T11.- TENDENCIAS OBSERVADAS Y PROYECCIONES FUTURAS RELATIVAS A FENÓMENOS EXTREMOS

Módulo 1.01.- Motores del clima, escenarios futuros y fenómenos extremos

Máster UIMP/CSIC en Cambio Global – Octubre 2013

Universitat de les Illes Balears

Romu Romero (Grupo de Meteorología – Dept. de Física)

3.8 Changes in Extreme Events

3.8.1 Background

There is increasing concern that extreme events may be changing in frequency and intensity as a result of human influences on climate. Climate change may be perceived most through the impacts of extremes, although these are to a large degree dependent on the system under consideration, including its vulnerability, resiliency and capacity for adaptation and mitigation; see the Working Group II contribution to the IPCC Fourth Assessment Report. Improvements in technology mean that people hear about extremes in most parts of the world within a few hours of their occurrence. Pictures shot by camcorders on the news may foster a belief that w
extremes are increasing in frequency, whether th
An extreme weather event becomes a disaster whe
or ecosystems are unable to cope with it effecti
human vulnerability (due to growing numbers of
in exposed and marginal areas or due to the de
more high-value property in high-risk zones) is
risk, while human endeavours (such as by local
try to mitigate possible effects.

extremes refer to rare events based on a statistical model of particular weather elements, and changes in extremes may relate to changes in the mean and variance in complicated ways. Changes in extremes are assessed at a range of temporal and spatial scales, for example, from extremely warm years globally to peak rainfall intensities locally, and examples are given in Box 3.6. To span this entire range, data are required at a daily (or shorter) time scale. However, the availability of observational data restricts the types of extremes that can be analysed. The rarer the event, the more difficult it is to identify long-term changes, simply because there are fewer cases to evaluate (Frei and Schär, 2001; Klein Tank and Können, 2003).

IPCC – AR4 (2007)

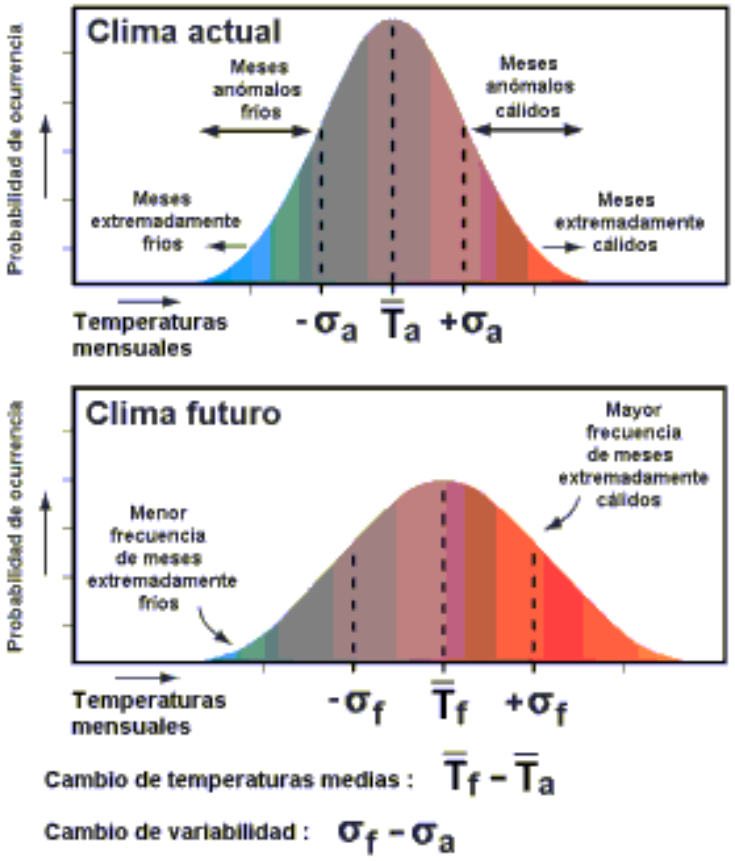

Figura 16. Ilustración esquemática de las distribuciones de frecuencia de las temperaturas mensuales en clima actual y en el clima proyectado.

Frequently Asked Question 3.3

Has there been a Change in Extreme Events like Heat Waves, Droughts, Floods and Hurricanes?

Since 1950, the number of heat waves has increased and widespread increases have occurred in the numbers of warm nights. The extent of regions affected by droughts has also increased as precipitation over land has marginally decreased while evaporation has increased due to warmer conditions. Generally, numbers of heavy daily precipitation events that lead to flooding have increased, but not everywhere. Tropical storm and hurricane frequencies vary considerably from year to year, but evidence suggests substantial increases in intensity and duration since the 1970s. In the extratropics, variations in tracks and intensity of storms reflect variations in major features of the atmospheric circulation, such as the North Atlantic Oscillation.

Table 3.6. *Global trends in extremes of temperature and precipitation as measured by the 10th and 90th percentiles (for 1961–1990). Trends with 5 and 95% confidence intervals and levels of significance (**bold**: <1%) were estimated by REML (see Appendix 3.A), which allows for serial correlation in the residuals of the data about the linear trend. All trends are based on annual averages. Values are % per decade. Based on Alexander et al. (2006).*

Series	Trend (% per decade) 1951–2003	1979–2003
TN10: % incidence of T_{min} below coldest decile.	**–1.17 ± 0.20**	**–1.24 ± 0.44**
TN90: % incidence of T_{min} above warmest decile.	**1.43 ± 0.42**	**2.60 ± 0.81**
TX10: % incidence of T_{max} below coldest decile.	**–0.63 ± 0.16**	**–0.91 ± 0.48**
TX90: % incidence of T_{max} above warmest decile.	**0.71 ± 0.35**	**1.74 ± 0.72**
PREC: % contribution of very wet days (above the 95th percentile) to the annual precipitation total.	**0.21 ± 0.10**	0.41 ± 0.38

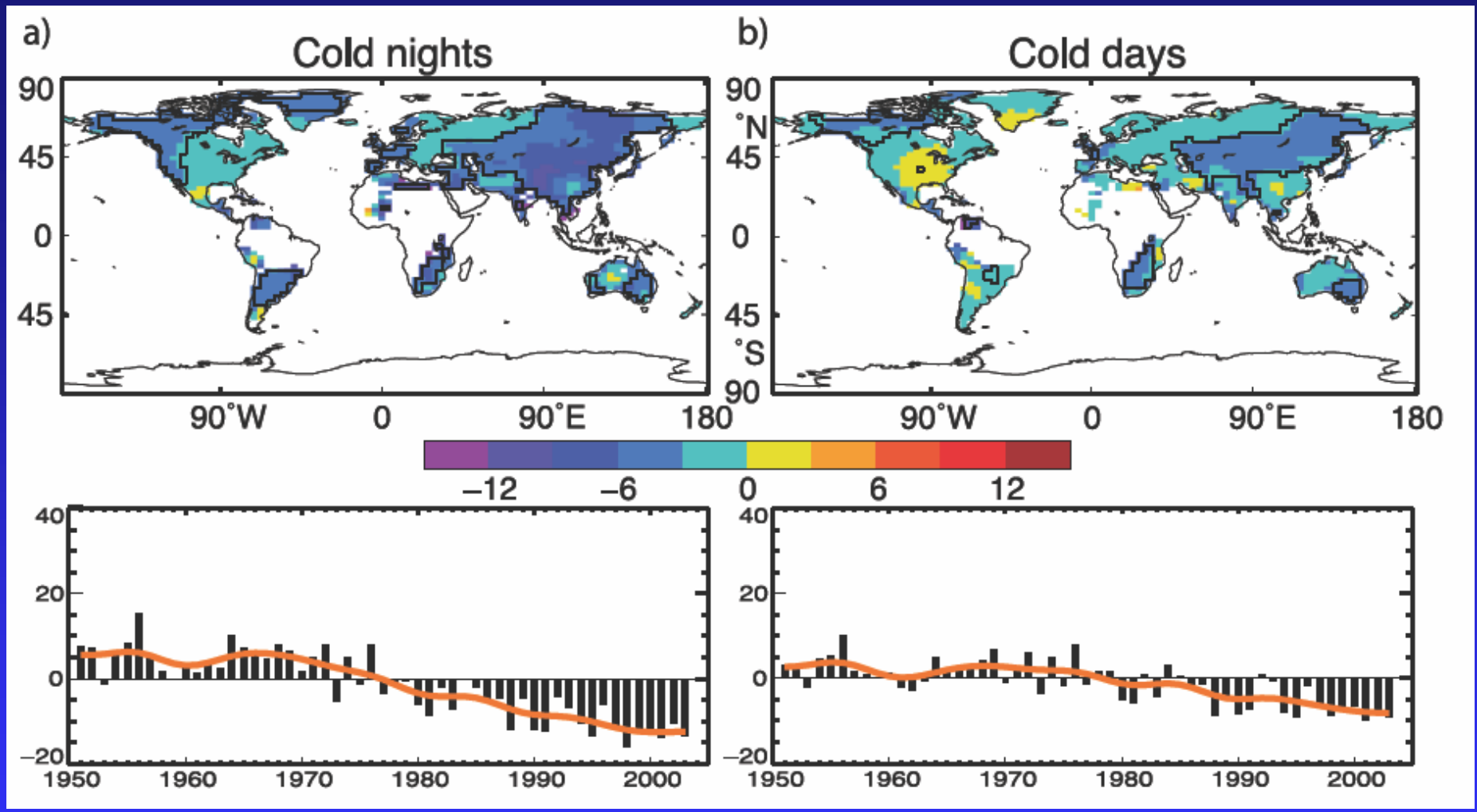
a)
Cold nights
b)
Cold days
90
45
0
45
90
°N
°S
90°W
0
90°E
180
−12
−6
0
6
12
40
20
0
−20
1950
1960
1970
1980
1990
2000

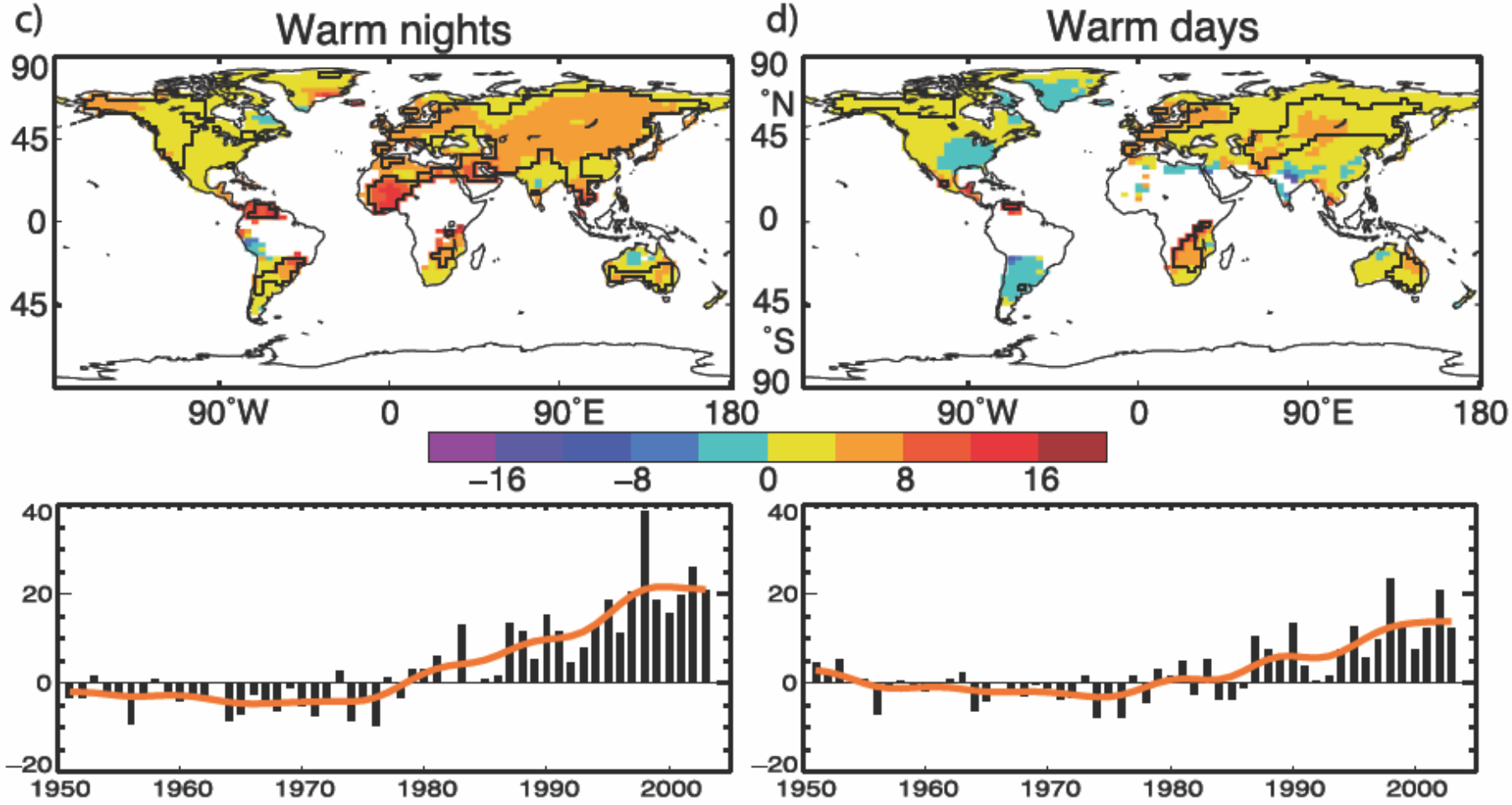

FAQ 3.3, Figure 1. *Observed trends (days per decade) for 1951 to 2003 in the frequency of extreme temperatures, defined based on 1961 to 1990 values, as maps for the 10th percentile: (a) cold nights and (b) cold days; and 90th percentile: (c) warm nights and (d) warm days. Trends were calculated only for grid boxes that had at least 40 years of data during this period and had data until at least 1999. Black lines enclose regions where trends are significant at the 5% level. Below each map are the global annual time series of anomalies (with respect to 1961 to 1990). The red line shows decadal variations. Trends are significant at the 5% level for all the global indices shown. Adapted from Alexander et al. (2006).*

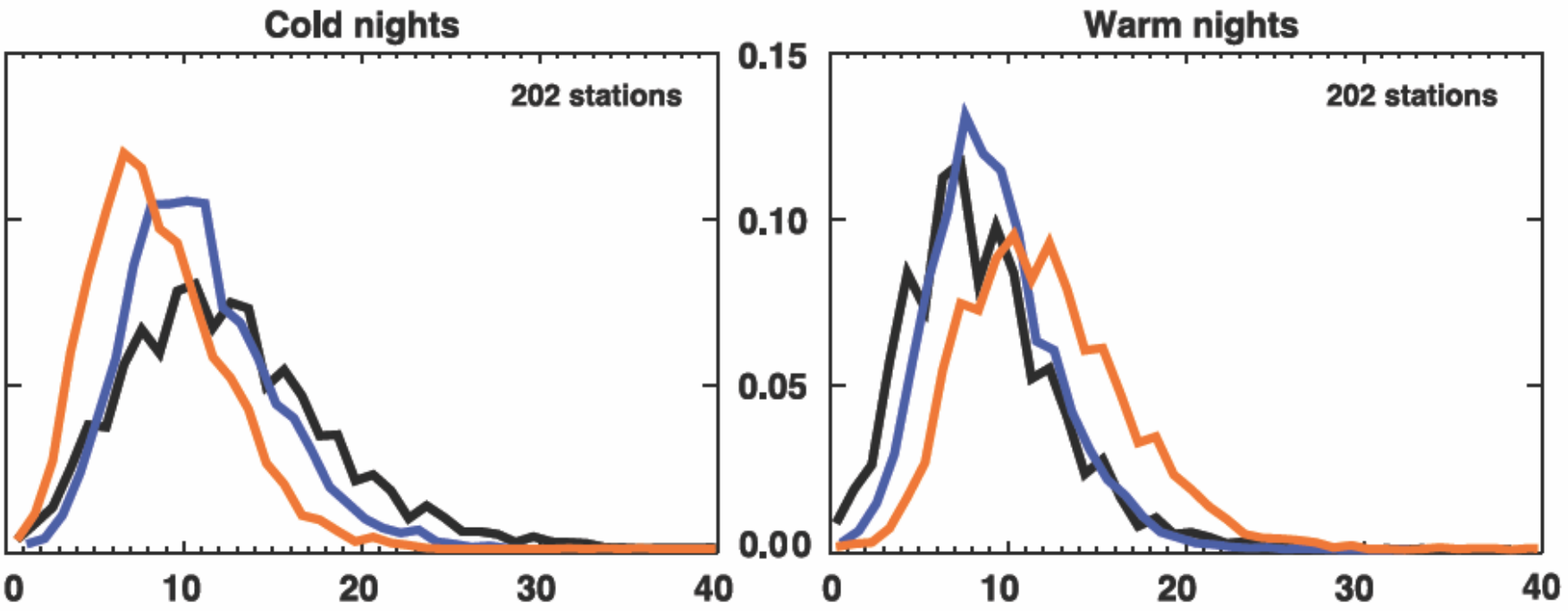

Figure 3.38. *Annual probability distribution functions for temperature indices for 202 global stations with at least 80% complete data between 1901 and 2003 for three time periods: 1901 to 1950 (black), 1951 to 1978 (blue) and 1979 to 2003 (red). The x-axis represents the percentage of time during the year when the indicators were below the 10th percentile for cold nights (left) or above the 90th percentile for warm nights (right). From Alexander et al. (2006).*

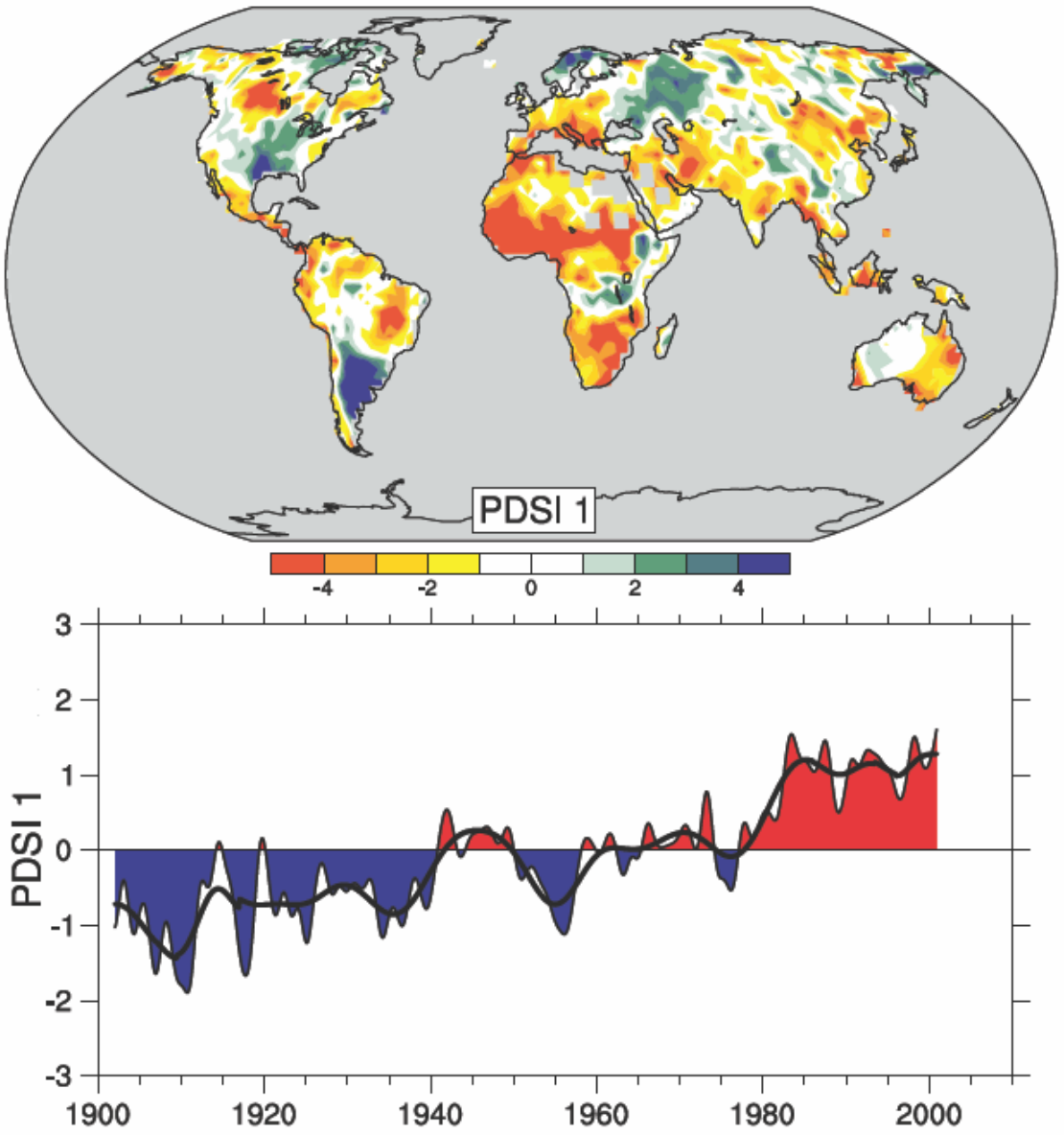

FAQ 3.2, Figure 1. *The most important spatial pattern (top) of the monthly Palmer Drought Severity Index (PDSI) for 1900 to 2002. The PDSI is a prominent index of drought and measures the cumulative deficit (relative to local mean conditions) in surface land moisture by incorporating previous precipitation and estimates of moisture drawn into the atmosphere (based on atmospheric temperatures) into a hydrological accounting system. The lower panel shows how the sign and strength of this pattern has changed since 1900. Red and orange areas are drier (wetter) than average and blue and green areas are wetter (drier) than average when the values shown in the lower plot are positive (negative). The smooth black curve shows decadal variations. The time series approximately corresponds to a trend, and this pattern and its variations account for 67% of the linear trend of PDSI from 1900 to 2002 over the global land area. It therefore features widespread increasing African drought, especially in the Sahel, for instance. Note also the wetter areas, especially in eastern North and South America and northern Eurasia. Adapted from Dai et al. (2004b).*

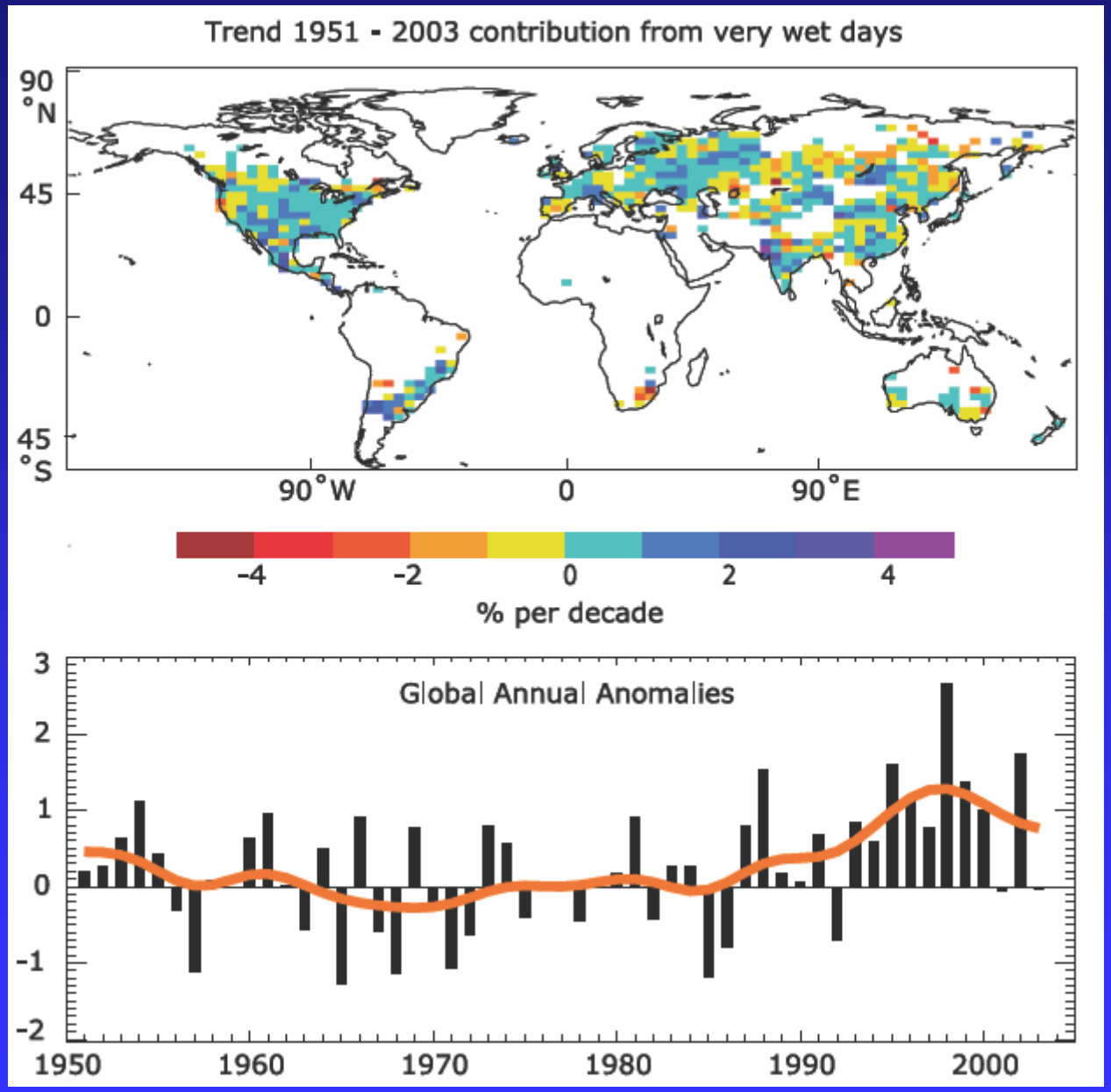
Trend 1951 - 2003 contribution from very wet days
90 °N
45
0
45 °S
90°W
0
90°E
-4
-2
0
2
4
% per decade
Global Annual Anomalies
3
2
1
0
-1
-2
1950
1960
1970
1980
1990
2000

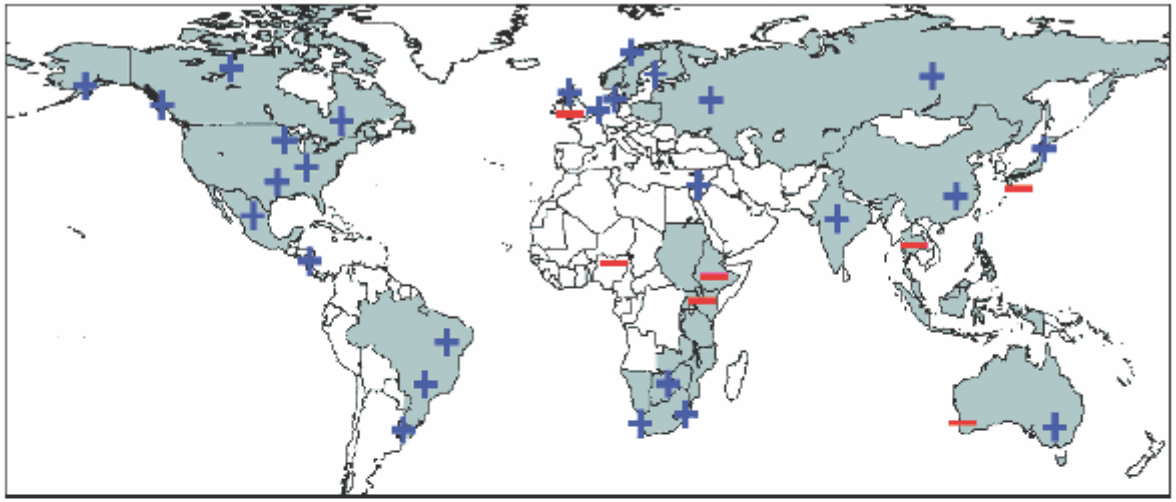

Figure 3.39. *(Top) Observed trends (% per decade) for 1951 to 2003 in the contribution to total annual precipitation from very wet days (95th percentile). Trends were only calculated for grid boxes where both the total and the 95th percentile had at least 40 years of data during this period and had data until at least 1999. (Middle) Anomalies (%) of the global annual time series (with respect to 1961 to 1990) defined as the percentage change of contributions of very wet days from the base period average (22.5%). The smooth red curve shows decadal variations (see Appendix 3.A). From Alexander et al. (2006). (Bottom) Regions where disproportionate changes in heavy and very heavy precipitation during the past decades were documented as either an increase (+) or decrease (–) compared to the change in the annual and/or seasonal precipitation (updated from Groisman et al., 2005). Thresholds used to define "heavy" and "very heavy" precipitation vary by season and region. However, changes in heavy precipitation frequencies are always greater than changes in precipitation totals and, in some regions, an increase in heavy and/or very heavy precipitation occurred while no change or even a decrease in precipitation totals was observed.*

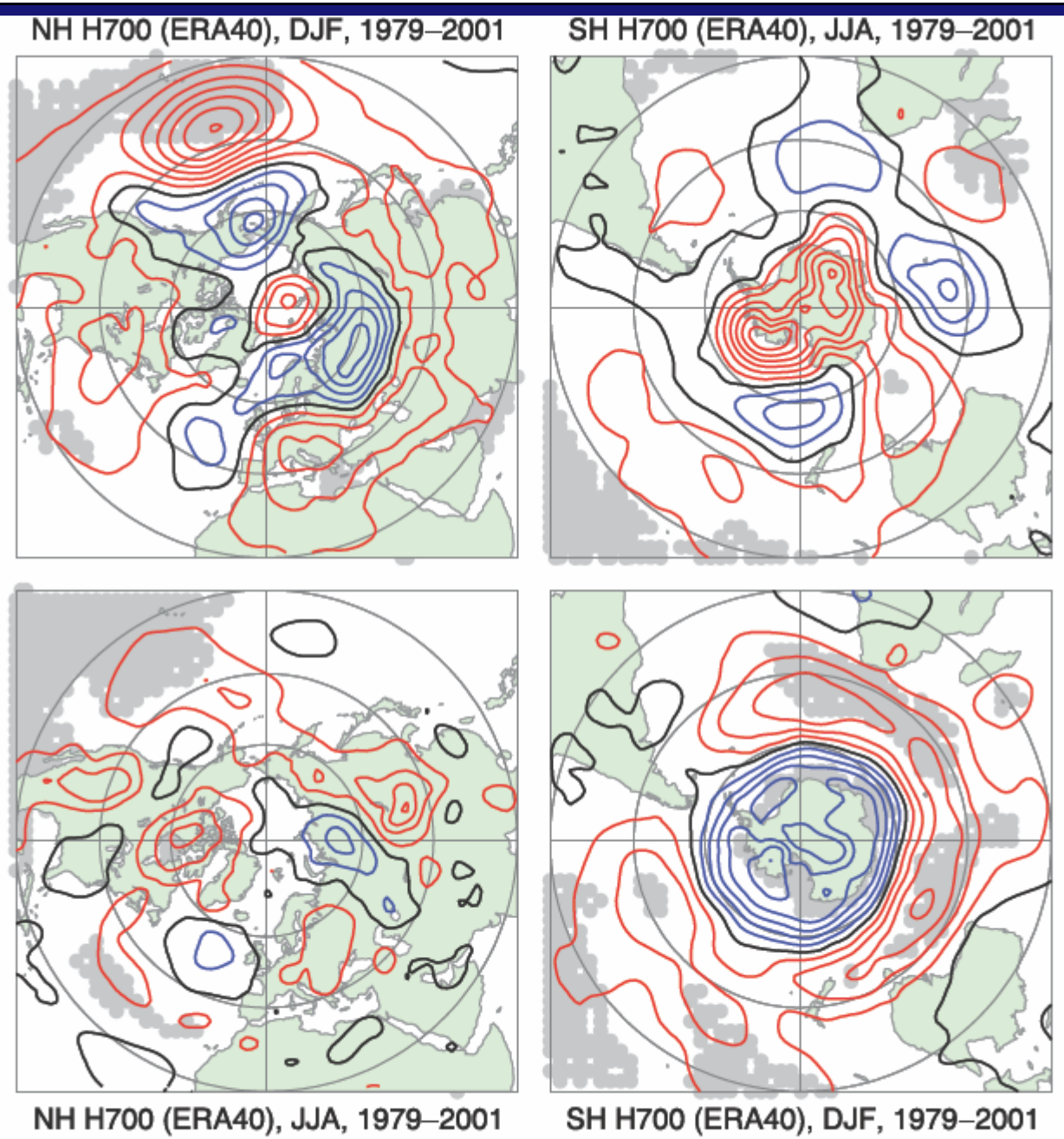

Figure 3.24. *Linear trends in ERA-40 700 hPa geopotential height from 1979 to 2001 for DJF (top left and bottom right) and JJA (bottom left and top right), for the NH (left) and SH (right). Trends are contoured in 5 gpm per decade and are calculated from seasonal means of daily 1200 UTC fields. Red contours are positive, blue negative and black zero; the grey background indicates 1% statistical significance using a standard least squares F-test and assuming independence between years.*

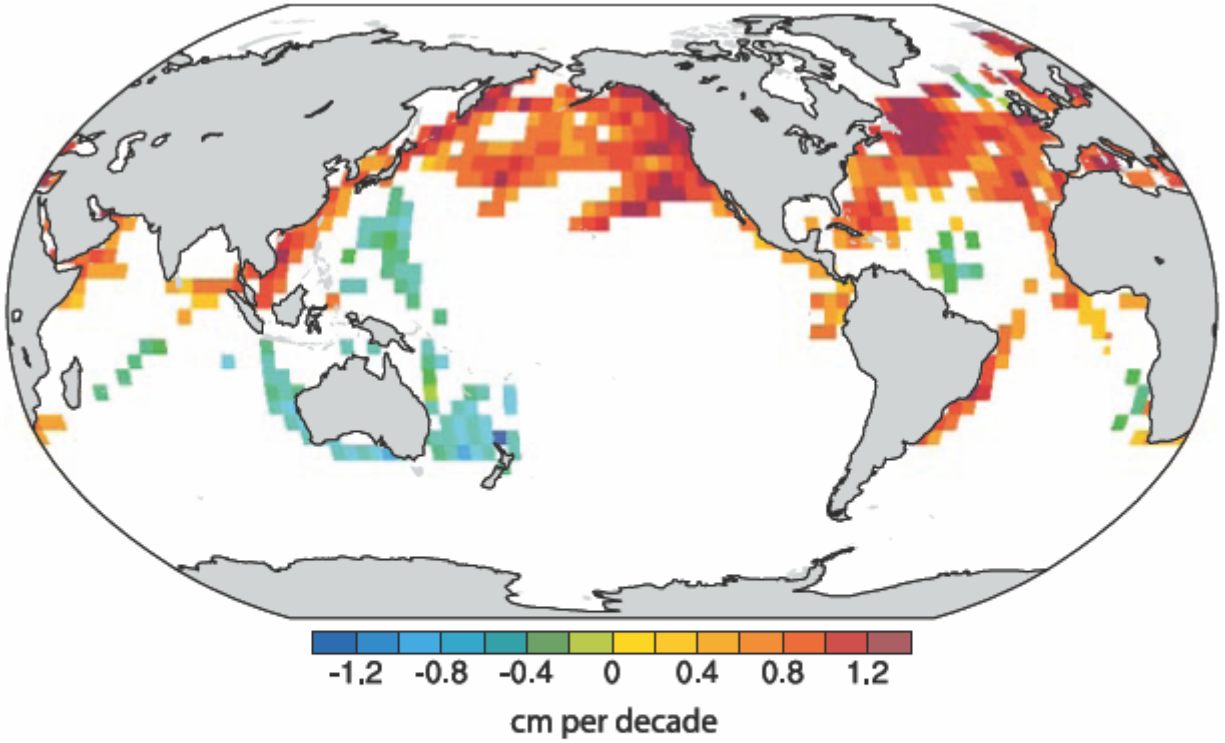

Figure 3.25. *Estimates of linear trends in significant wave height (cm per decade) for regions along the major ship routes of the global ocean for 1950 to 2002. Trends are shown only for locations where they are significant at the 5% level. Adapted from Gulev and Grigorieva (2004).*

Table 3.7. *Definition of phenomena used to assess extremes in Table 3.8*

PHENOMENON	Definition
Low-temperature days/ nights and frost days	Percentage of days with temperature (maximum for days, minimum for nights) not exceeding some threshold, either fixed (frost days) or varying regionally (cold days/cold nights), based on the 10th percentile of the daily distribution in the reference period (1961–1990).
High-temperature days/nights	See low-temperature days/nights, but now exceeding the 90th percentile.
Cold spells/snaps	Episode of several consecutive low-temperature days/nights.
Warm spells (heat waves)	Episode of several consecutive high-temperature days/nights.
Cool seasons/warm seasons	Seasonal averages (rather than daily temperatures) exceeding some threshold.
Heavy precipitation events (events that occur every year)	Percentage of days (or daily precipitation amount) with precipitation exceeding some threshold, either fixed or varying regionally, based on the 95th or 99th percentile of the daily distribution in the reference period (1961–1990).
Rare precipitation events (with return periods >~10 yr)	As for heavy precipitation events, but for extremes further into the tail of the distribution.
Drought (season/year)	Precipitation deficit; or based on the PDSI (see Box 3.1).

Tropical cyclones (frequency, intensity, track, peak wind, peak precipitation)	Tropical storm with thresholds crossed in terms of estimated wind speed and organisation. Hurricanes in categories 1 to 5, according to the Saffir-Simpson scale, are defined as storms with wind speeds of 33 to 42 m s^{-1}, 43 to 49 m s^{-1}, 50 to 58 m s^{-1}, 59 to 69 m s^{-1}, and >70 m s^{-1}, respectively. NOAA's ACE index is a measure of the total seasonal activity that accounts for the collective intensity and duration of tropical storms and hurricanes during a given tropical cyclone season.
Extreme extratropical storms (frequency, intensity, track, surface wind, wave height)	Intense low-pressure systems that occur throughout the mid-latitudes of both hemispheres fueled by temperature gradients and acting to reduce them.
Small-scale severe weather phenomena	Extreme events, such as tornadoes, hail, thunderstorms, dust storms and other severe local weather.

Table 3.8. *Change in extremes for phenomena over the specified region and period, with the level of confidence and section where the phenomenon is discus*

PHENOMENON	Change	Region	Period	Confidence
Low-temperature days/nights and frost days	Decrease, more so for nights than days	Over 70% of global land area	1951–2003 (last 150 years for Europe and China)	*Very likely*
High-temperature days/nights	Increase, more so for nights than days	Over 70% of global land area	1951–2003	*Very likely*
Cold spells/snaps (episodes of several days)	Insufficient studies, but daily temperature changes imply a decrease			
Warm spells (heat waves) (episodes of several days)	Increase: implicit evidence from changes of daily temperatures	Global	1951–2003	*Likely*
Cool seasons/ warm seasons (seasonal averages)	Some new evidence for changes in inter-seasonal variability	Central Europe	1961–2004	*Likely*

Heavy precipitation events (that occur every year)	Increase, generally beyond that expected from changes in the mean (disproportionate)	Many mid-latitude regions (even where reduction in total precipitation)	1951–2003	*Likely*
Rare precipitation events (with return periods > ~10 yr)	Increase	Only a few regions have sufficient data for reliable trends (e.g., UK and USA)	Various since 1893	*Likely* (consistent with changes inferred for more robust statistics)
Drought (season/year)	Increase in total area affected	Many land regions of the world	Since 1970s	*Likely*
Tropical cyclones	Trends towards longer lifetimes and greater storm intensity, but no trend in frequency	Tropics	Since 1970s	*Likely;* more confidence in frequency and intensity
Extreme extratropical storms	Net increase in frequency/intensity and poleward shift in track	NH land	Since about 1950	*Likely*
Small-scale severe weather phenomena	Insufficient studies for assessment			

Frequently Asked Question 9.1

Can Individual Extreme Events be Explained by Greenhouse Warming?

Changes in climate extremes are expected as the climate warms in response to increasing atmospheric greenhouse gases resulting from human activities, such as the use of fossil fuels. However, determining whether a specific, single extreme event is due to a specific cause, such as increasing greenhouse gases, is difficult, if not impossible, for two reasons: 1) extreme events are usually caused by a combination of factors and 2) a wide range of extreme events is a normal occurrence even in an unchanging climate. Nevertheless, analysis of the warming observed over the past century suggests that the likelihood of some extreme events, such as heat waves, has increased due to greenhouse warming, and that the likelihood of others, such as frost or extremely cold nights, has decreased. For example, a recent study estimates that human influences have more than doubled the risk of a very hot European summer like that of 2003.

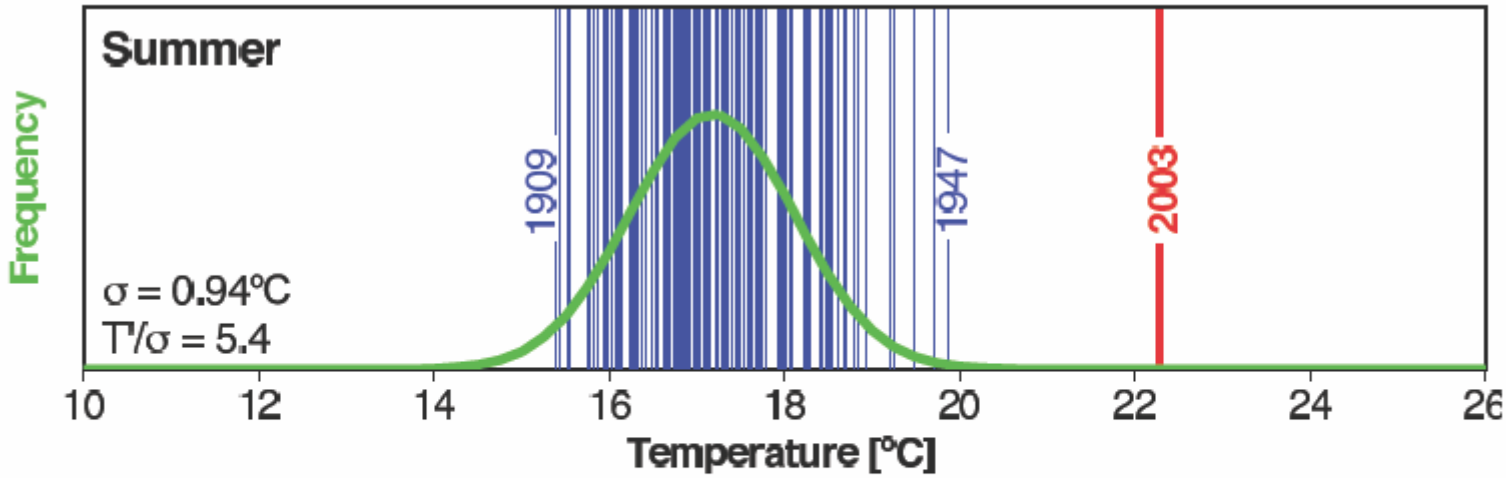

FAQ 9.1, Figure 1. *Summer temperatures in Switzerland from 1864 to 2003 are, on average, about 17°C, as shown by the green curve. During the extremely hot summer of 2003, average temperatures exceeded 22°C, as indicated by the red bar (a vertical line is shown for each year in the 137-year record). The fitted Gaussian distribution is indicated in green. The years 1909, 1947 and 2003 are labelled because they represent extreme years in the record. The values in the lower left corner indicate the standard deviation (σ) and the 2003 anomaly normalised by the 1864 to 2000 standard deviation (T'/σ). From Schär et al. (2004).*

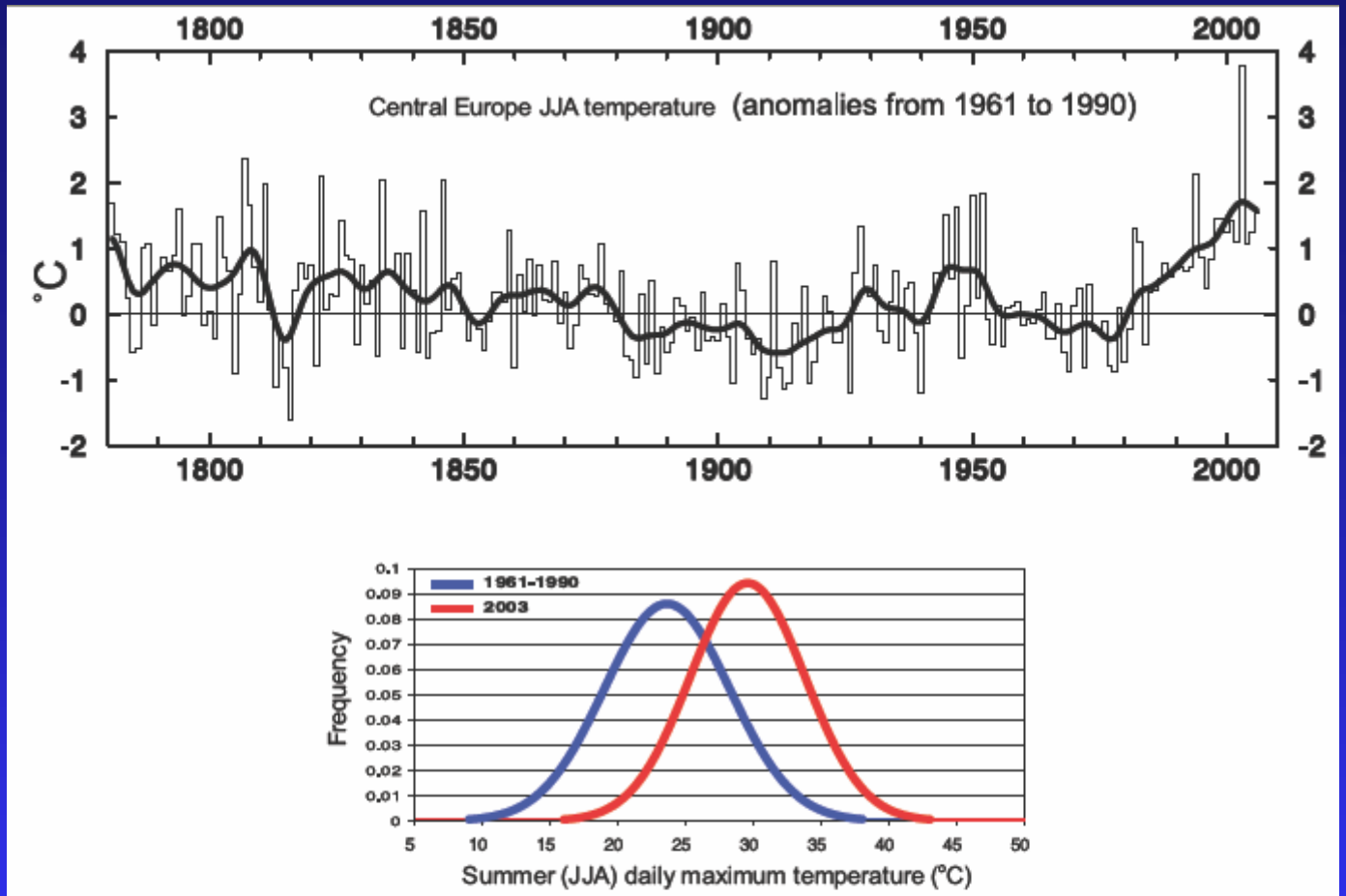

Box 3.6, Figure 2. *Long time series of JJA temperature anomalies in Central Europe relative to the 1961 to 1990 mean (top). The smooth curve shows decadal variations (see Appendix 3.A). In the summer of 2003, the value of 3.8°C far exceeded the next largest anomaly of 2.4°C in 1807, and the highly smoothed Gaussian distribution (bottom) of maximum temperatures (red) compared with normal (blue) at Basel, Switzerland (Beniston and Diaz, 2004) shows how the whole distribution shifted.*

Extremos de Temperatura

Mallorca

Anual

Temperaturas máximas i mínimas diarias

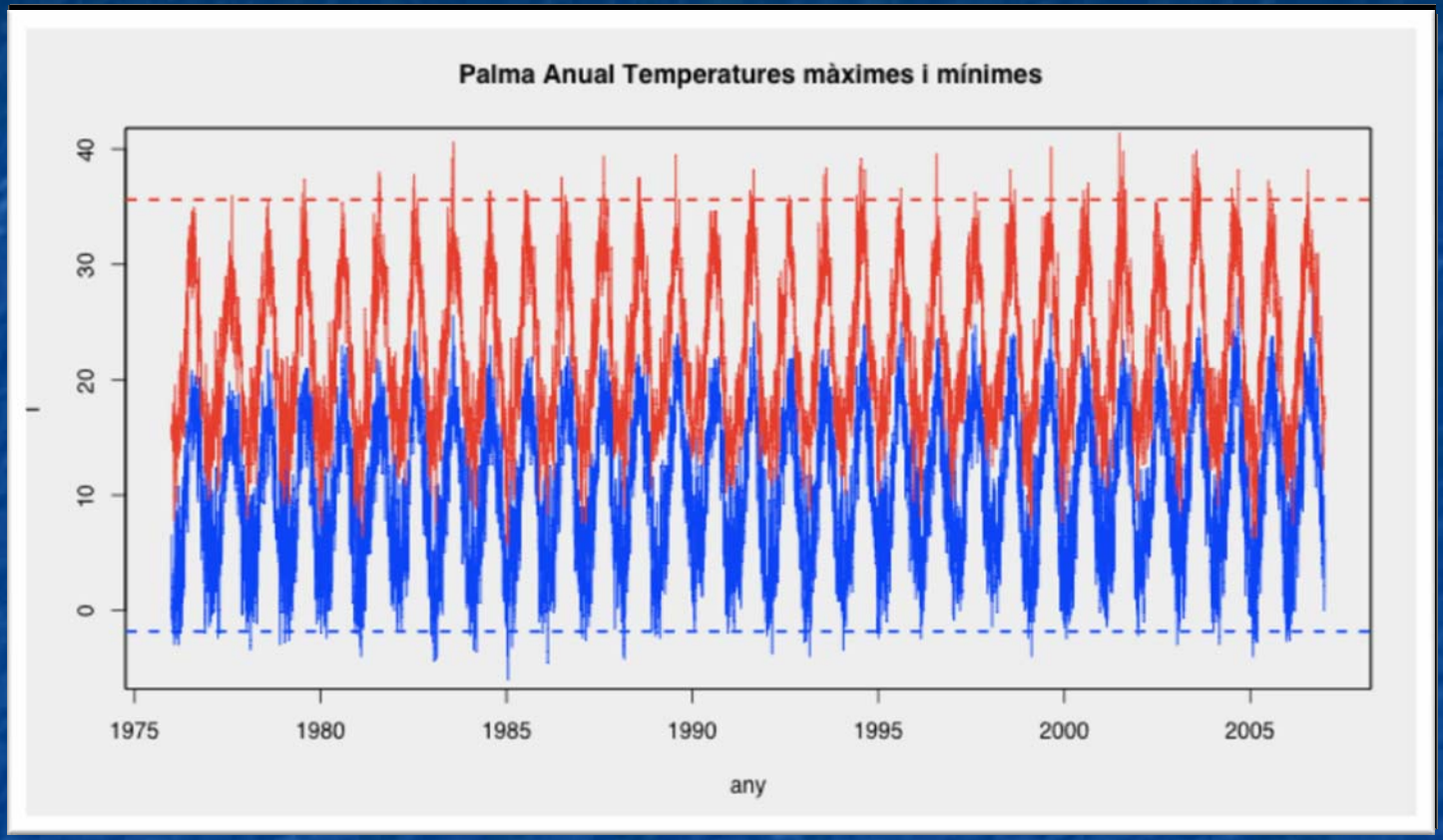

Temperaturas máximas diarias

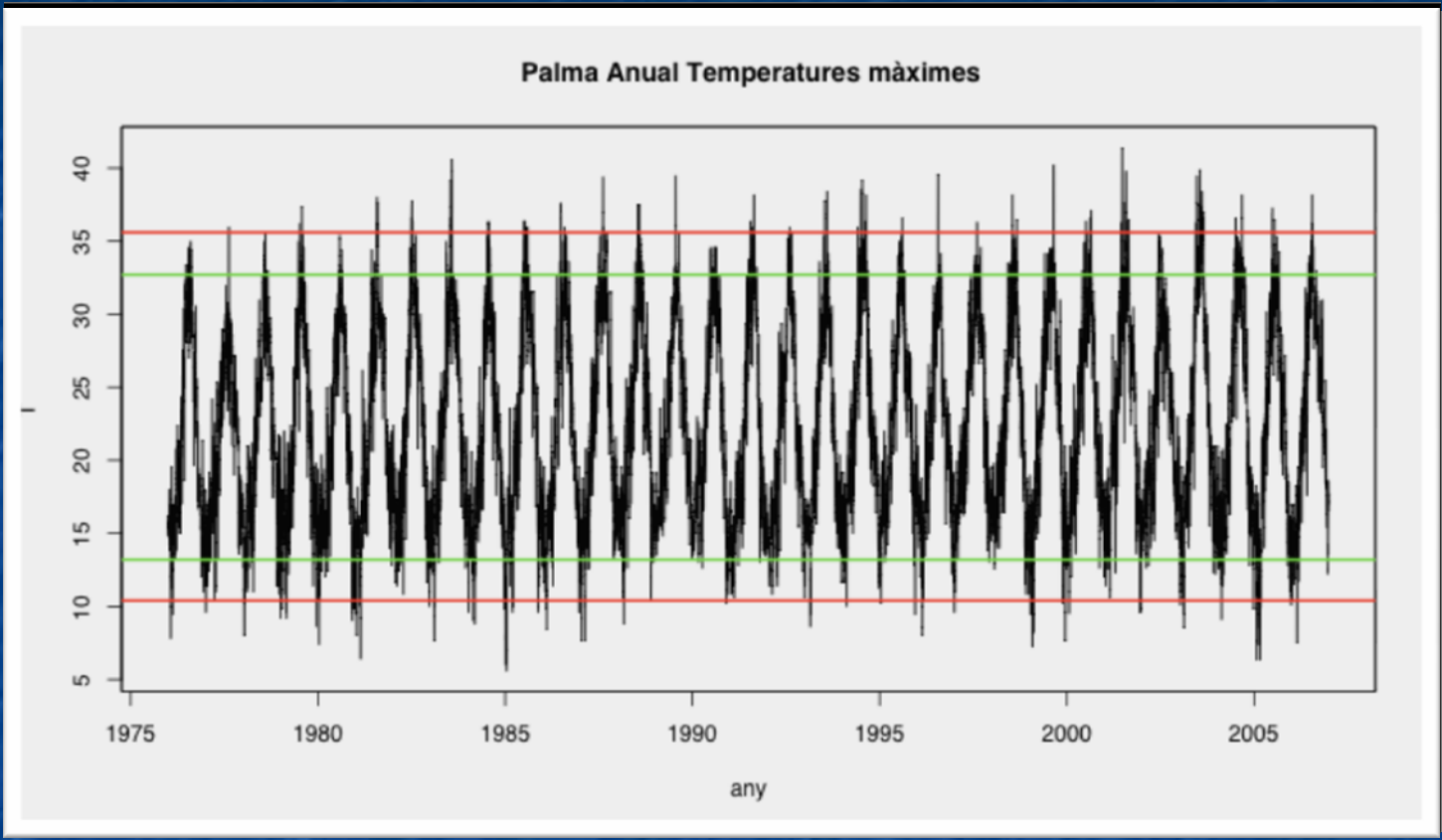

Temperaturas mínimas diarias

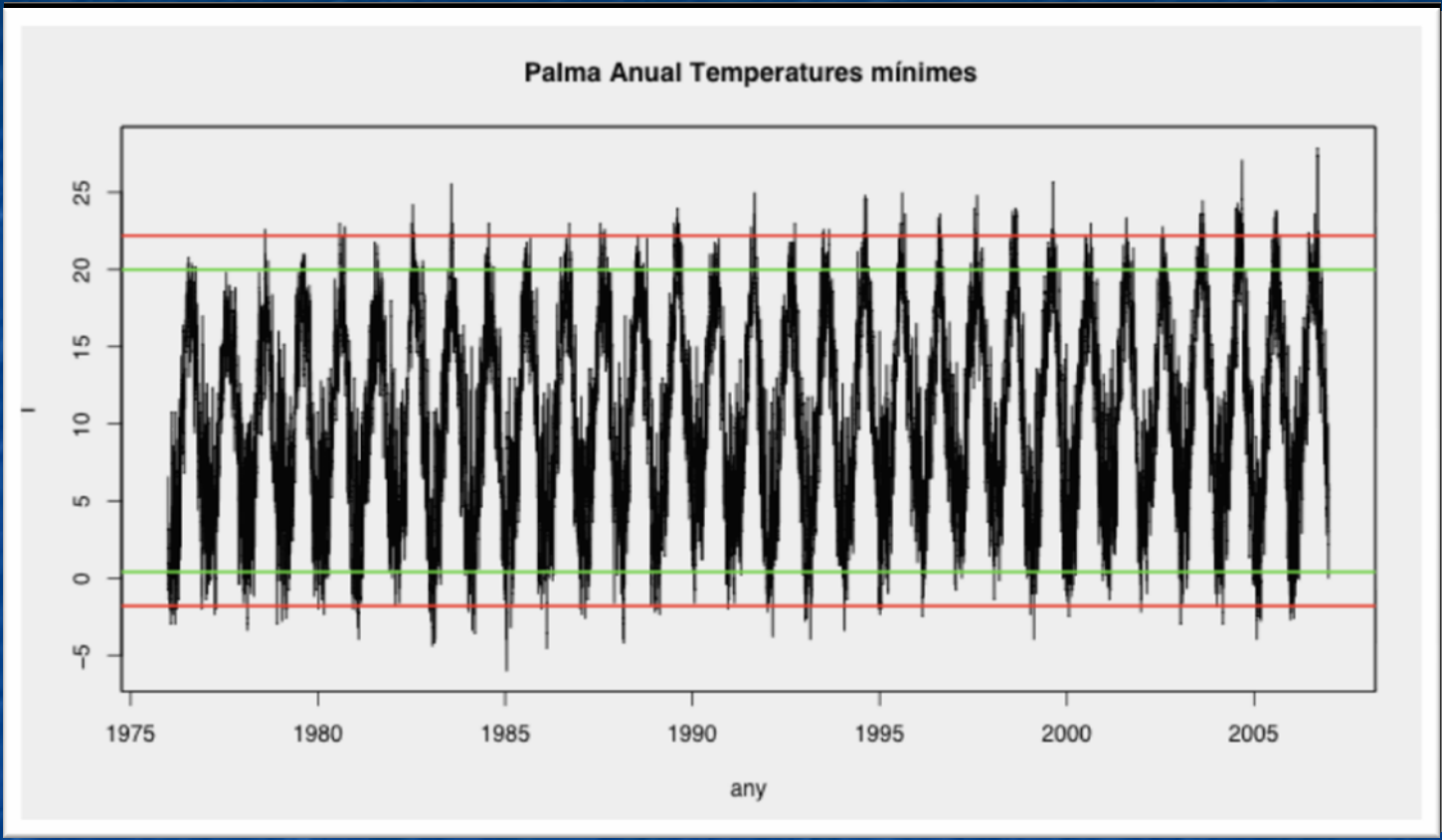

Histograma temperaturas máximas

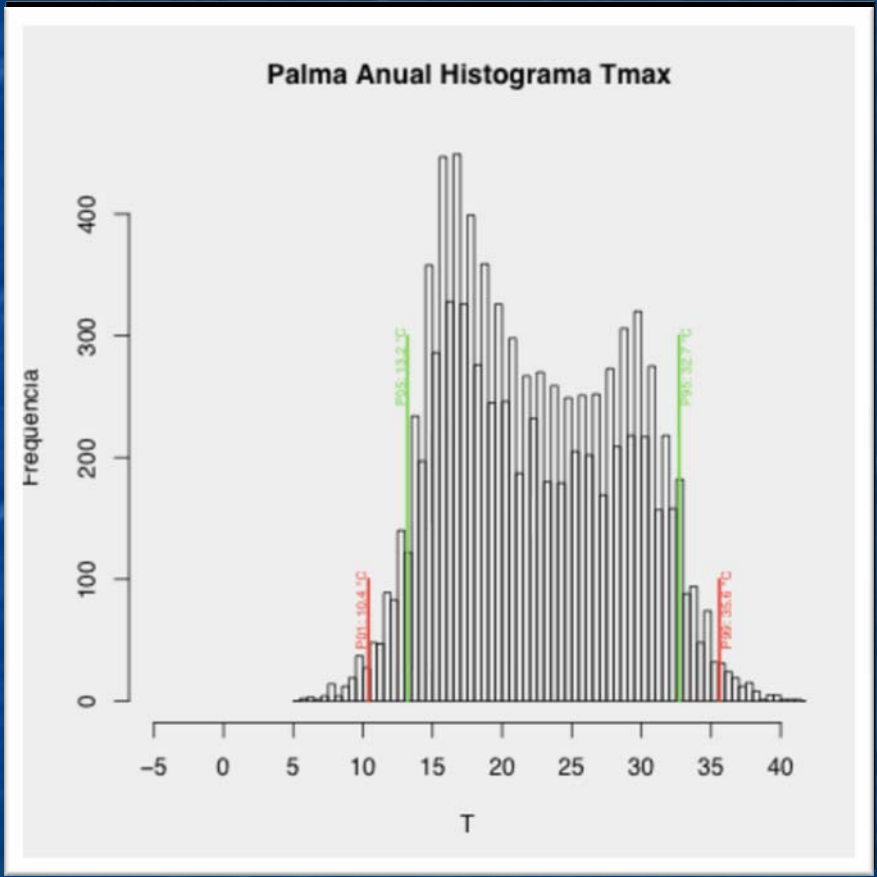

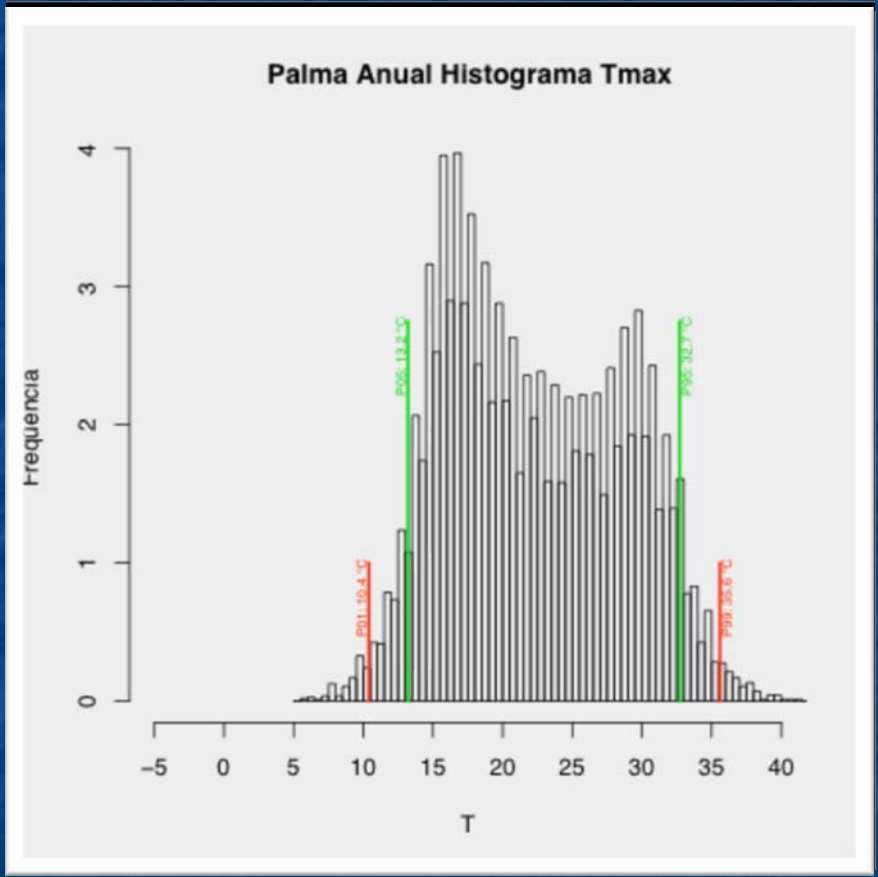

Histograma temperaturas mínimas

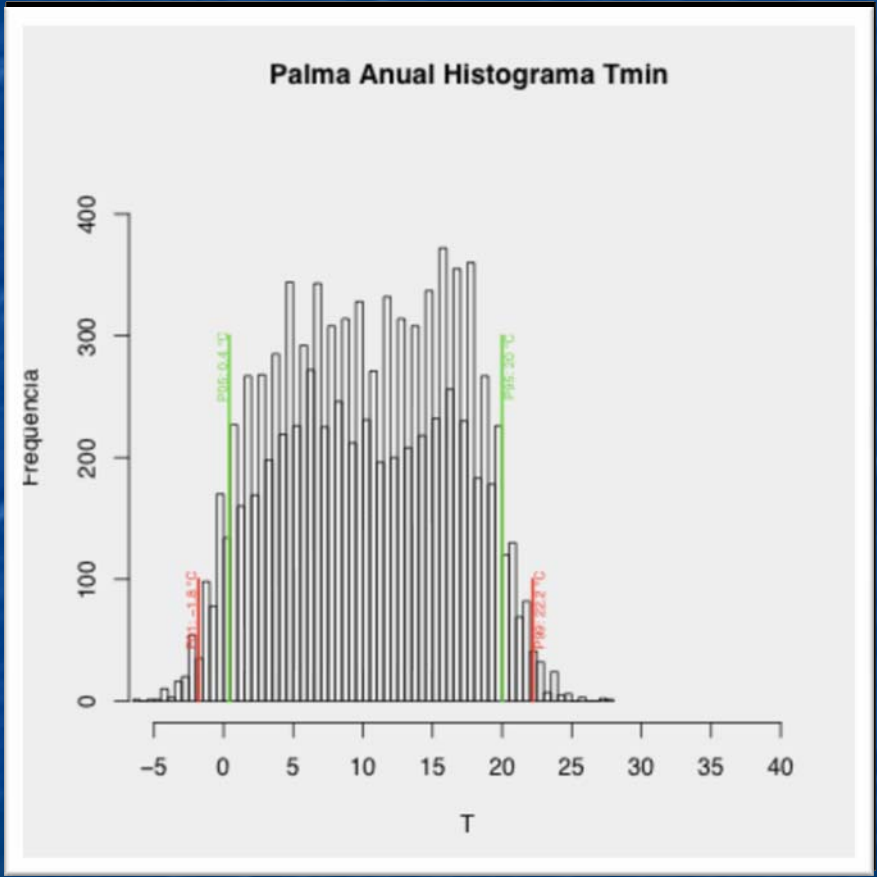

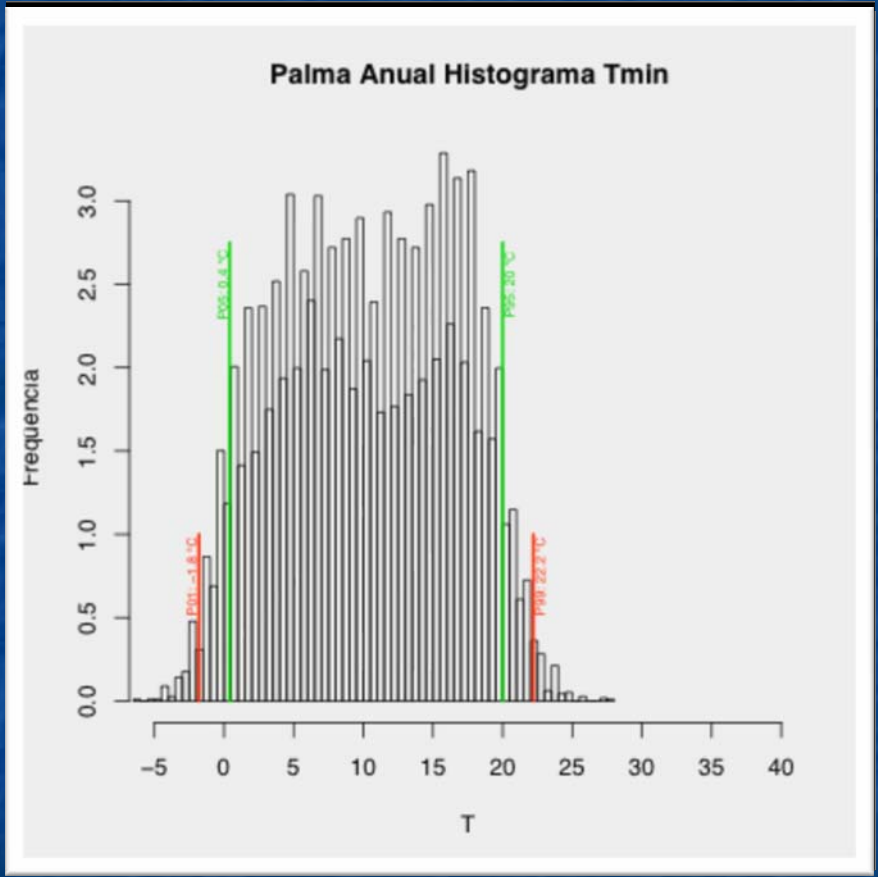

Temperaturas - Extremos

Máximas			
Tmax 1%	10.4ºC	Tmax 99%	35.6ºC
Tmax 5%	13.2ºC	Tmax 95%	32.7ºC
Tmax 10%	14.6ºC	Tmax 90%	31.2ºC
Tmax 20%	16.2ºC	Tmax 80%	29.0ºC

Mínimas			
Tmin 1%	-1.8ºC	Tmin 99%	22.2ºC
Tmin 5%	0.4ºC	Tmin 95%	20.0ºC
Tmin 10%	1.8ºC	Tmin 90%	18.6ºC
Tmin 20%	4.2ºC	Tmin 80%	16.6ºC

Temperaturas máximas (99%)

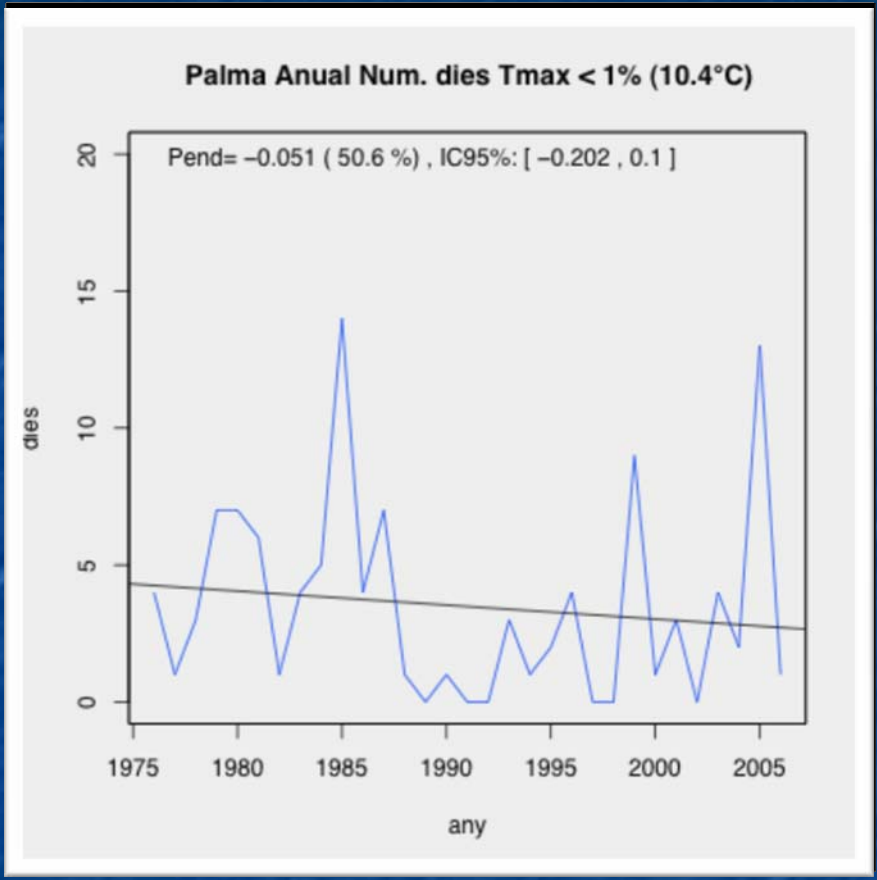

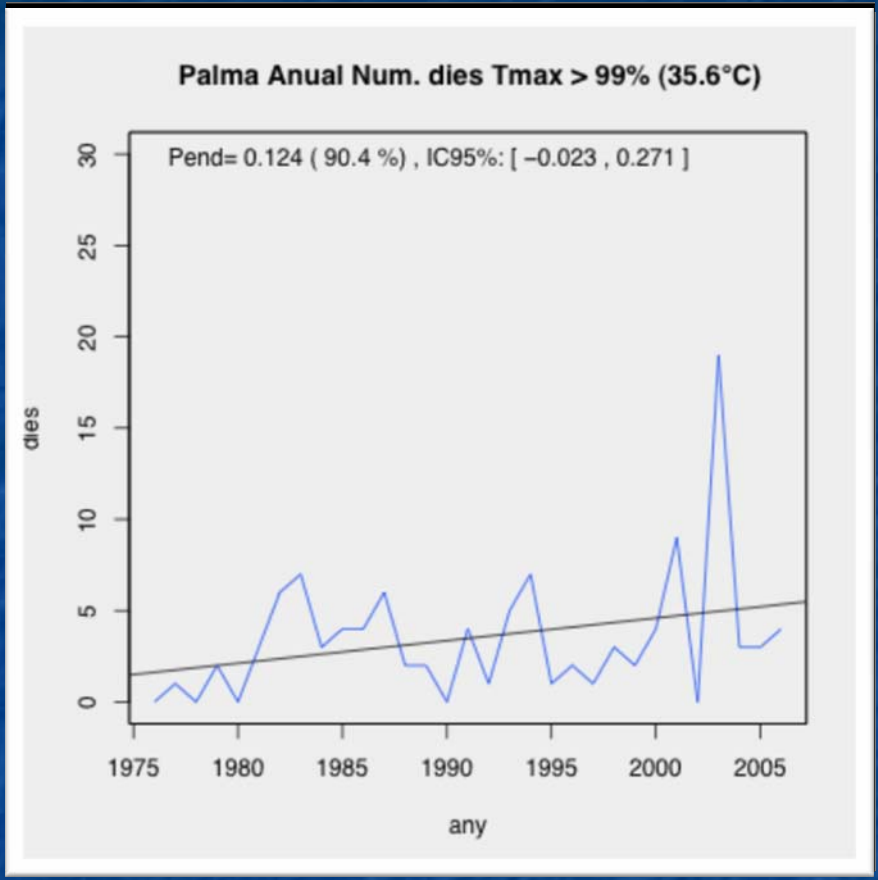

Temperaturas máximas (95%)

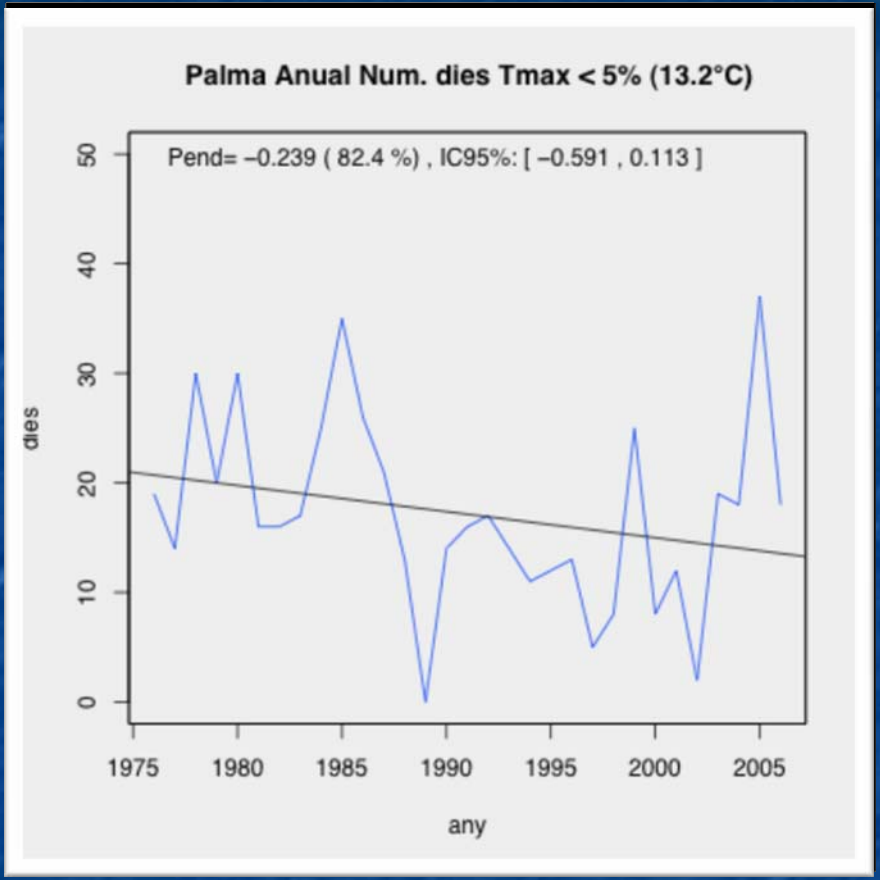

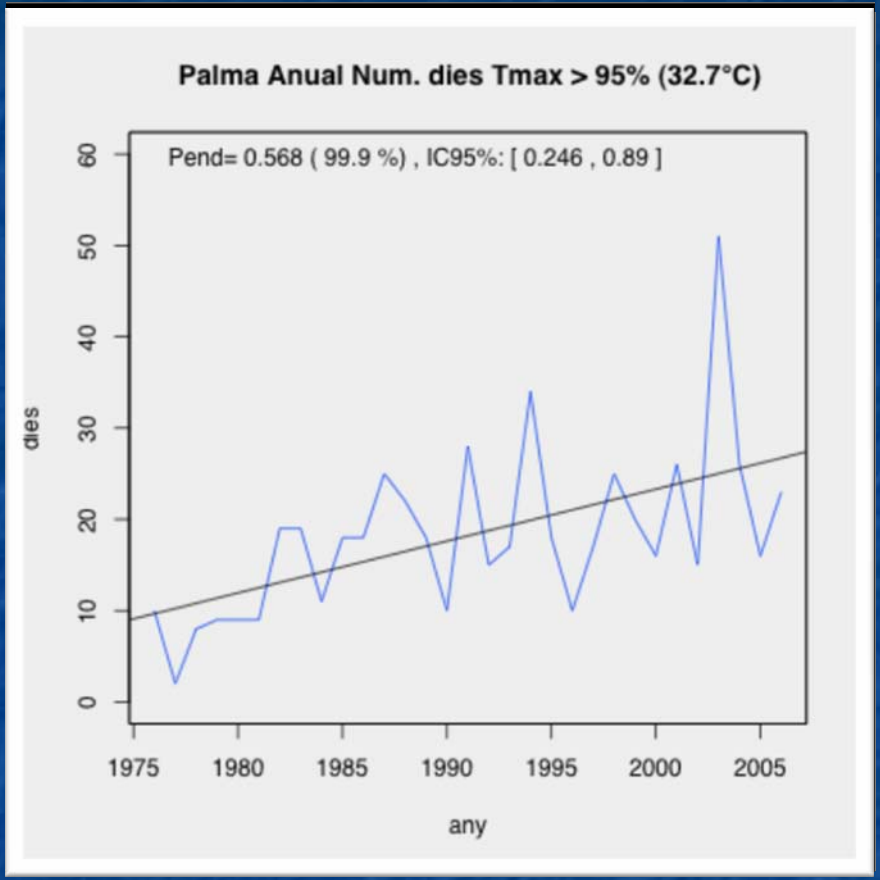

Temperaturas mínimas (99%)

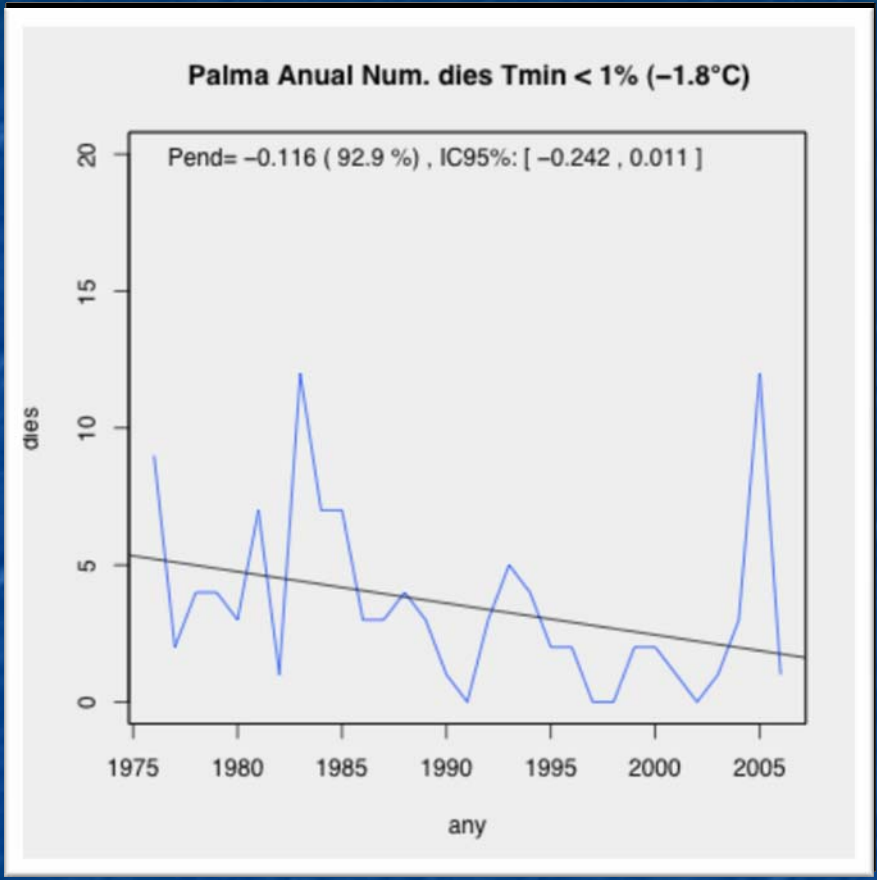

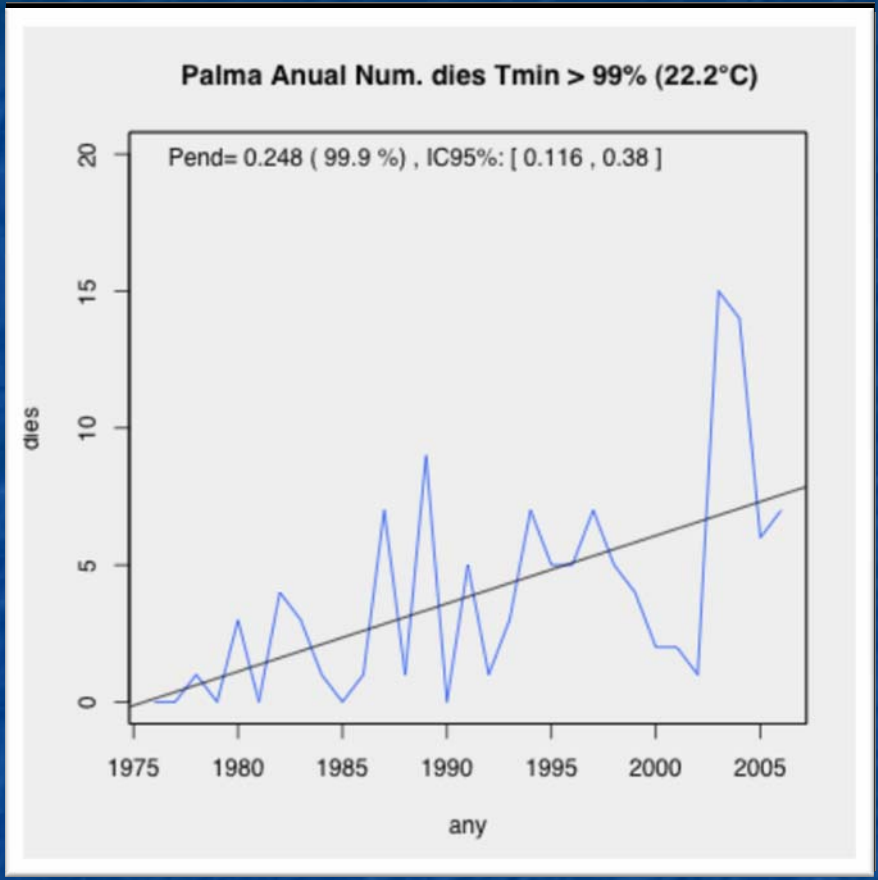

Temperaturas mínimas (95%)

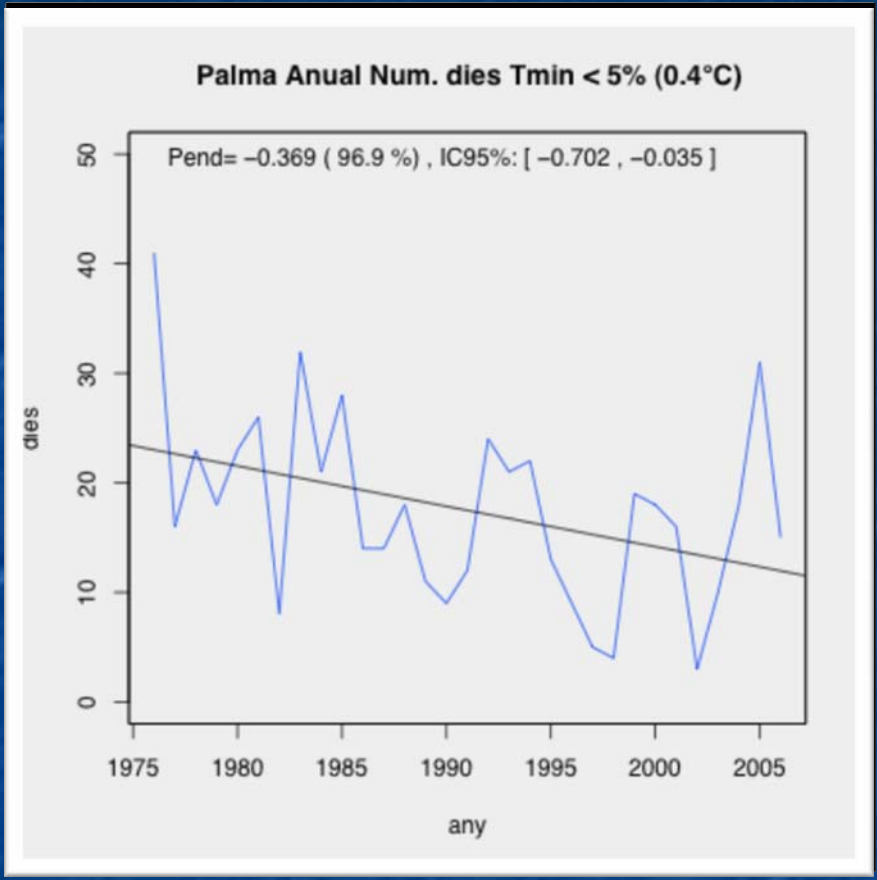

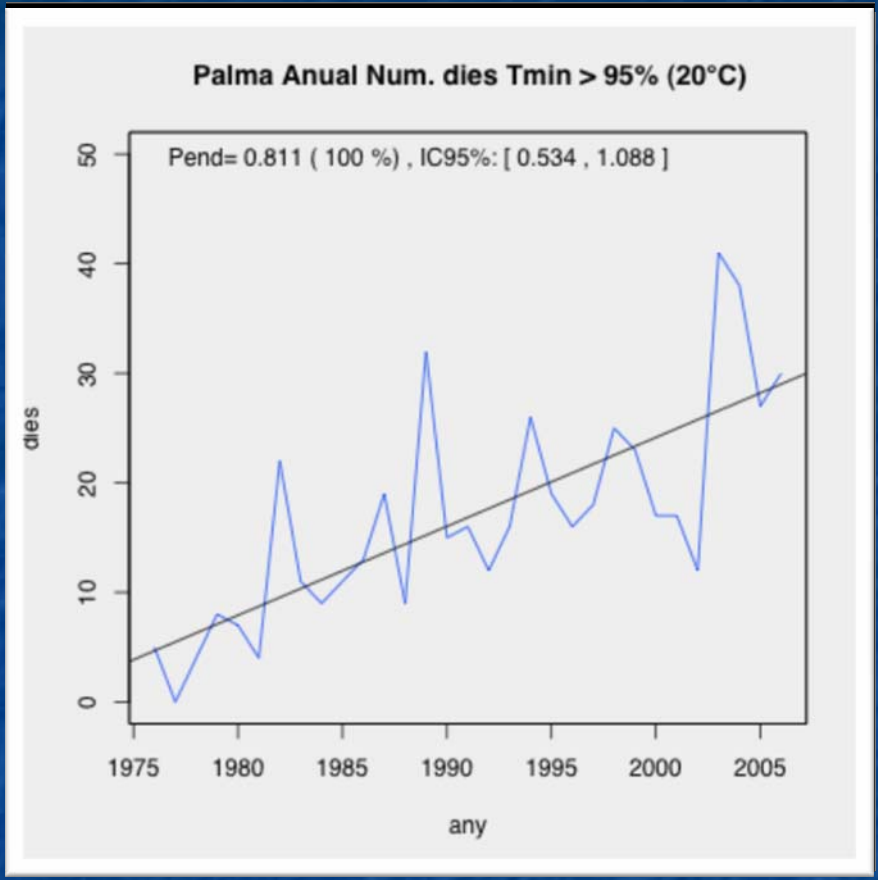

Invierno

Histograma temperaturas máximas

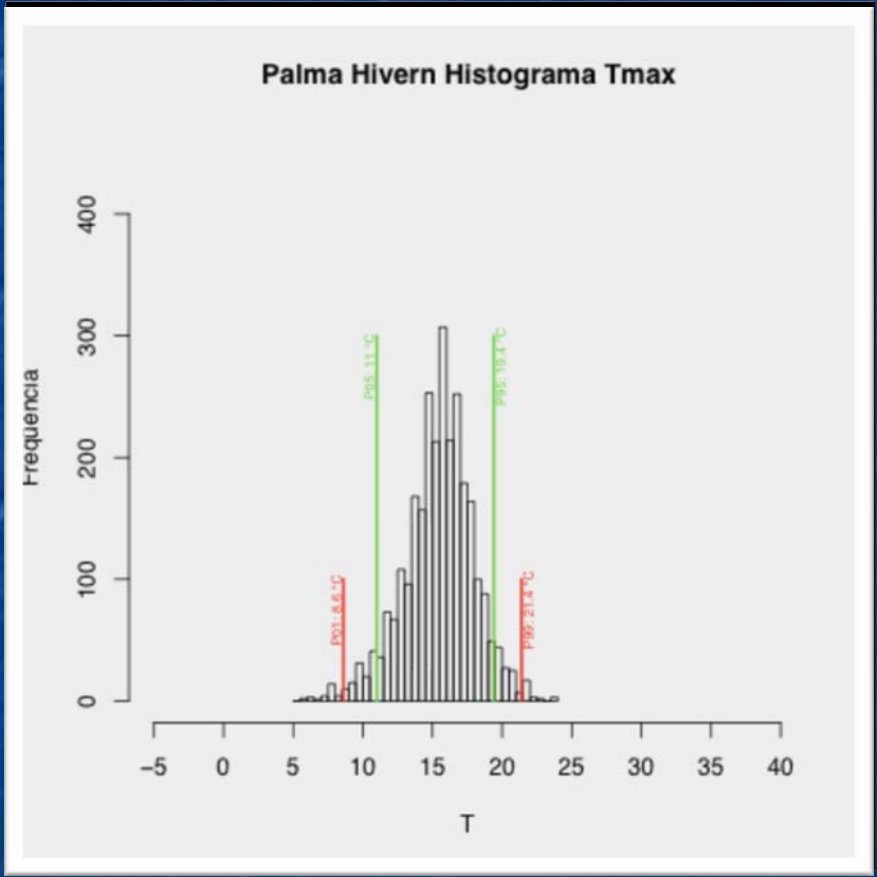

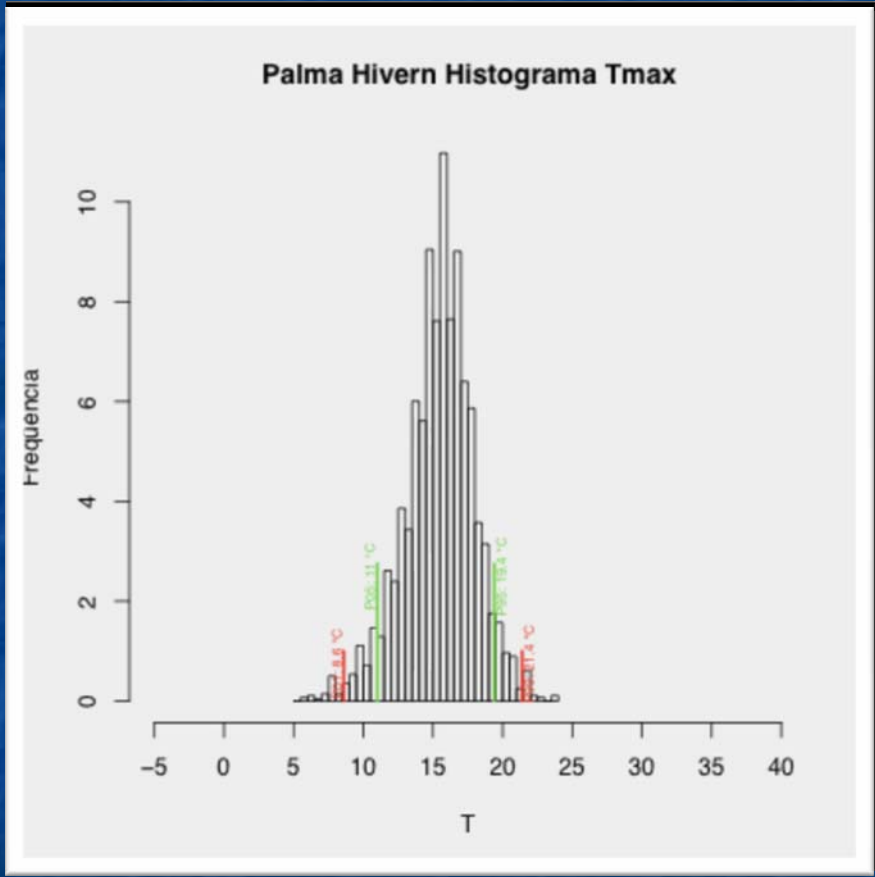

Histograma temperaturas mínimas

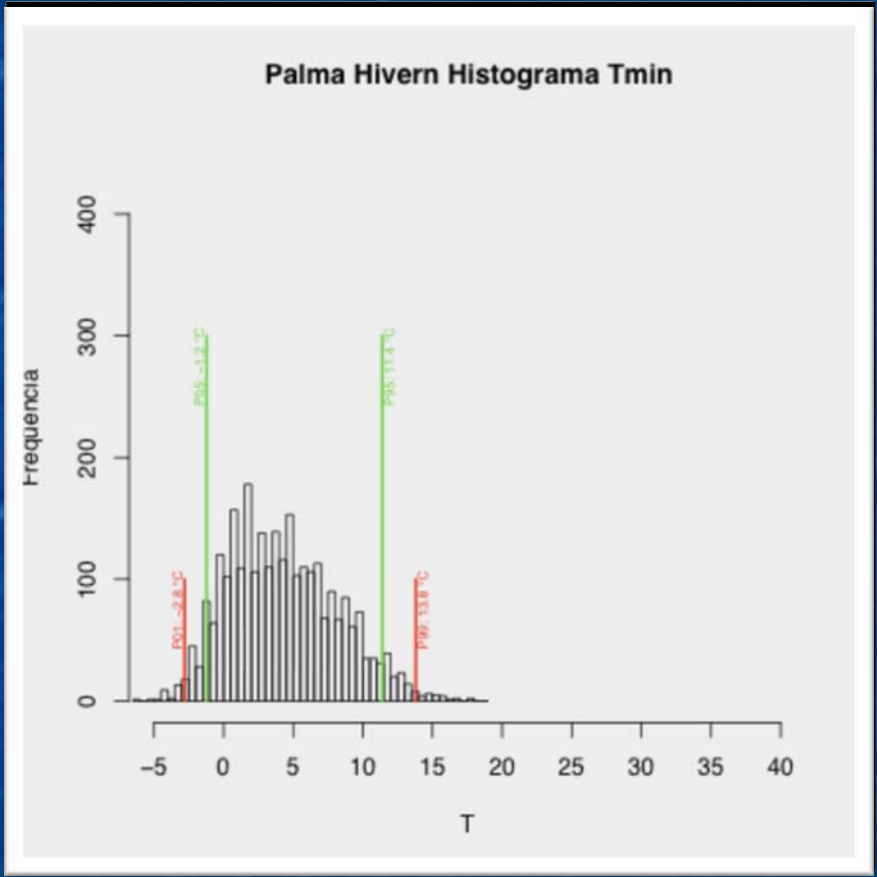

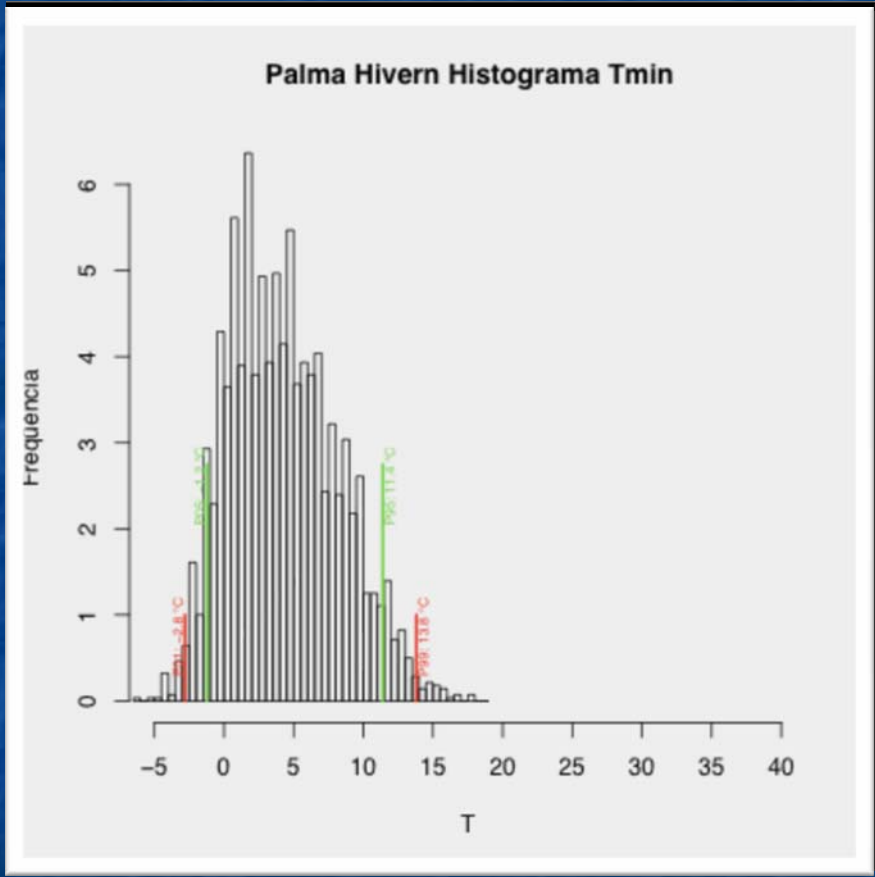

Temperaturas - Extremos

Máximas			
Tmax 1%	8.6ºC	Tmax 99%	21.4ºC
Tmax 5%	11.0ºC	Tmax 95%	19.4ºC
Tmax 10%	12.4ºC	Tmax 90%	18.5ºC
Tmax 20%	13.6ºC	Tmax 80%	17.5ºC

Mínimas			
Tmin 1%	-2.8ºC	Tmin 99%	13.8ºC
Tmin 5%	-1.2ºC	Tmin 95%	11.4ºC
Tmin 10%	-0.4ºC	Tmin 90%	9.6ºC
Tmin 20%	0.8ºC	Tmin 80%	7.8ºC

Temperaturas máximas (99%)

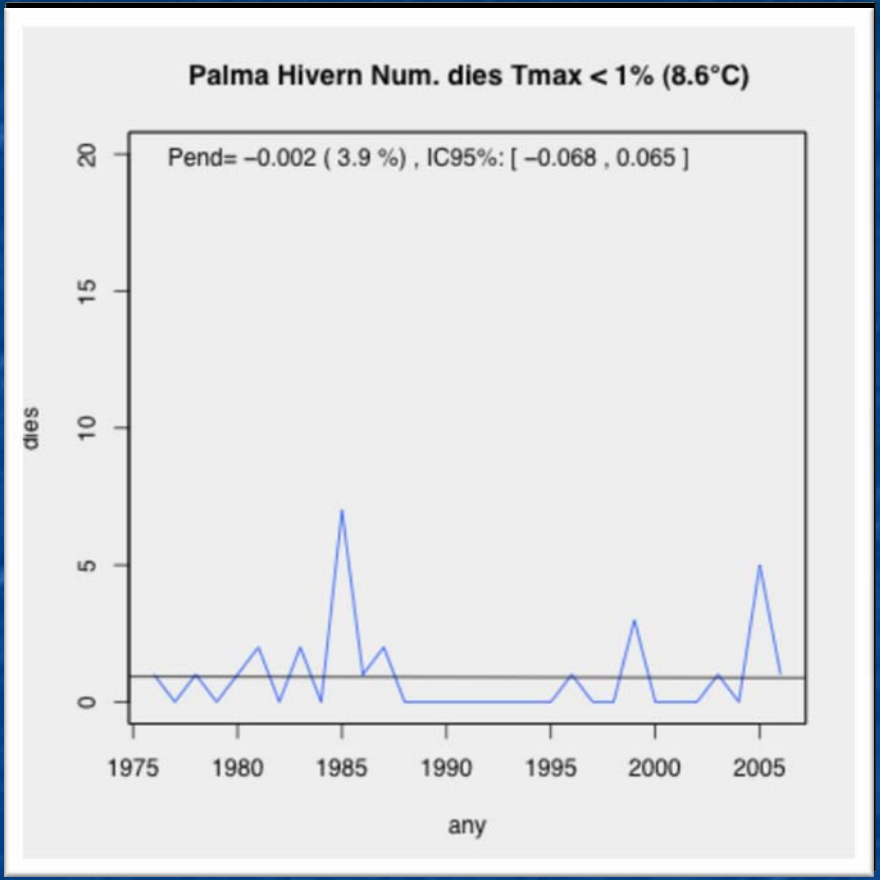

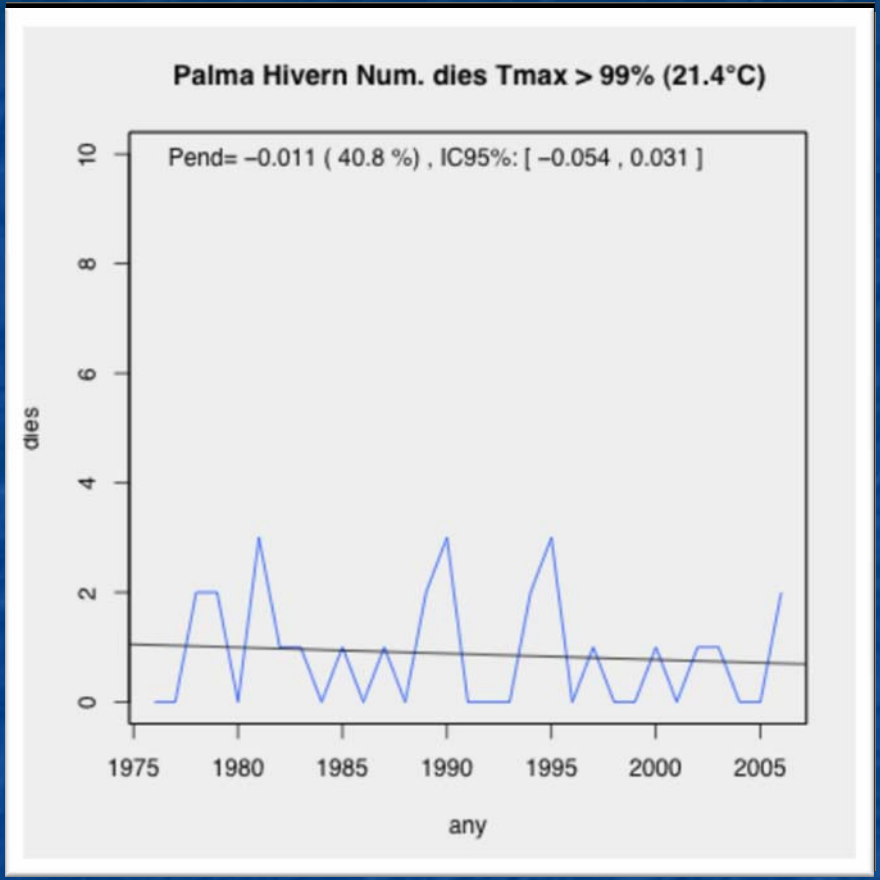

Temperaturas máximas (95%)

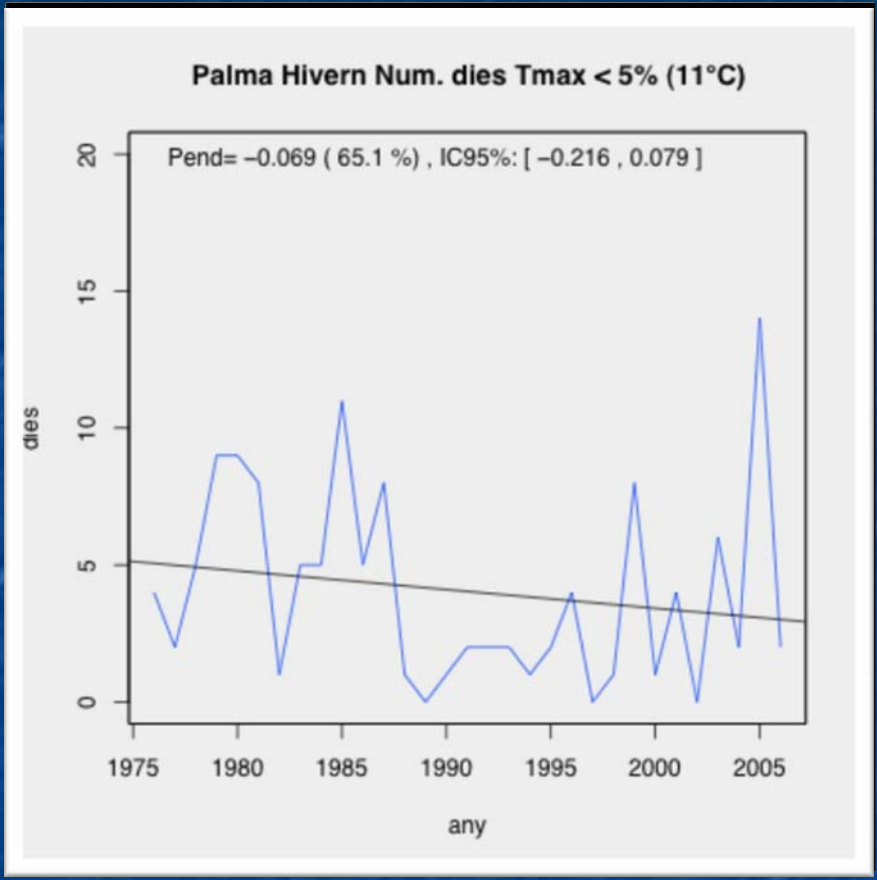

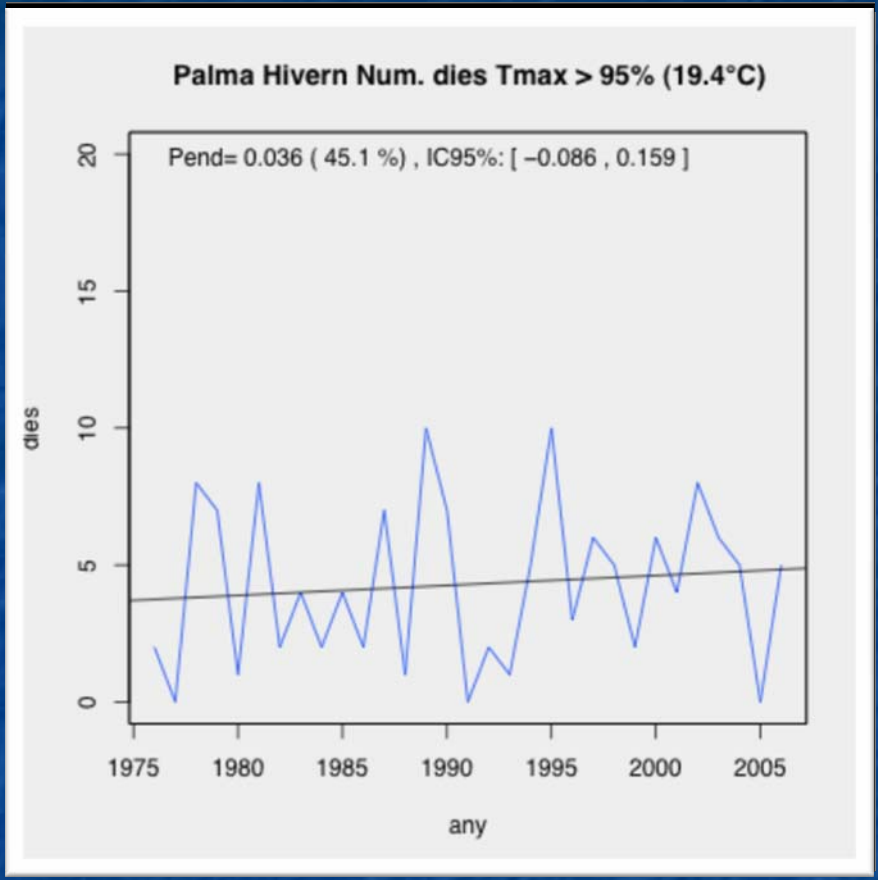

Temperaturas mínimas (99%)

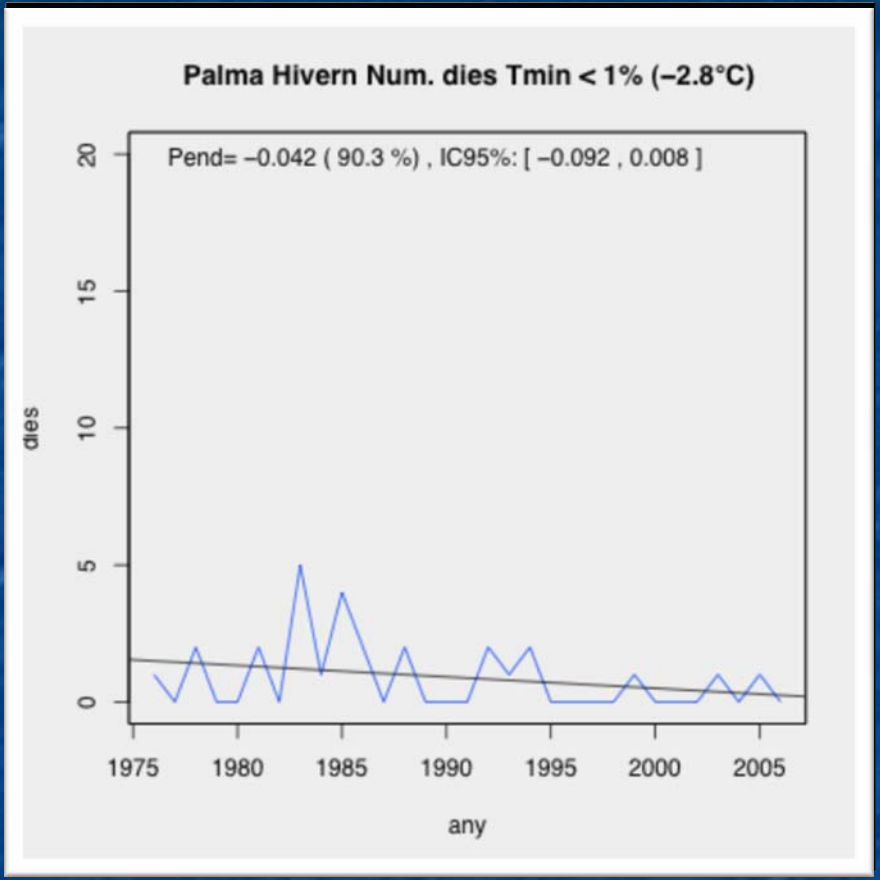

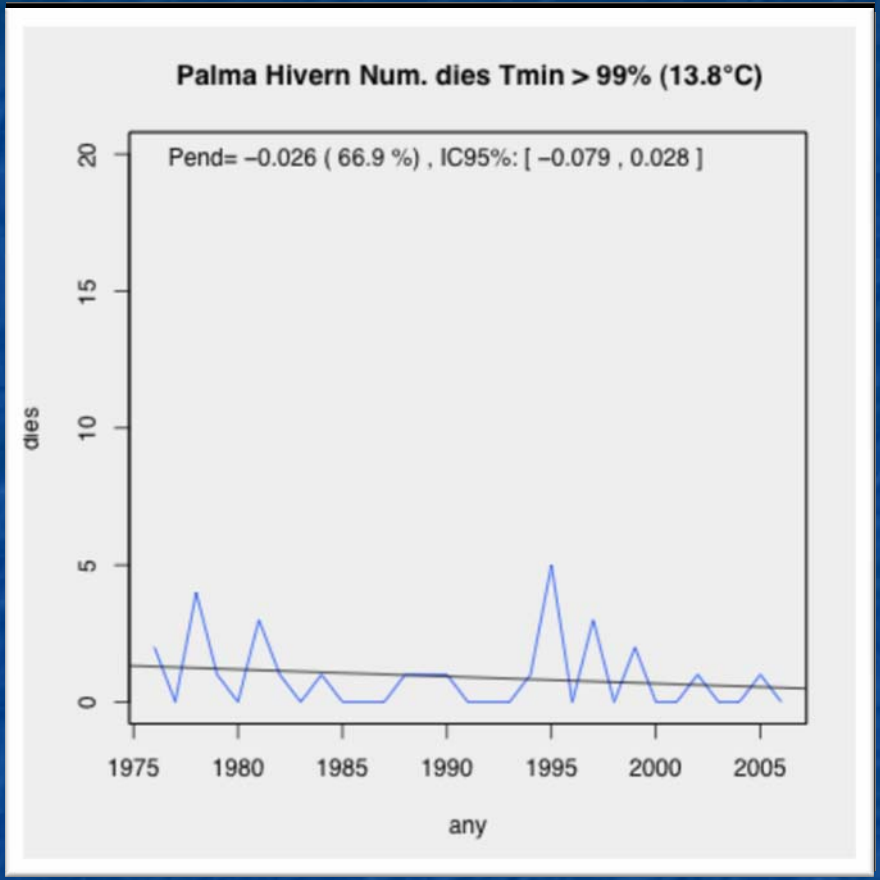

Temperaturas mínimas (95%)

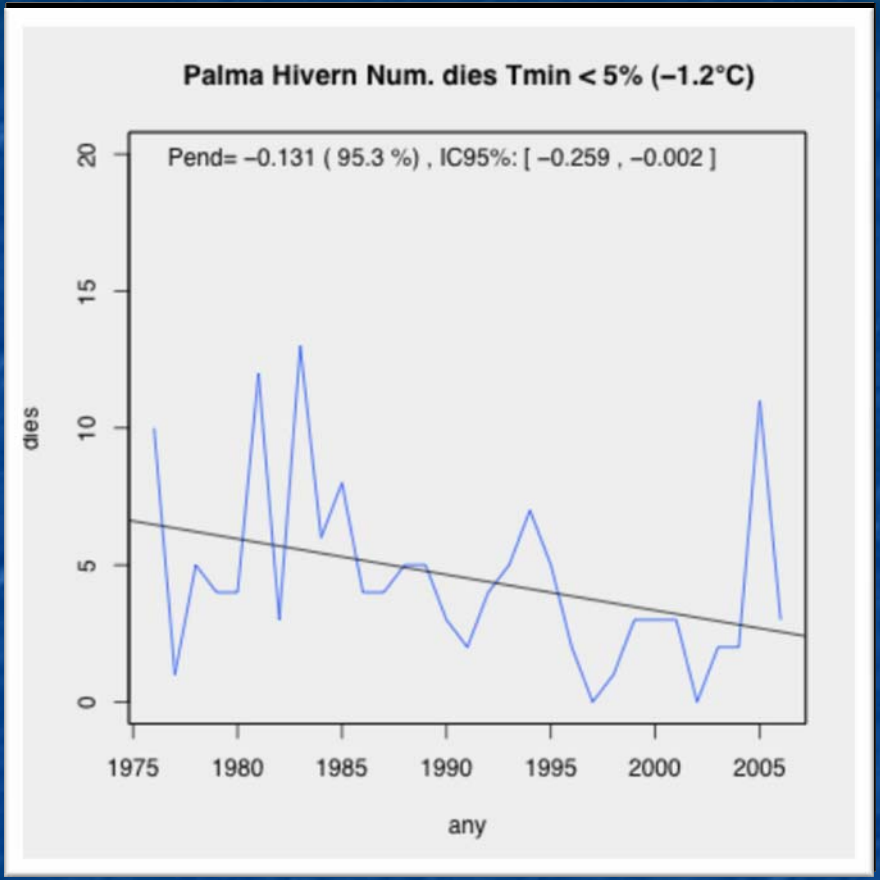

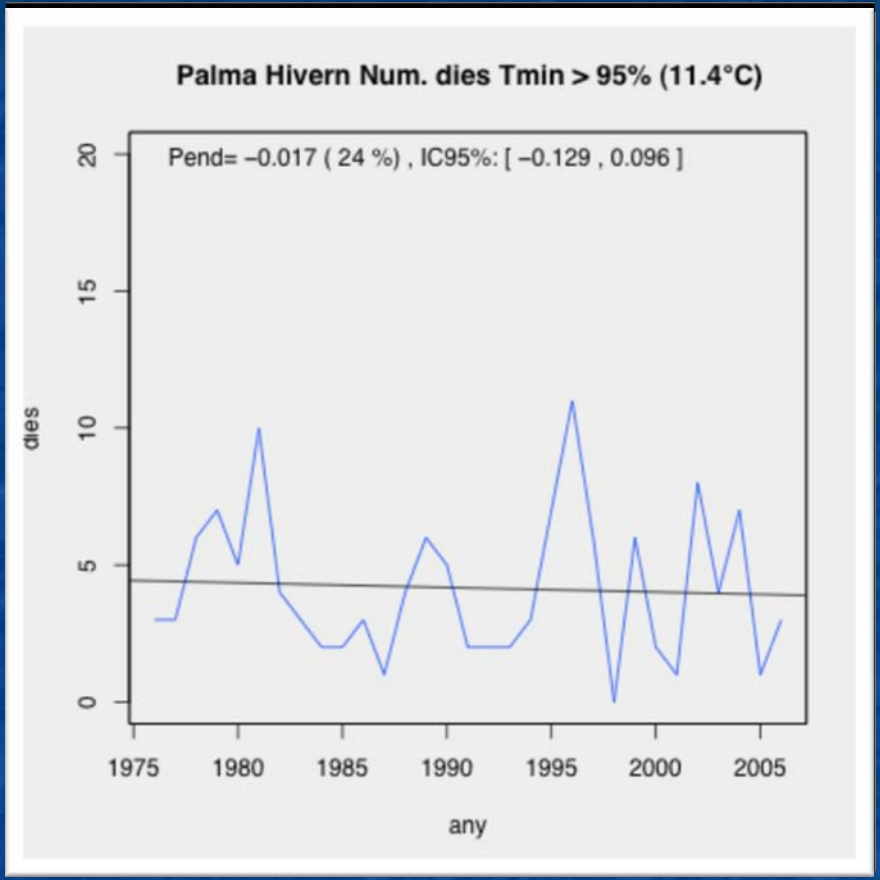

Primavera

Histograma temperaturas máximas

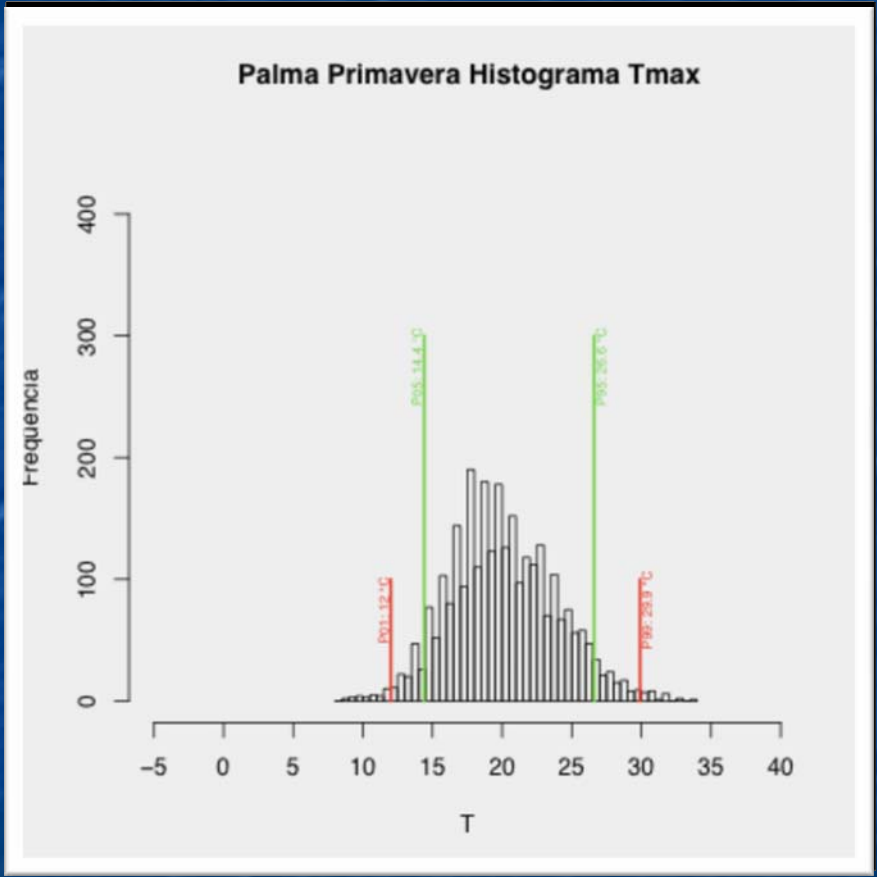

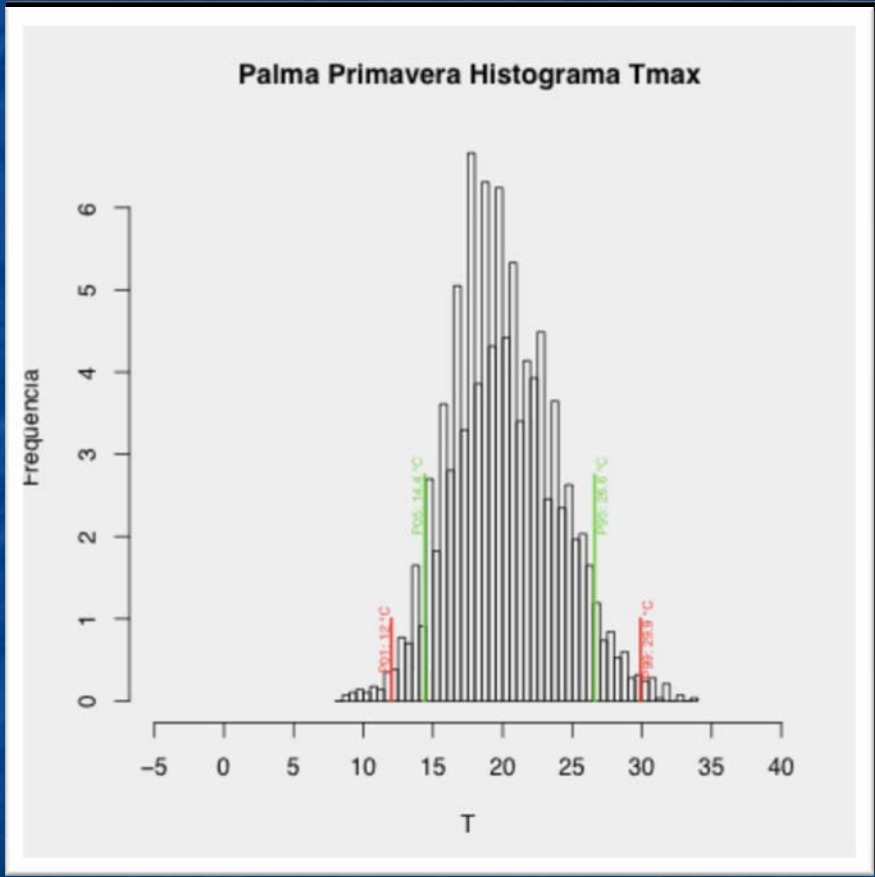

Histograma temperaturas mínimas

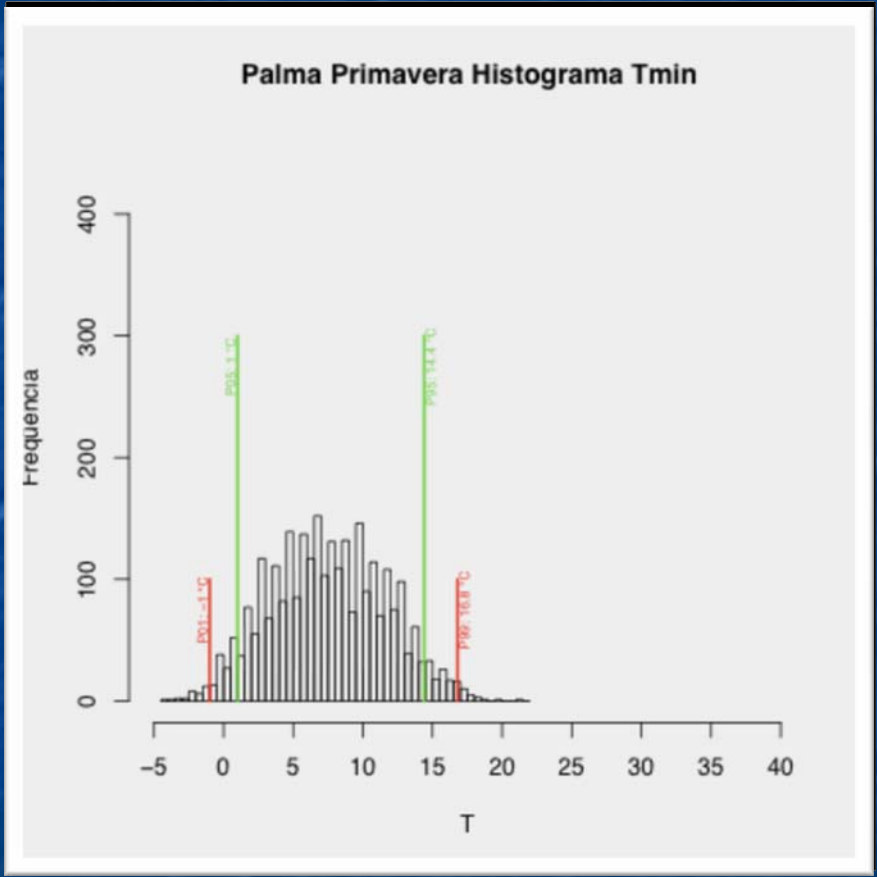

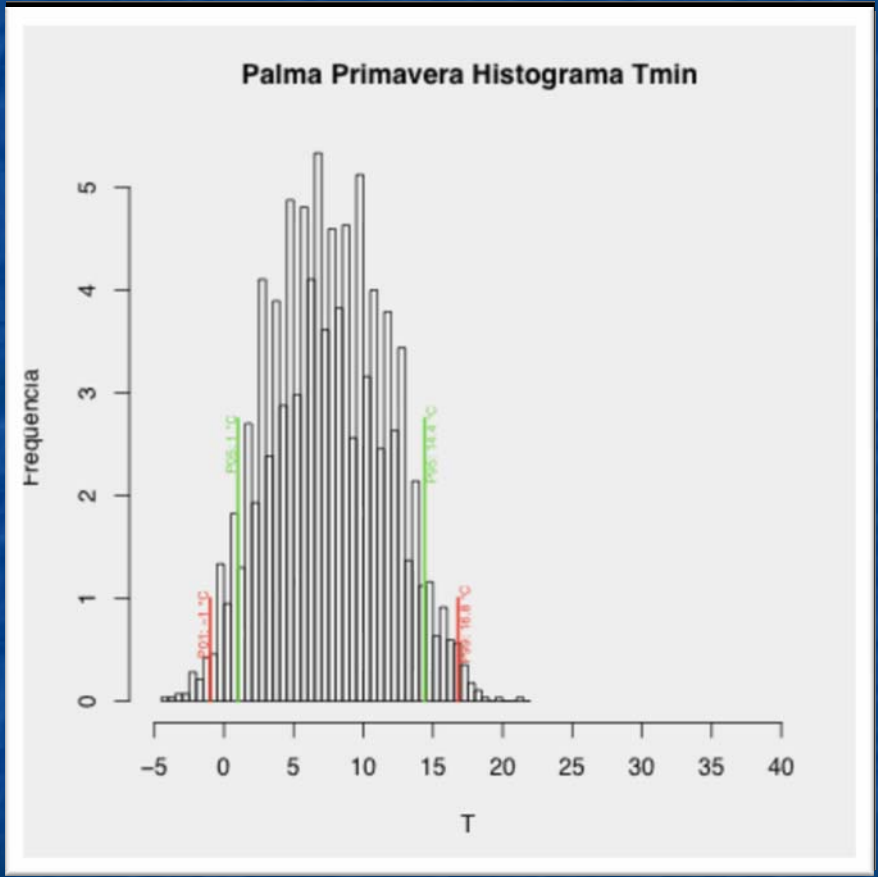

Temperaturas - Extremos

Máximas			
Tmax 1%	12.0ºC	Tmax 99%	29.9ºC
Tmax 5%	14.4ºC	Tmax 95%	26.6ºC
Tmax 10%	15.5ºC	Tmax 90%	25.4ºC
Tmax 20%	17.0ºC	Tmax 80%	23.5ºC

Mínimas			
Tmin 1%	-1.0ºC	Tmin 99%	16.8ºC
Tmin 5%	1.0ºC	Tmin 95%	14.4ºC
Tmin 10%	2.2ºC	Tmin 90%	13.0ºC
Tmin 20%	3.8ºC	Tmin 80%	11.4ºC

Temperaturas máximas (99%)

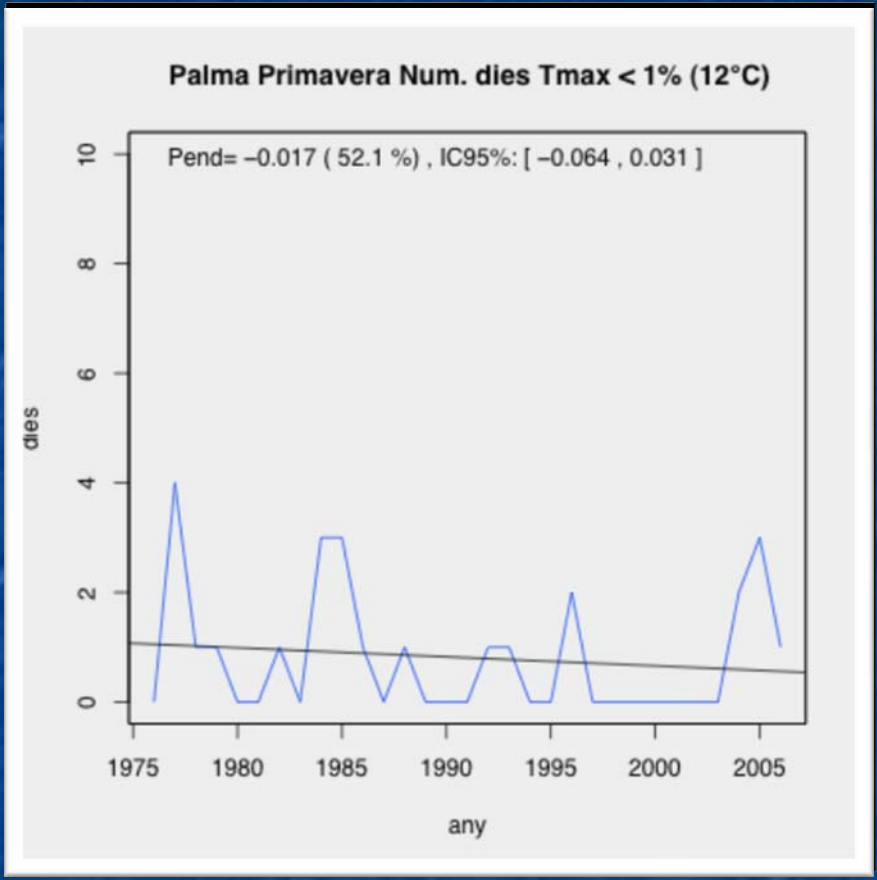

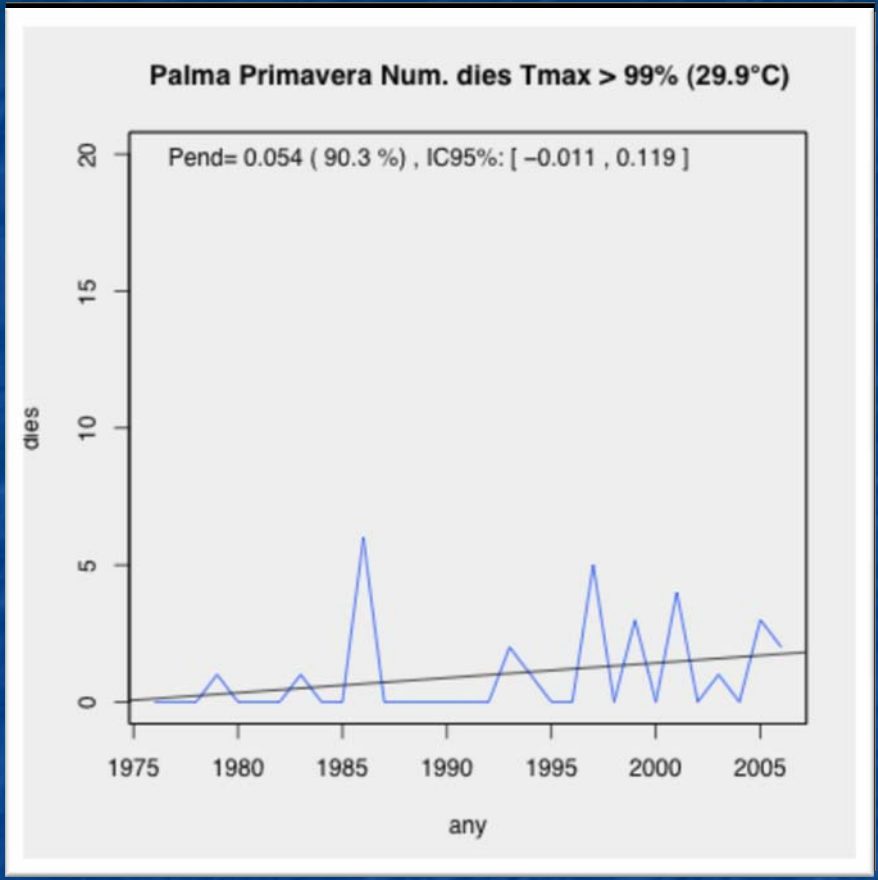

Temperaturas máximas (95%)

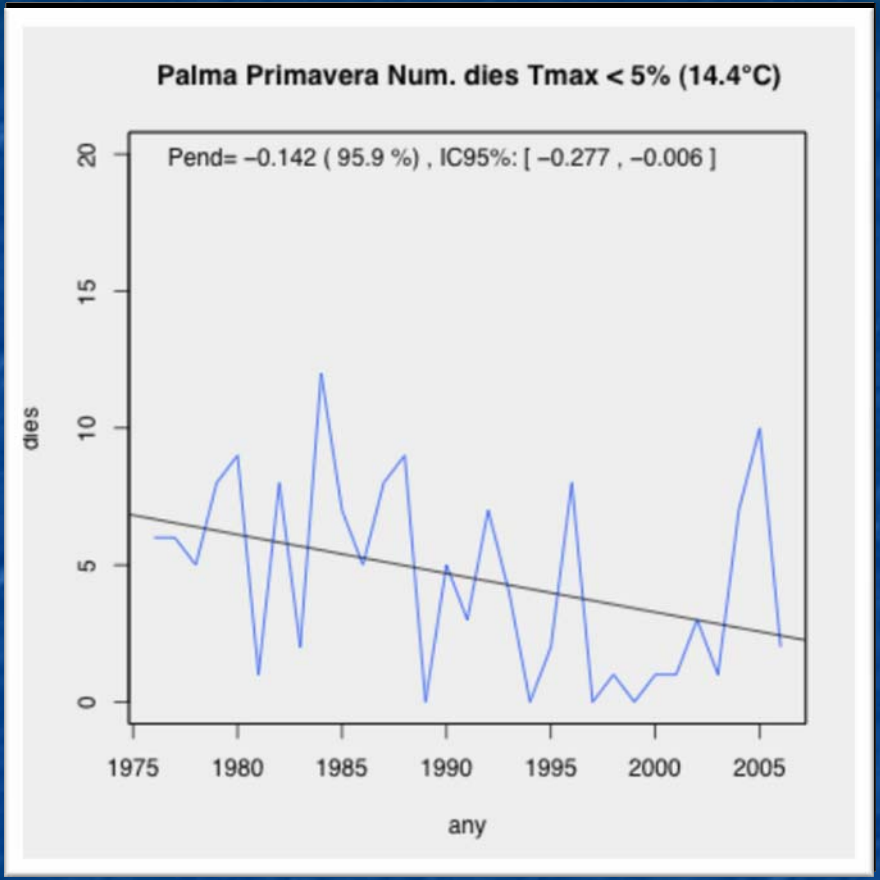

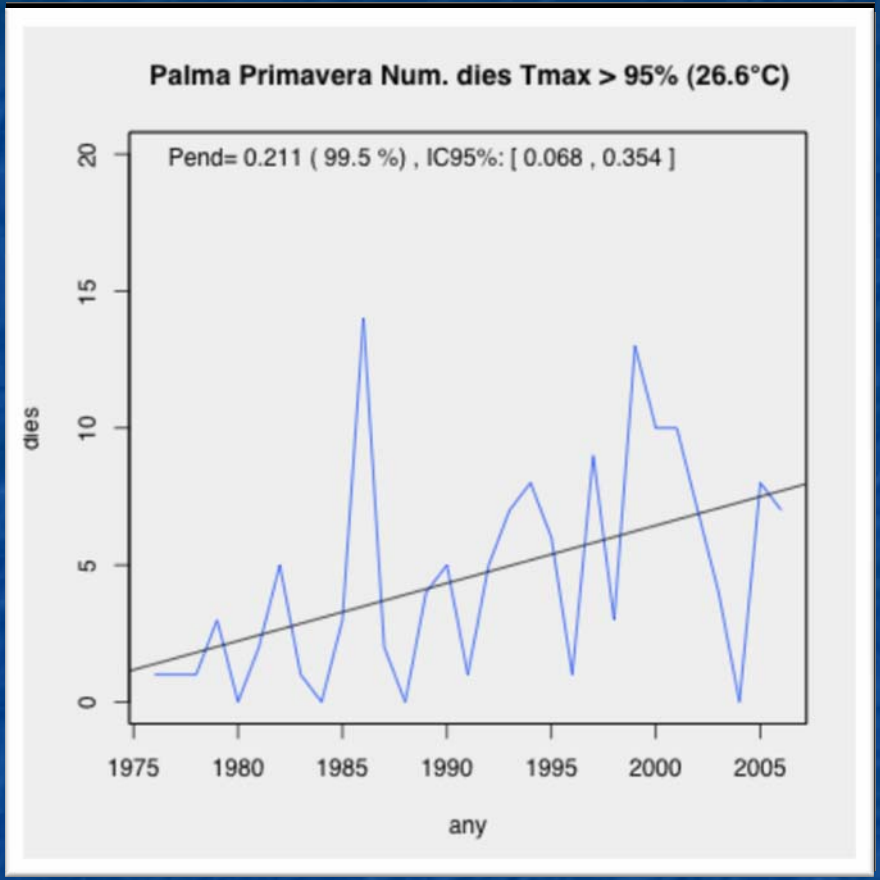

Temperaturas mínimas (99%)

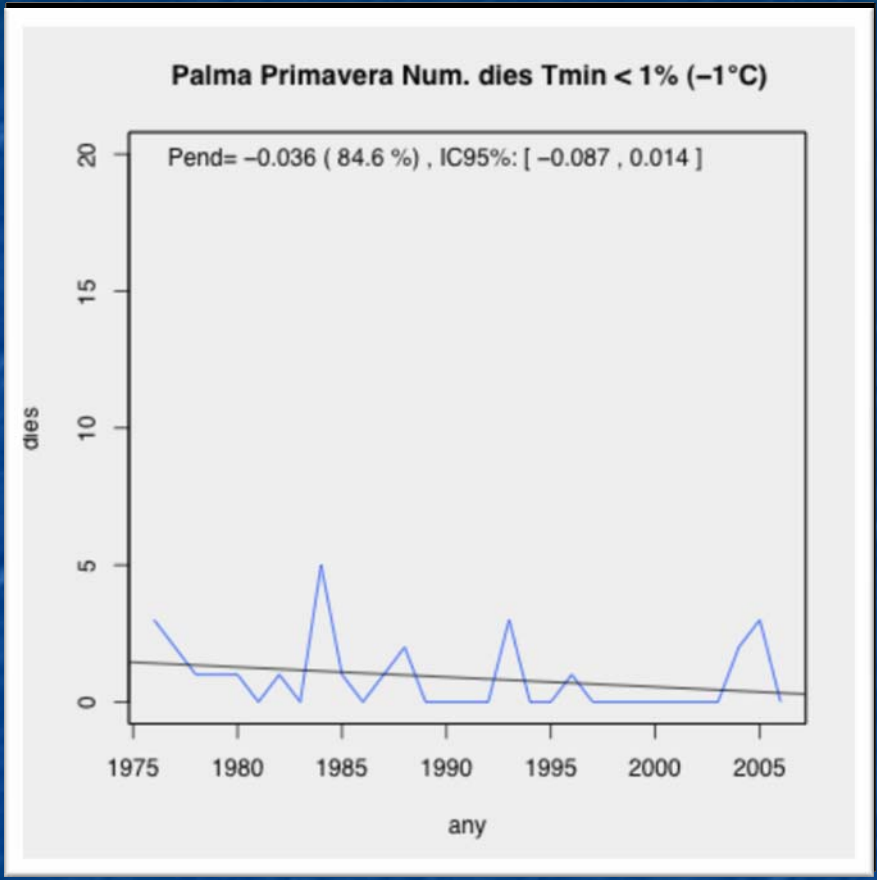

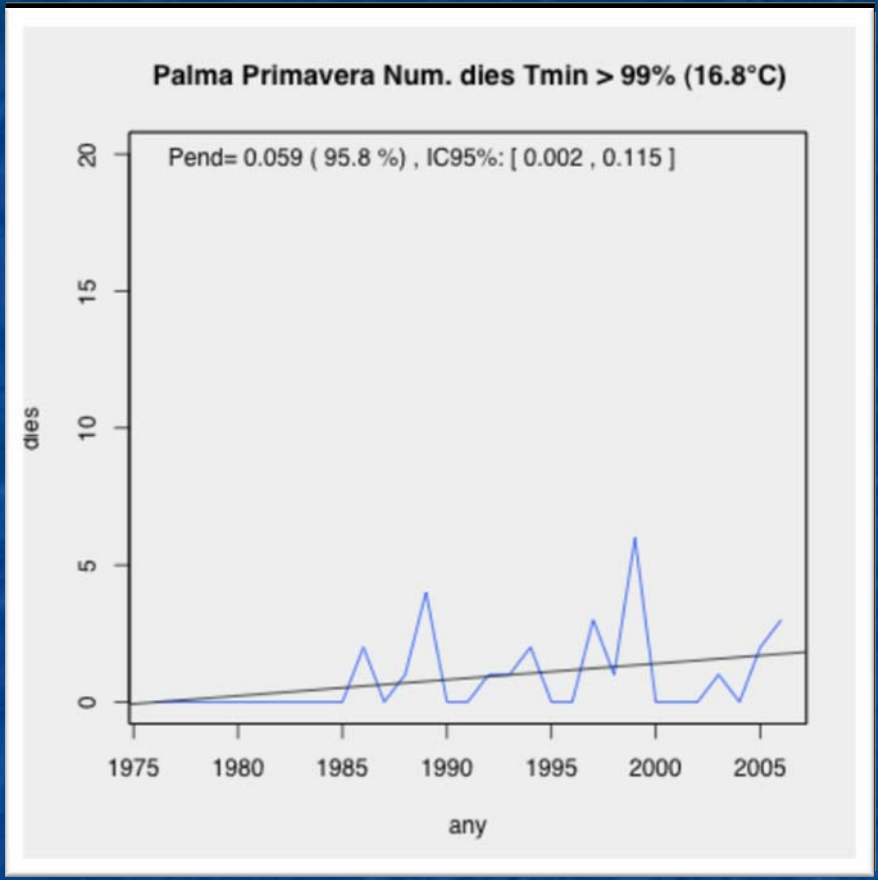

Temperaturas mínimas (95%)

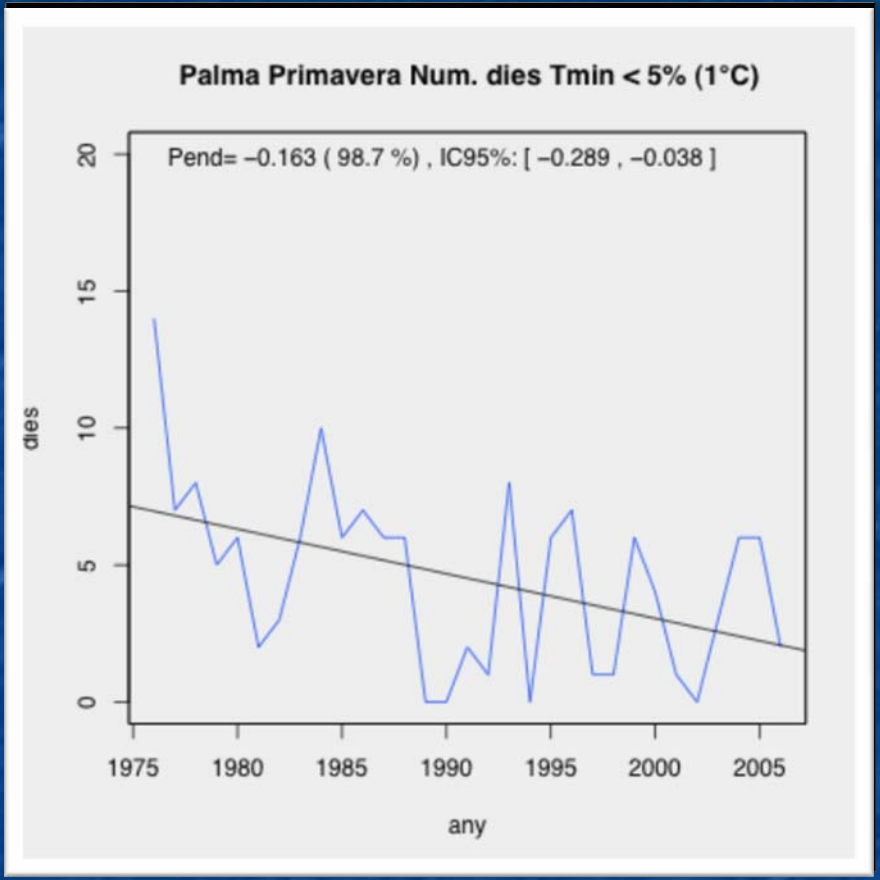

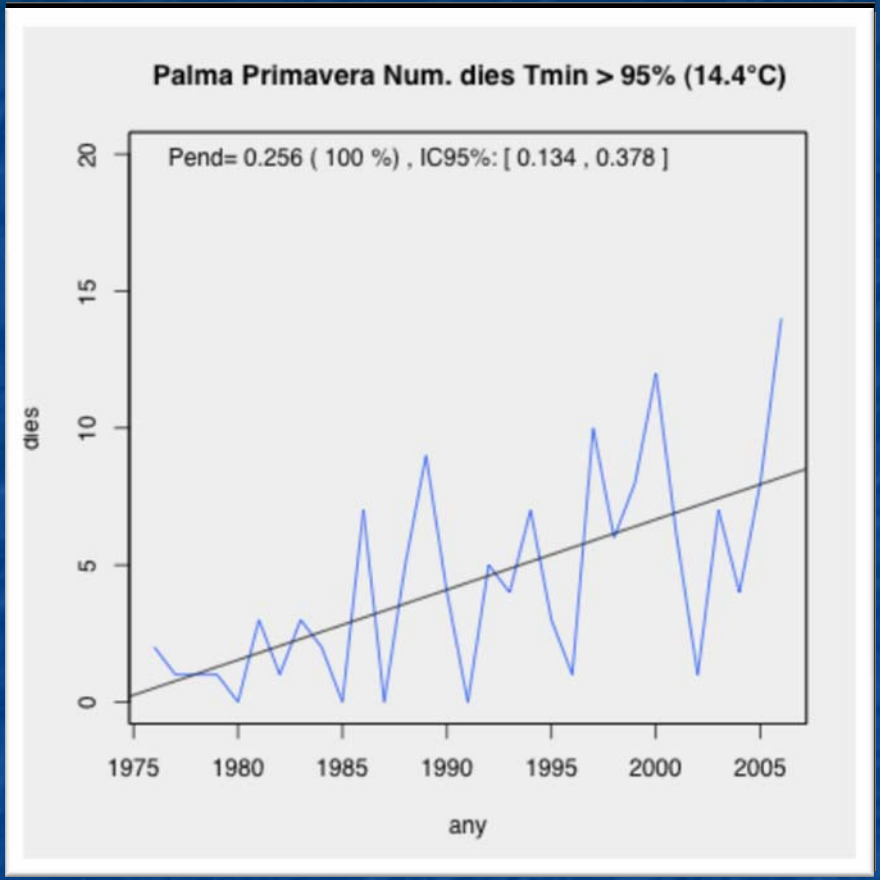

Verano

Histograma temperaturas máximas

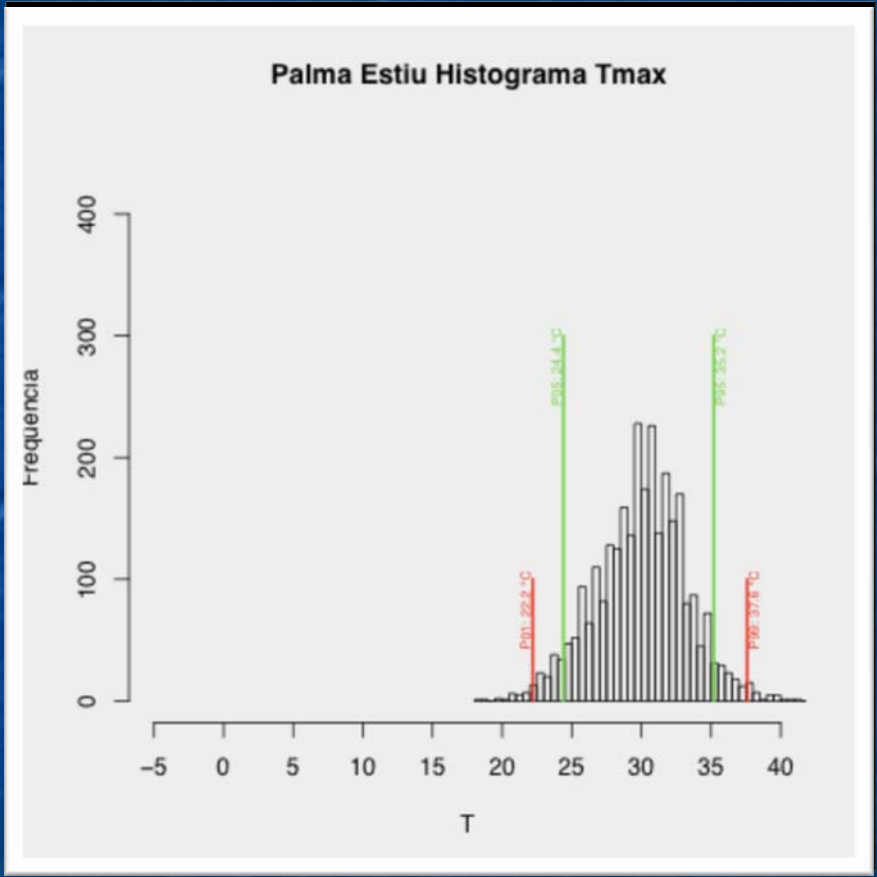

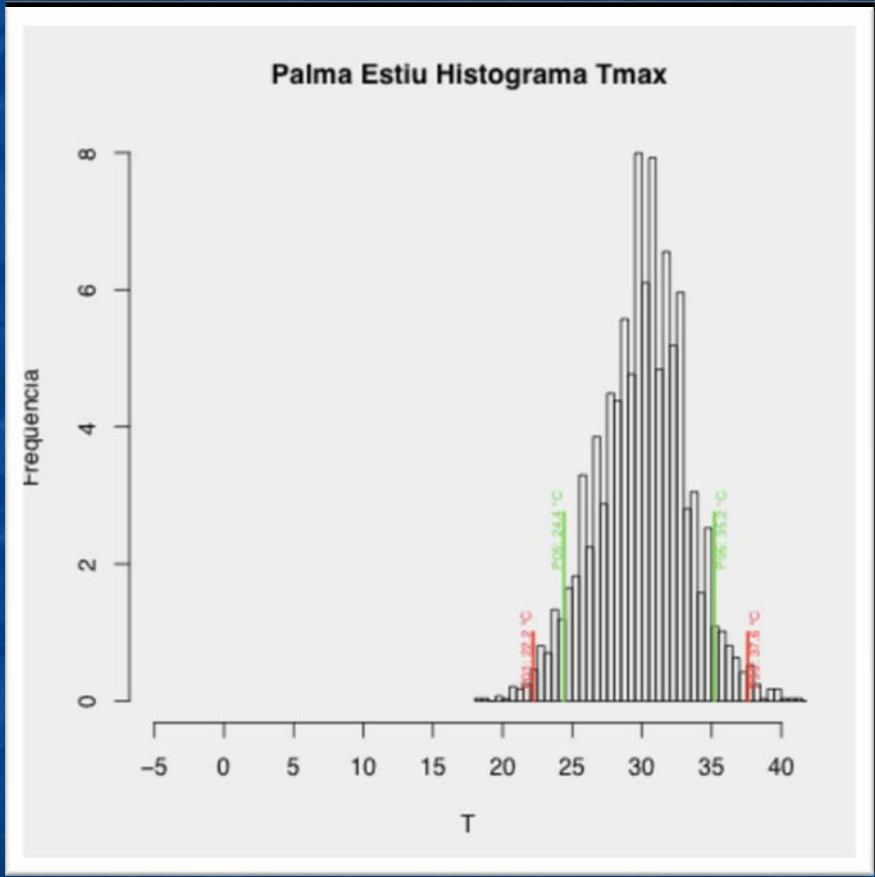

Histograma temperaturas mínimas

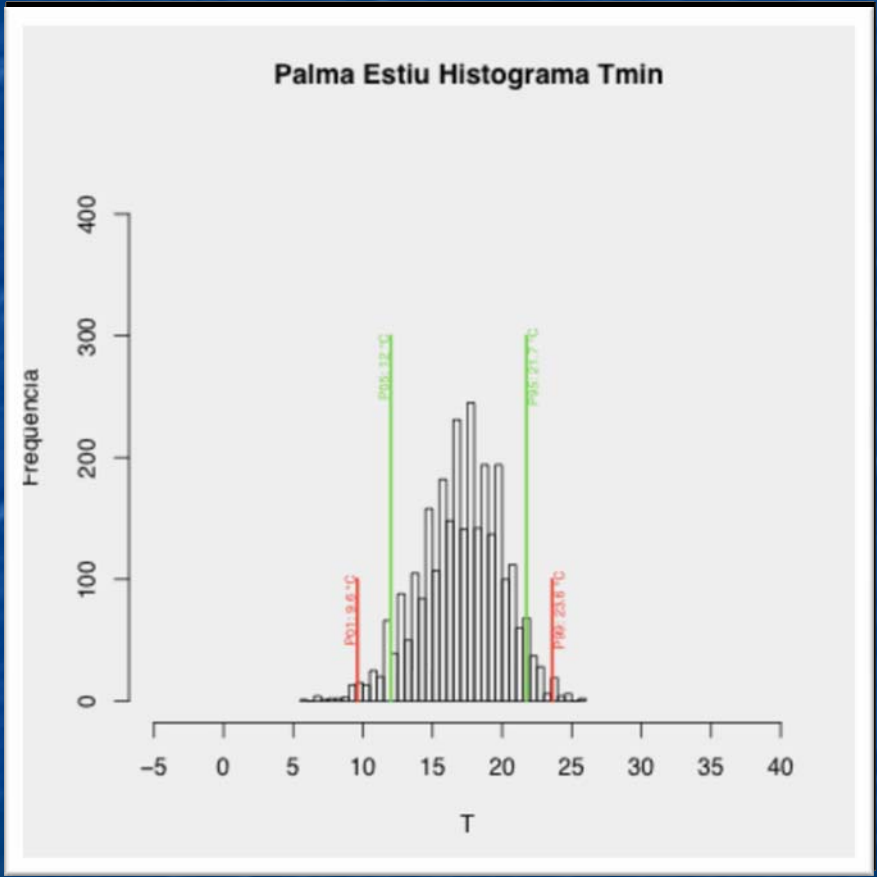

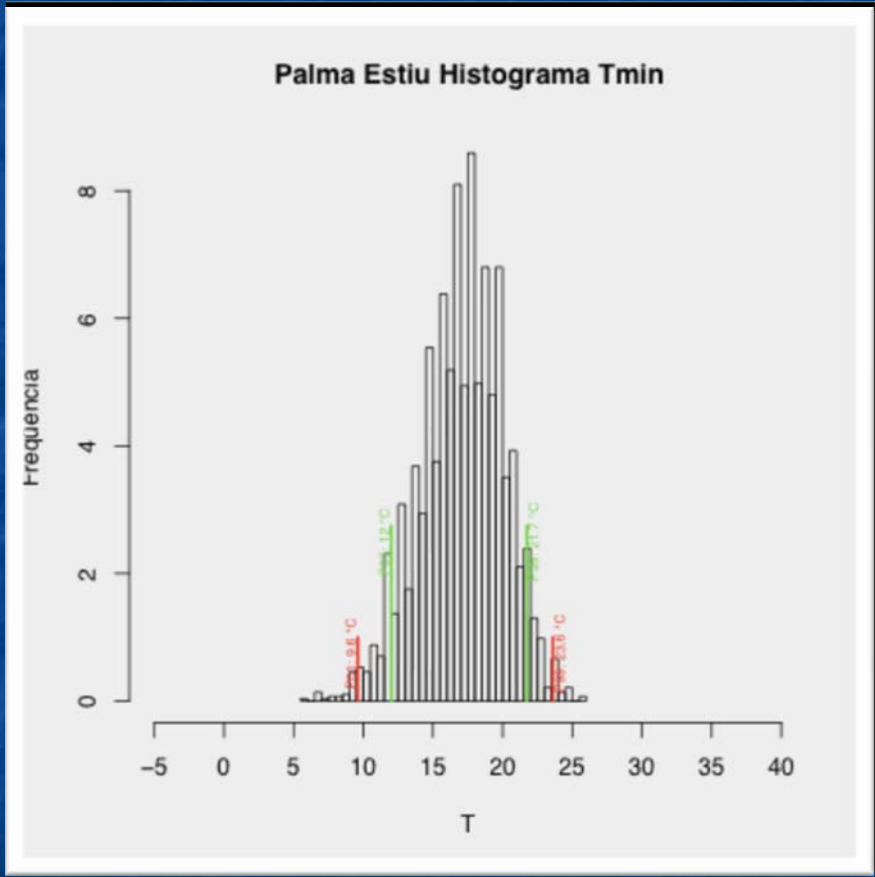

Temperaturas - Extremos

Màximes			
Tmax 1%	22.2ºC	Tmax 99%	37.6ºC
Tmax 5%	24.4ºC	Tmax 95%	35.2ºC
Tmax 10%	25.6ºC	Tmax 90%	34.0ºC
Tmax 20%	27.4ºC	Tmax 80%	32.6ºC

Mínimes			
Tmin 1%	9.6ºC	Tmin 99%	23.6ºC
Tmin 5%	12.0ºC	Tmin 95%	21.7ºC
Tmin 10%	13.0ºC	Tmin 90%	20.8ºC
Tmin 20%	14.6ºC	Tmin 80%	19.8ºC

Temperaturas máximas (99%)

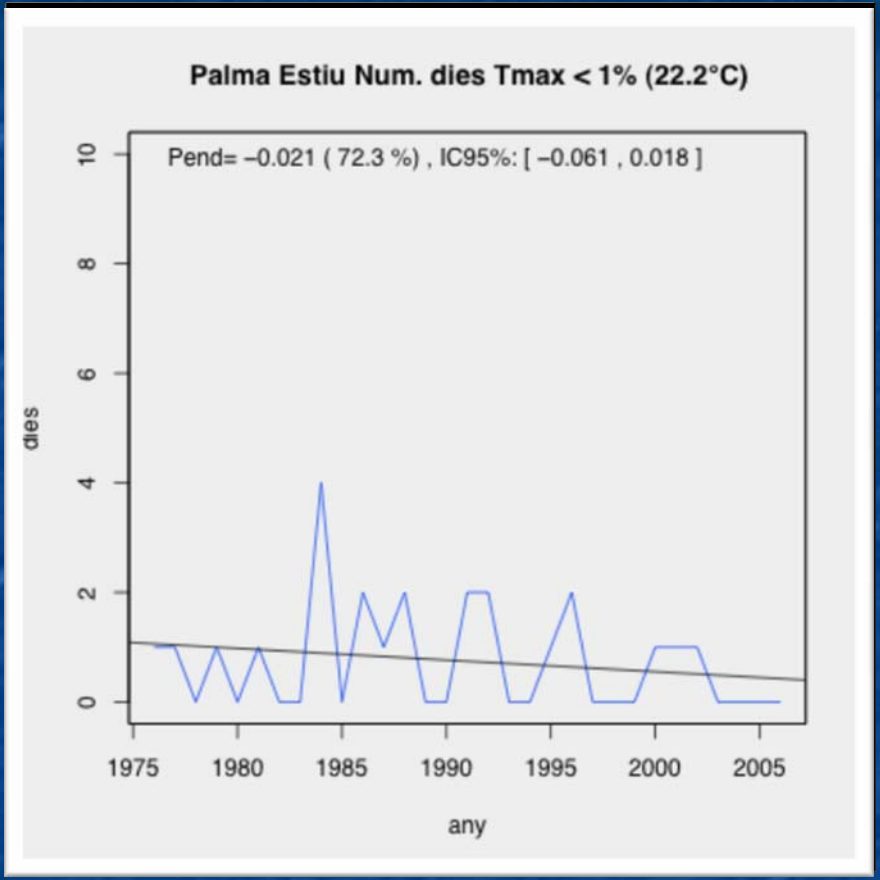

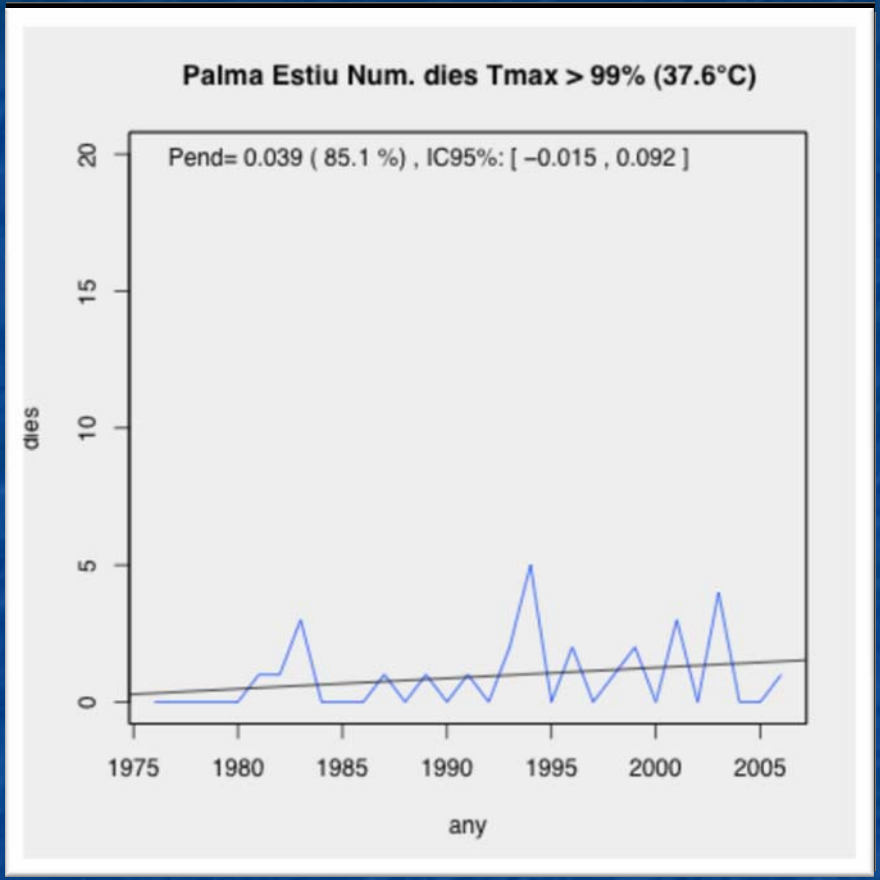

Temperaturas máximas (95%)

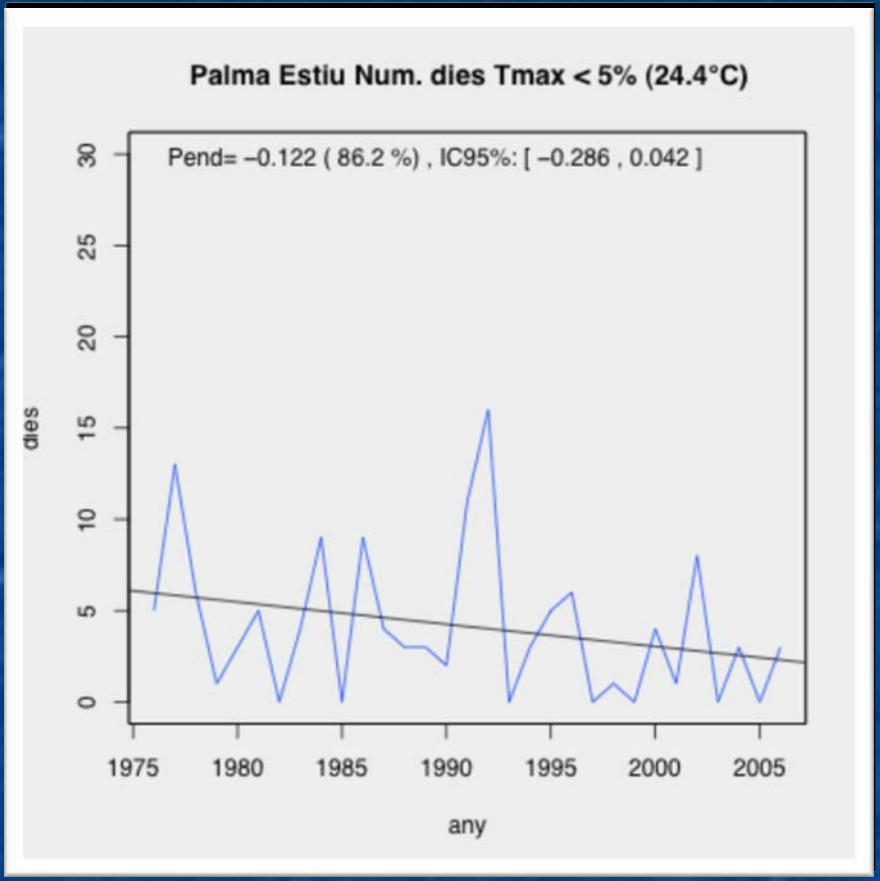

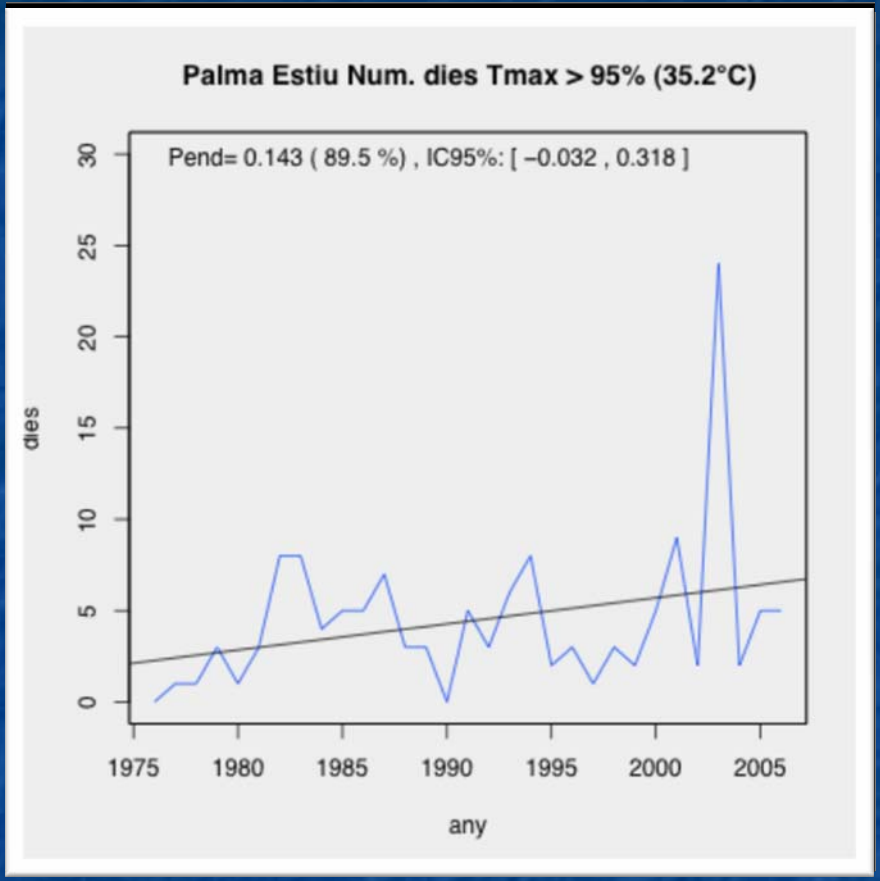

Temperaturas mínimas (99%)

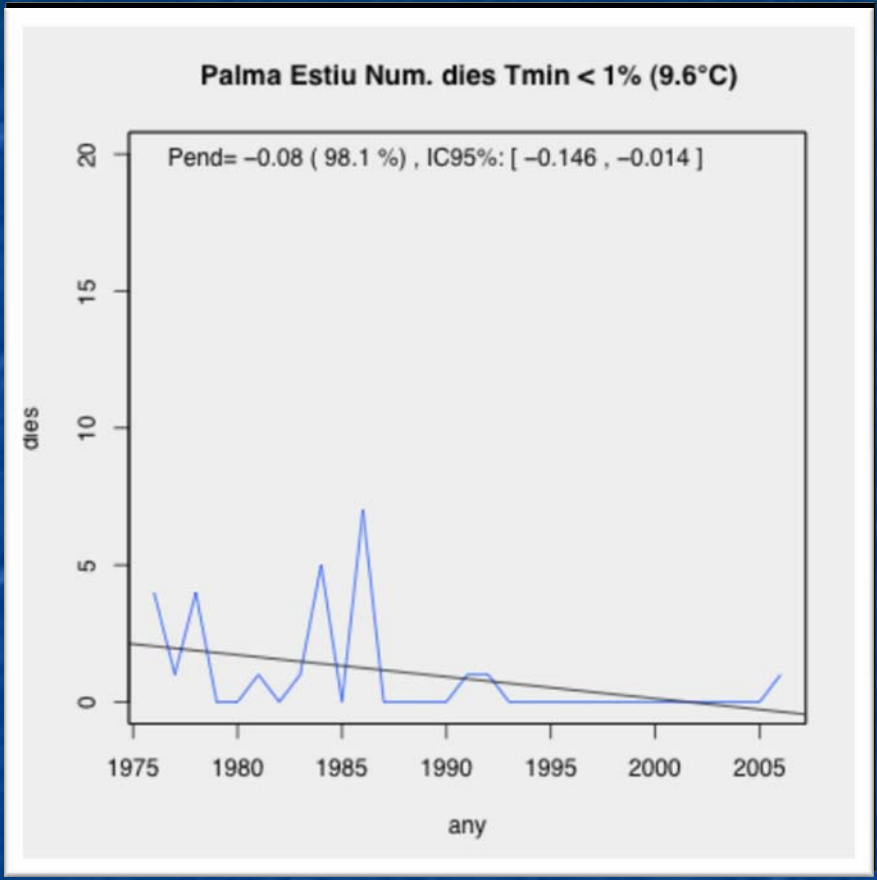

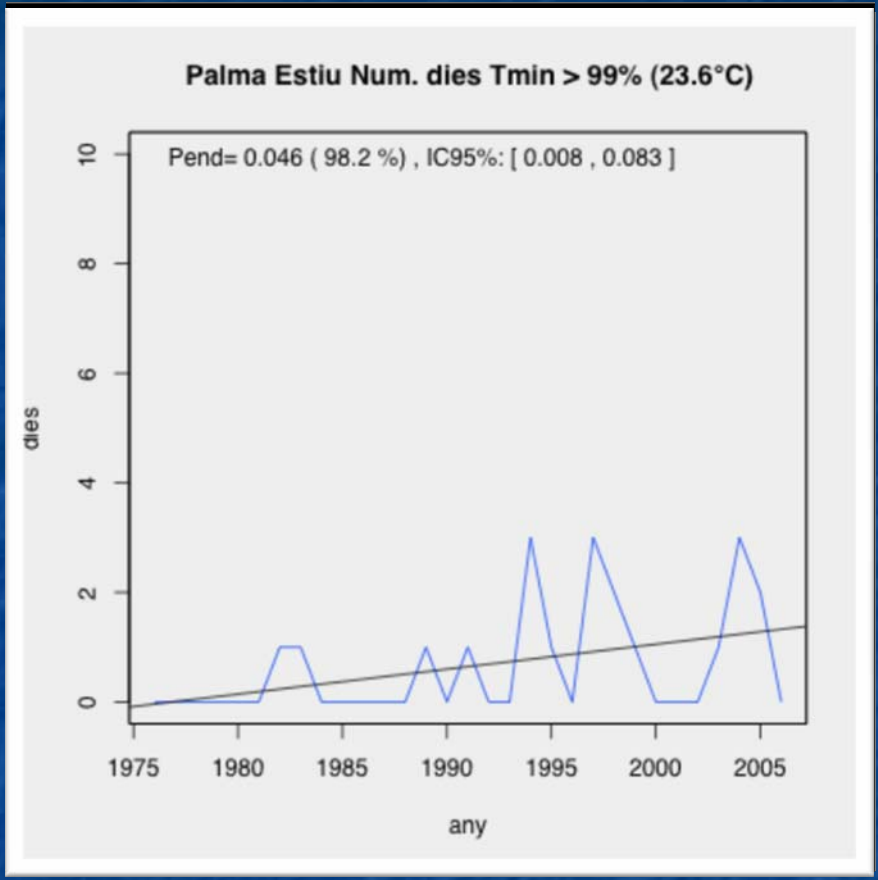

Temperaturas mínimas (95%)

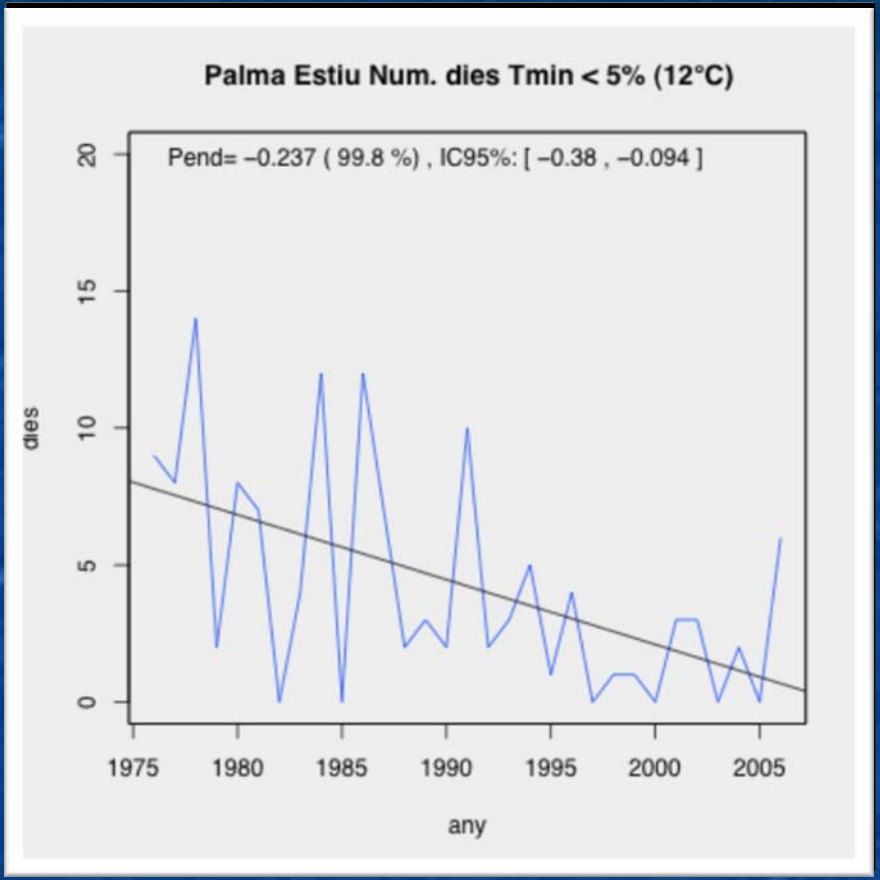

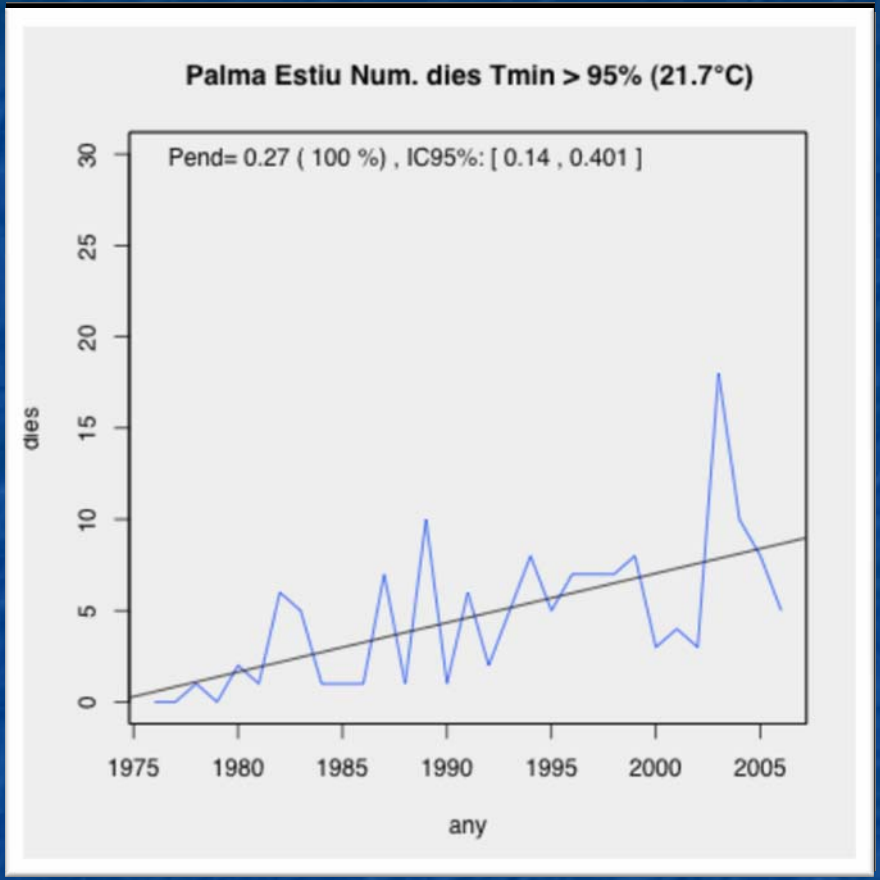

Otoño

Histograma temperaturas máximas

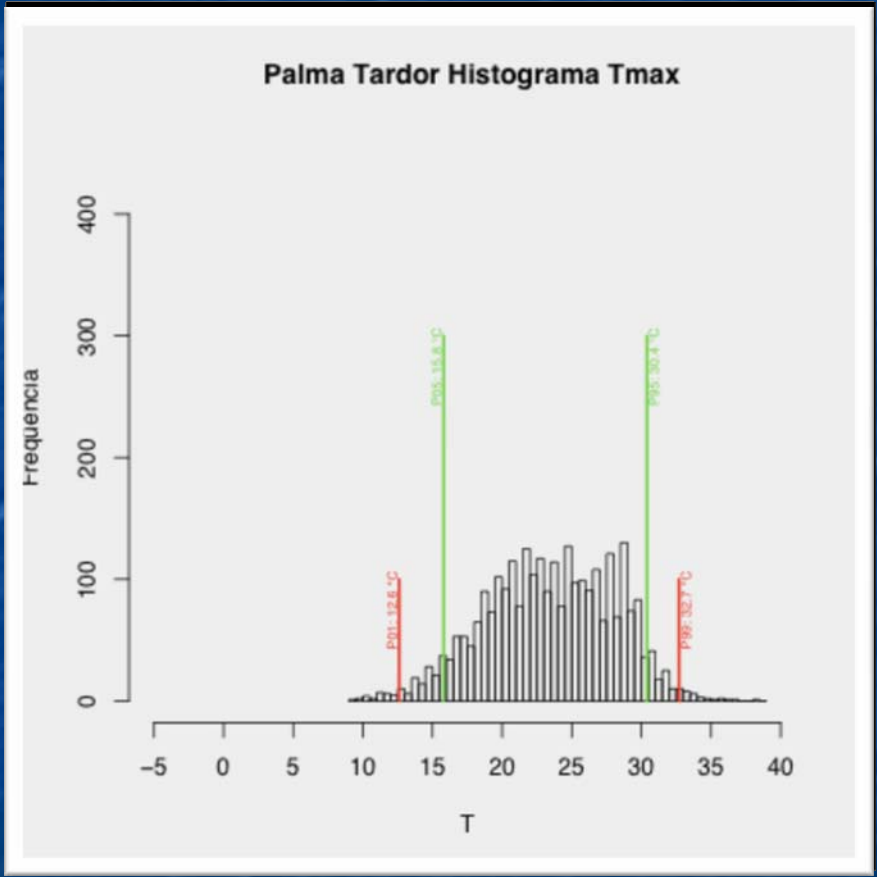

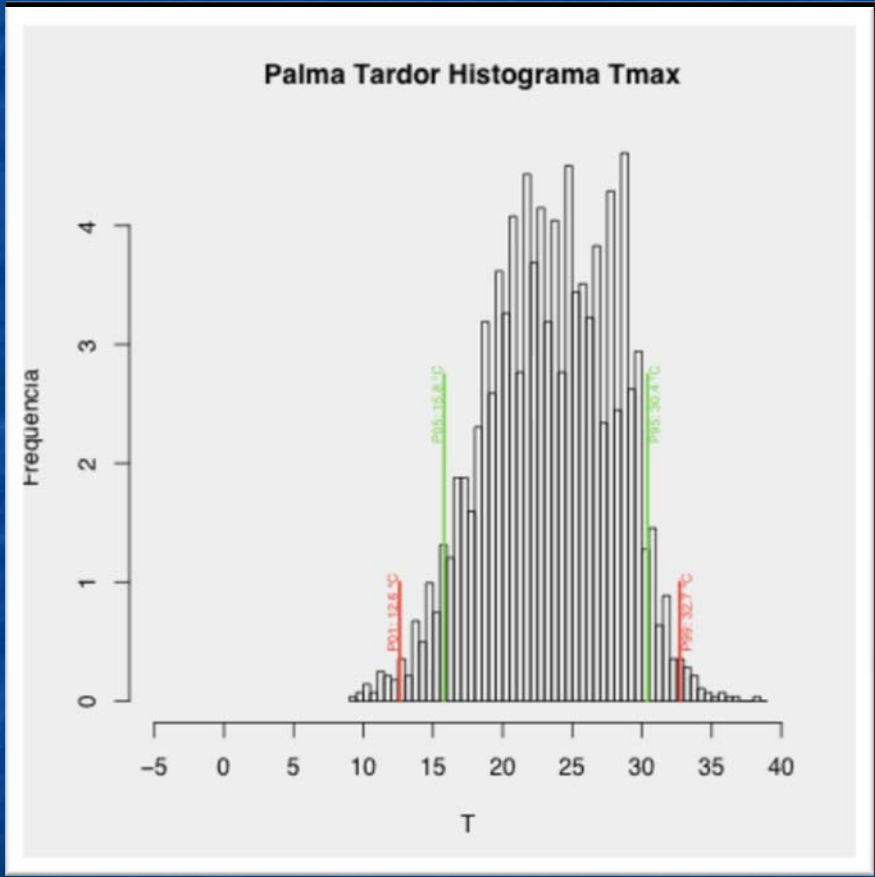

Histograma temperaturas mínimas

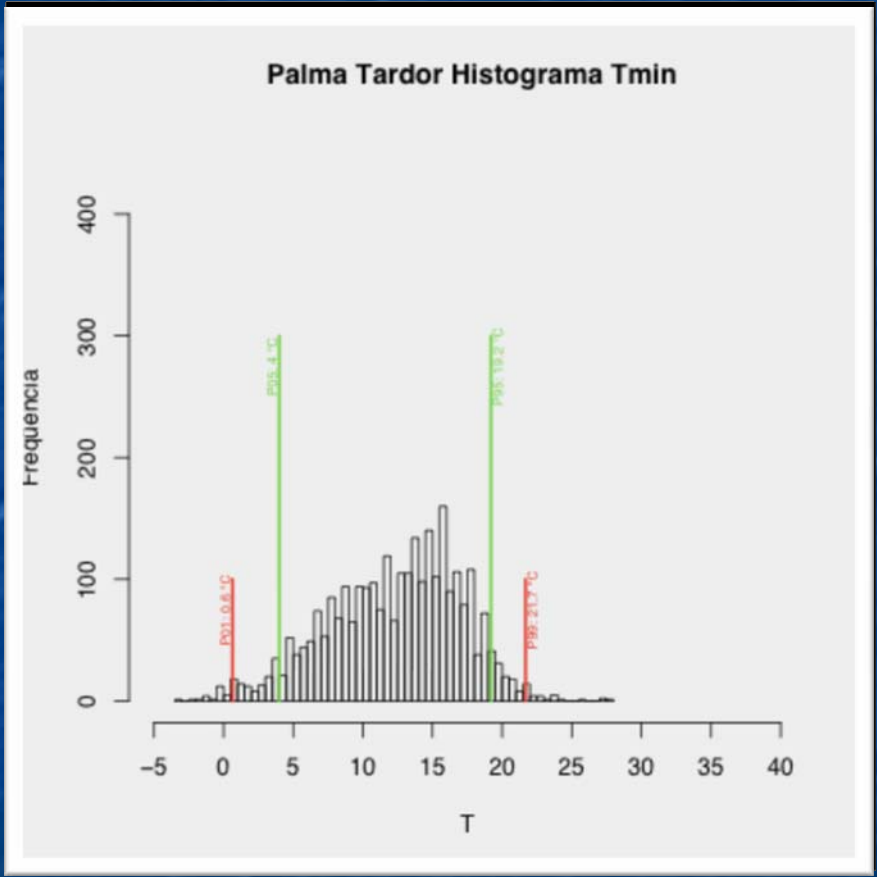

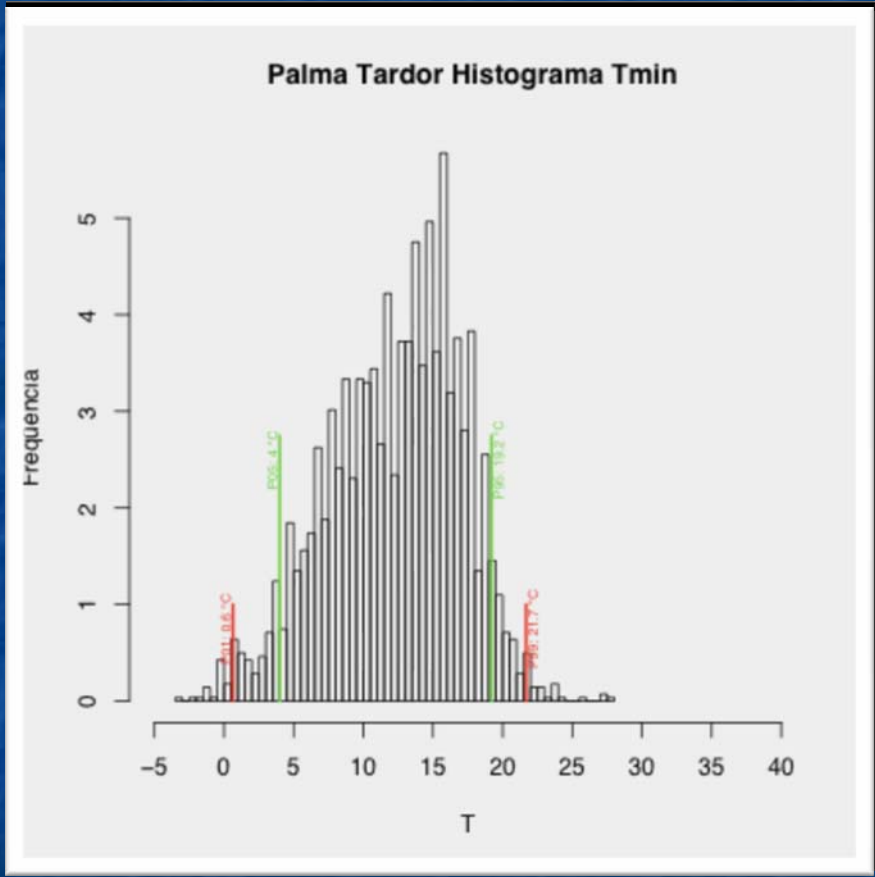

Temperaturas - Extremos

Màximes			
Tmax 1%	12.6ºC	Tmax 99%	32.7ºC
Tmax 5%	15.8ºC	Tmax 95%	30.4ºC
Tmax 10%	17.4ºC	Tmax 90%	29.4ºC
Tmax 20%	19.5ºC	Tmax 80%	28.0ºC

Mínimes			
Tmin 1%	0.6ºC	Tmin 99%	21.7ºC
Tmin 5%	4.0ºC	Tmin 95%	19.2ºC
Tmin 10%	5.8ºC	Tmin 90%	18.0ºC
Tmin 20%	8.2ºC	Tmin 80%	16.5ºC

Temperaturas máximas (99%)

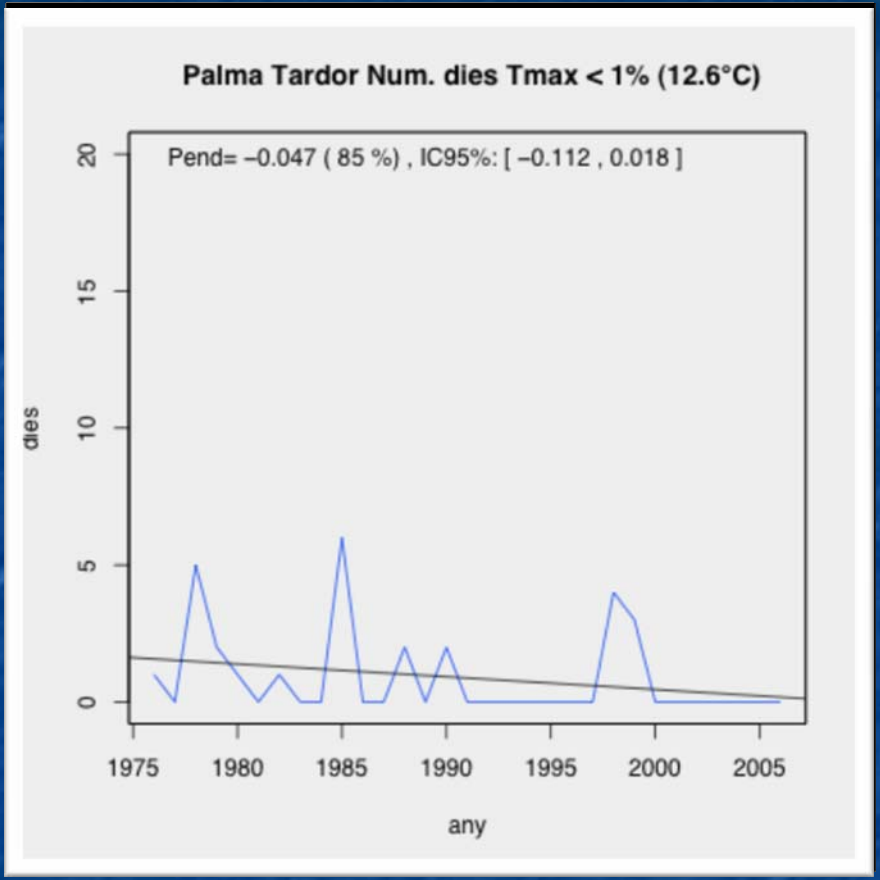

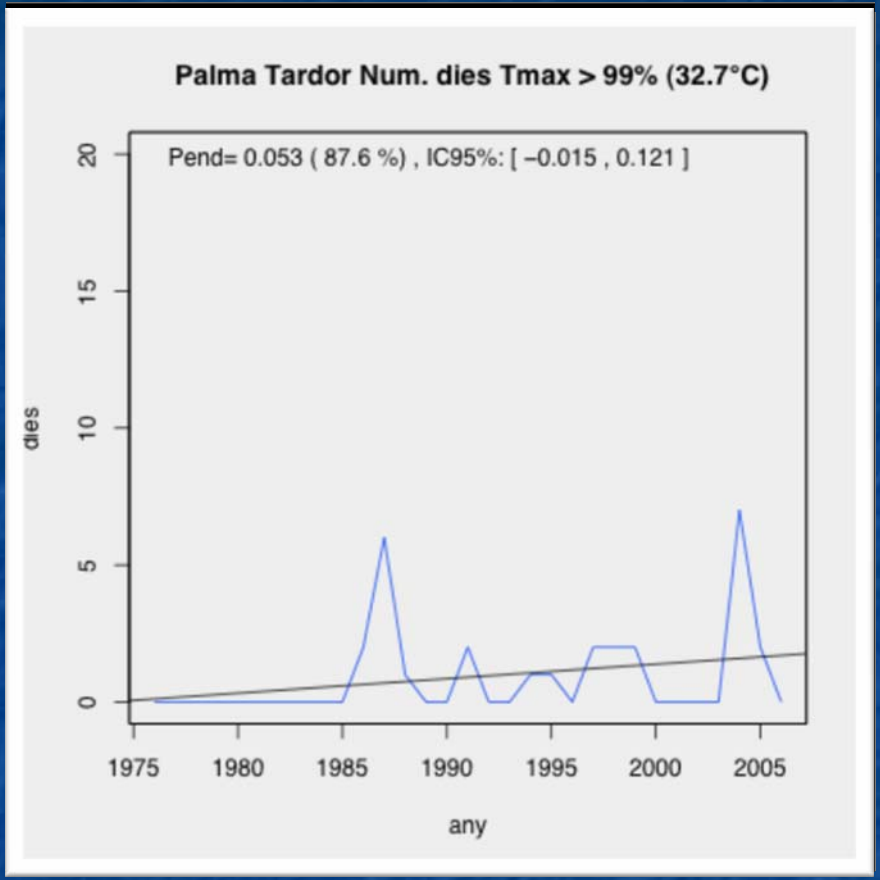

Temperaturas máximas (95%)

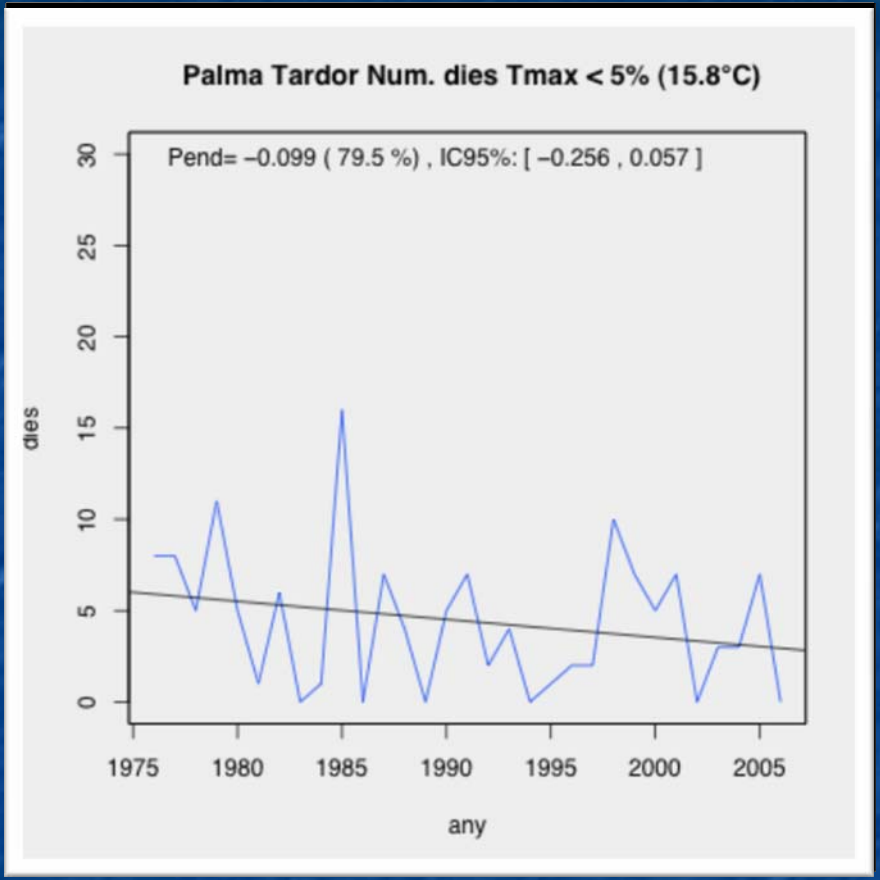

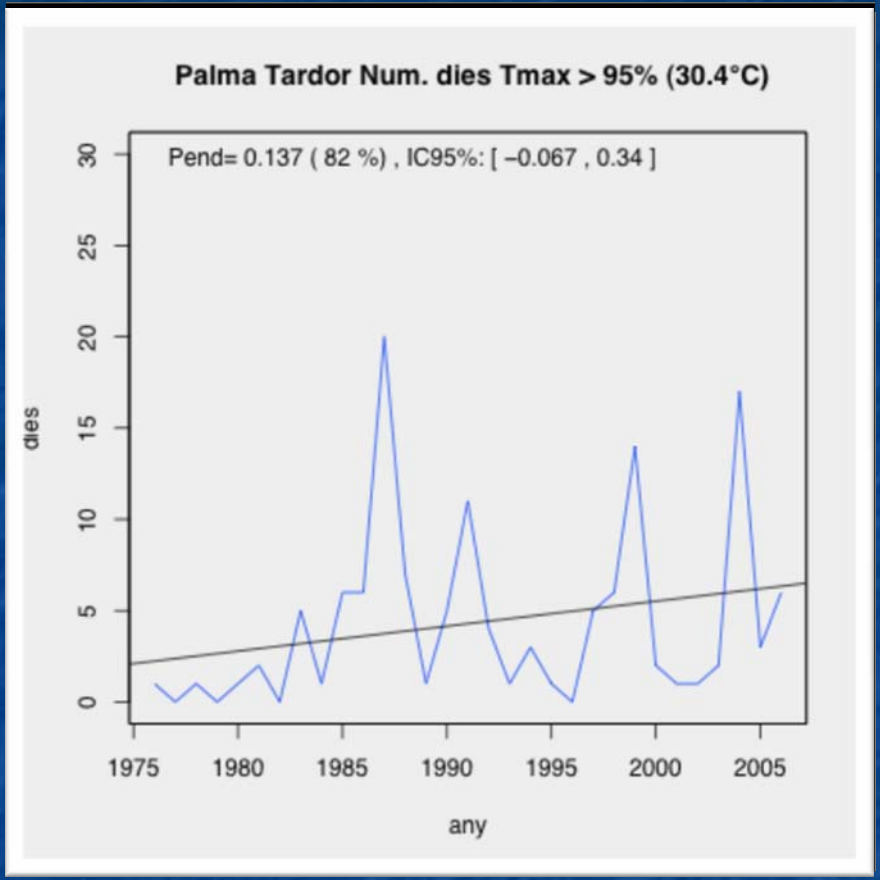

Temperaturas mínimas (99%)

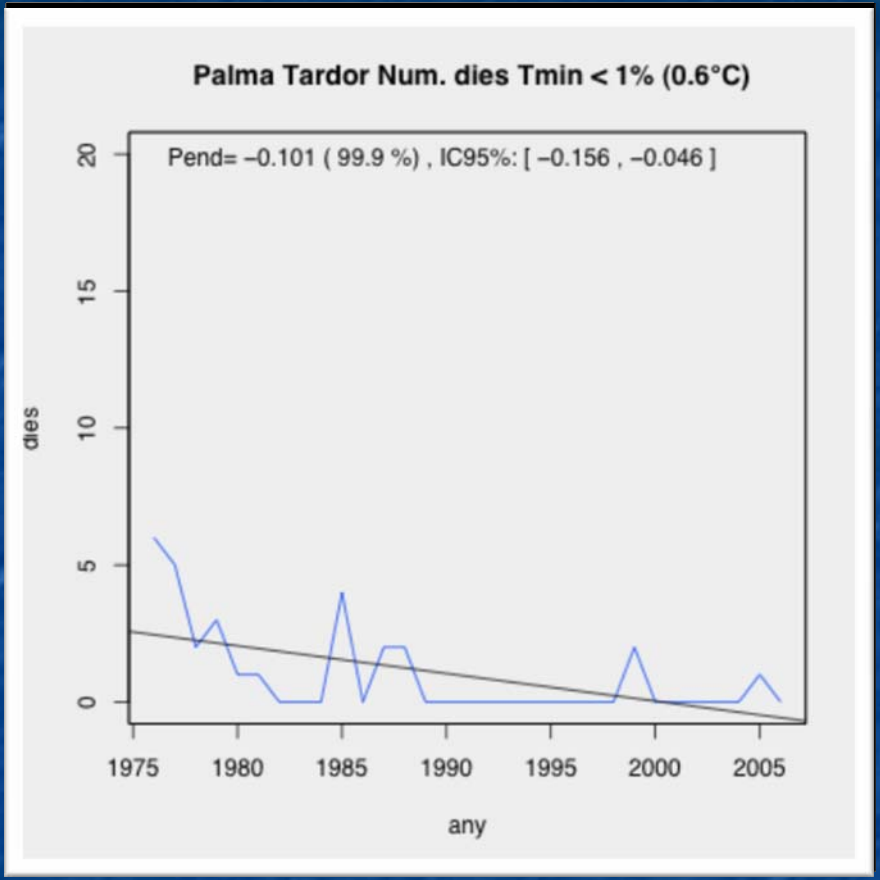

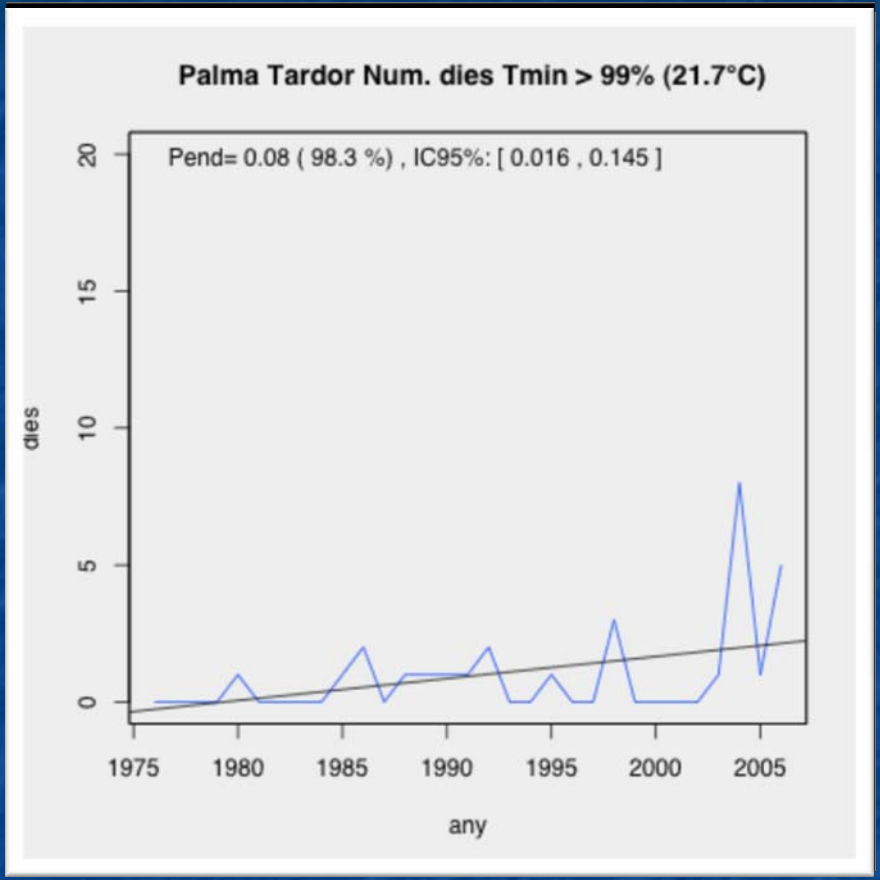

Temperaturas mínimas (95%)

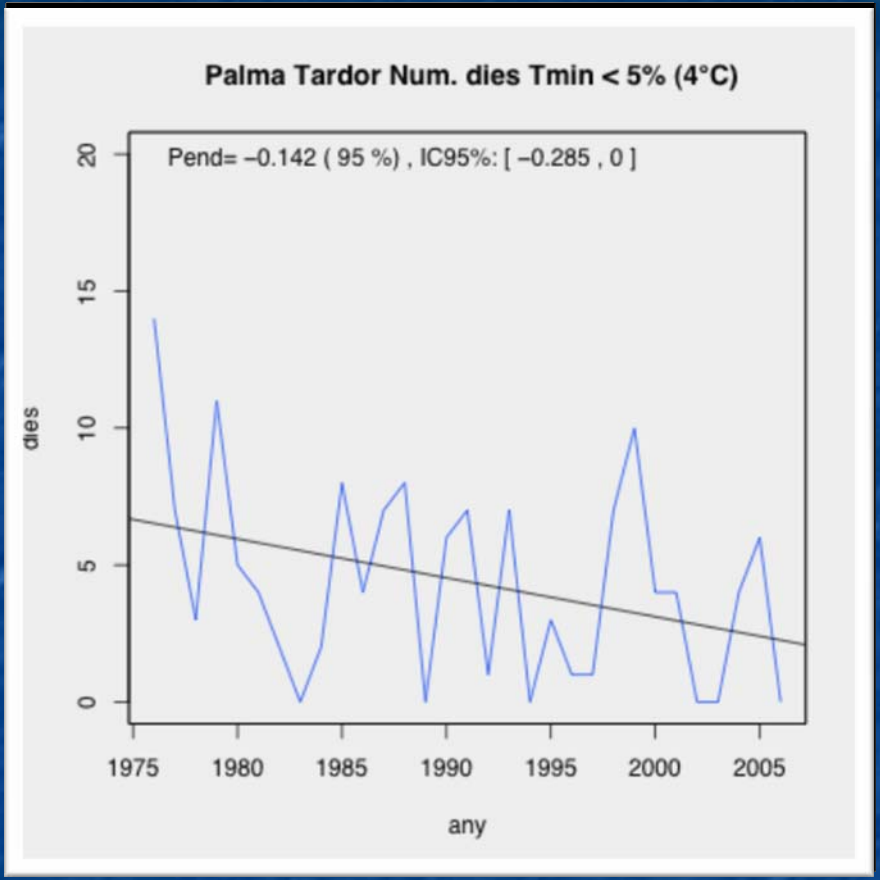

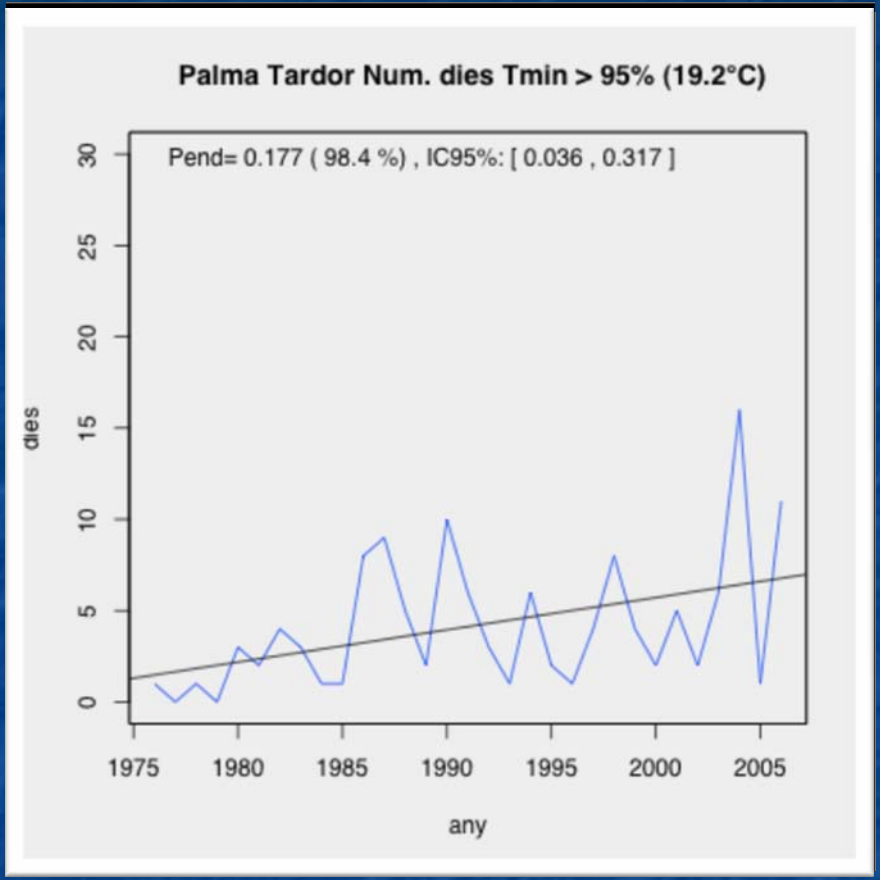

Extremos de Precipitación

Islas Baleares

Daily precipitation categories

Category	Precipitation (mm)
“trace”	<1
a	1-4
b	4-16
c1	16-32
c2	32-64
d1	64-128
d2	>128

Categories

Category	Mean (days/ yr)	Trend (days/100 yr)	Statistical Confidence in trend (+ or -)
trace	17.65	+3.79	Very likely
a	19.36	+7.01	Virtually certain
b	23.99	-4.86	Likely
c1	7.63	-4.20	Virtually certain
c2	2.79	-1.40	Likely
d1	0.45	+0.07	About as likely as not
d2	0.04	+0.04	About as likely as not

Frequently Asked Question 10.1

Are Extreme Events, Like Heat Waves, Droughts or Floods, Expected to Change as the Earth's Climate Changes?

Yes; the type, frequency and intensity of extreme events are expected to change as Earth's climate changes, and these changes could occur even with relatively small mean climate changes. Changes in some types of extreme events have already been observed, for example, increases in the frequency and intensity of heat waves and heavy precipitation events (see FAQ 3.3).

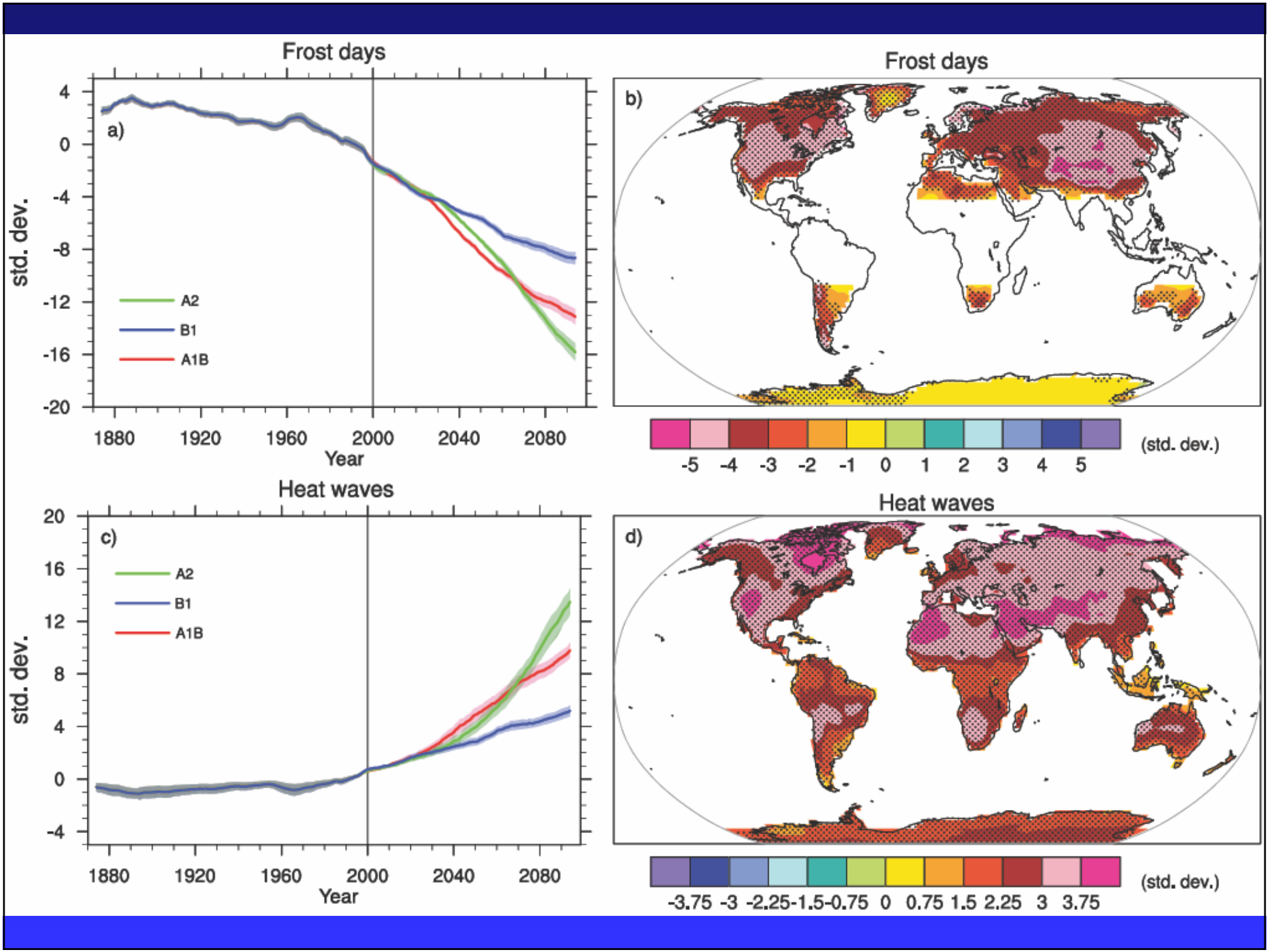
Frost days
a)
std. dev.
4
0
-4
-8
-12
-16
-20
A2
B1
A1B
1880
1920
1960
2000
2040
2080
Year
Frost days
b)
-5 -4 -3 -2 -1 0 1 2 3 4 5
(std. dev.)
Heat waves
c)
std. dev.
20
16
12
8
4
0
-4
A2
B1
A1B
1880
1920
1960
2000
2040
2080
Year
Heat waves
d)
-3.75 -3 -2.25 -1.5 -0.75 0 0.75 1.5 2.25 3 3.75
(std. dev.)

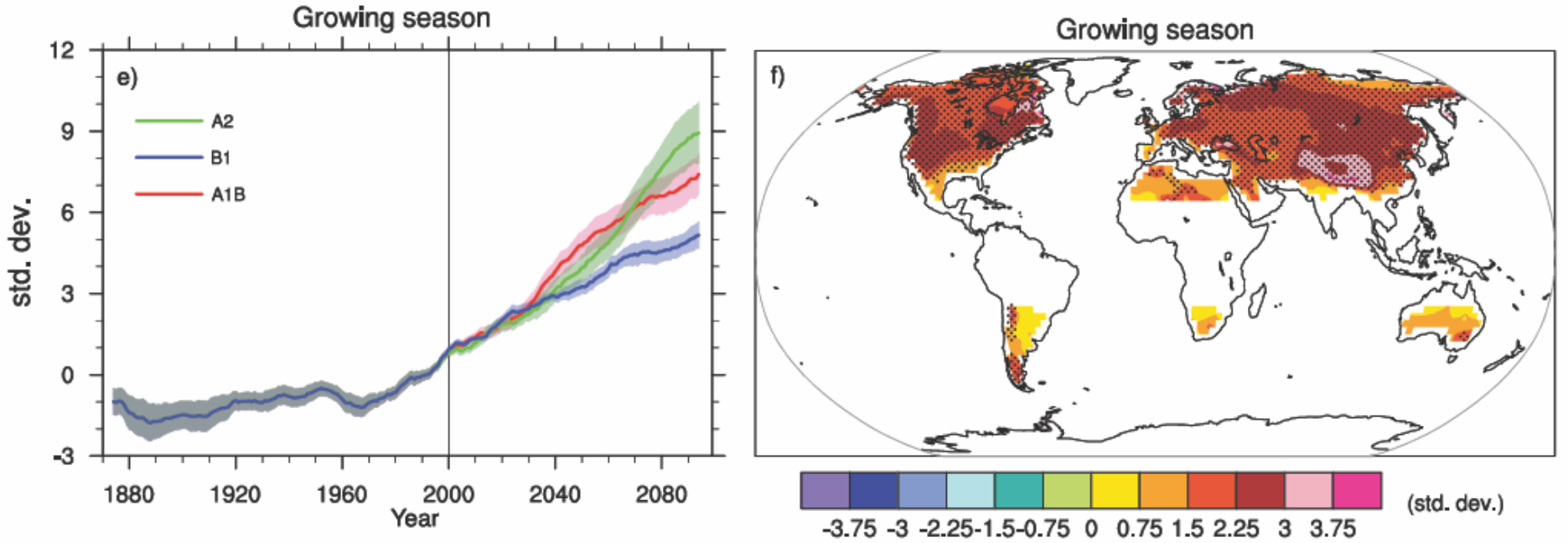

Figure 10.19. *Changes in extremes based on multi-model simulations from nine global coupled climate models, adapted from Tebaldi et al. (2006). (a) Globally averaged changes in the frost day index (defined as the total number of days in a year with absolute minimum temperature below 0°C) for a low (SRES B1), middle (SRES A1B) and high (SRES A2) scenario. (b) Changes in spatial patterns of simulated frost days between two 20-year means (2080–2099 minus 1980–1999) for the A1B scenario. (c) Globally averaged changes in heat waves (defined as the longest period in the year of at least five consecutive days with maximum temperature at least 5°C higher than the climatology of the same calendar day). (d) Changes in spatial patterns of simulated heat waves between two 20-year means (2080–2099 minus 1980–1999) for the A1B scenario. (e) Globally averaged changes in growing season length (defined as the length of the period between the first spell of five consecutive days with mean temperature above 5°C and the last such spell of the year). (f) Changes in spatial patterns of simulated growing season length between two 20-year means (2080–2099 minus 1980–1999) for the A1B scenario. Solid lines in (a), (c) and (e) show the 10-year smoothed multi-model ensemble means; the envelope indicates the ensemble mean standard deviation. Stippling in (b), (d) and (f) denotes areas where at least five of the nine models concur in determining that the change is statistically significant. Extreme indices are calculated only over land. Frost days and growing season are only calculated in the extratropics. Extremes indices are calculated following Frich et al. (2002). Each model's time series was centred around its 1980 to 1999 average and normalised (rescaled) by its standard deviation computed (after de-trending) over the period 1960 to 2099. The models were then aggregated into an ensemble average, both at the global and at the grid-box level. Thus, changes are given in units of standard deviations.*

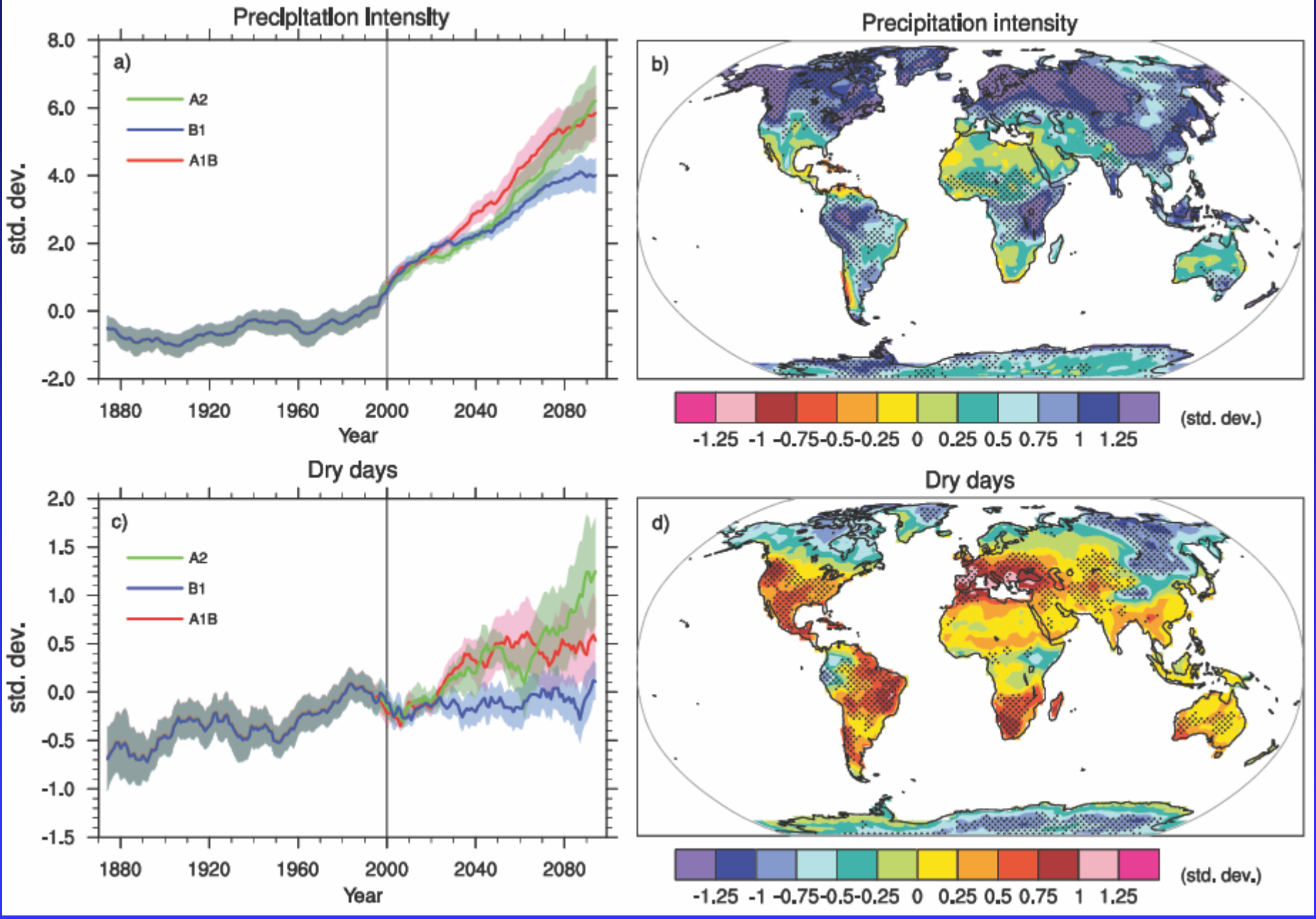
Precipitation Intensity
a)
A2
B1
A1B
std. dev.
8.0
6.0
4.0
2.0
0.0
-2.0
1880
1920
1960
2000
2040
2080
Year
Precipitation intensity
b)
-1.25 -1 -0.75 -0.5 -0.25 0 0.25 0.5 0.75 1 1.25
(std. dev.)
Dry days
c)
A2
B1
A1B
std. dev.
2.0
1.5
1.0
0.5
0.0
-0.5
-1.0
-1.5
1880
1920
1960
2000
2040
2080
Year
Dry days
d)
-1.25 -1 -0.75 -0.5 -0.25 0 0.25 0.5 0.75 1 1.25
(std. dev.)

Figure 10.18. *Changes in extremes based on multi-model simulations from nine global coupled climate models, adapted from Tebaldi et al. (2006). (a) Globally averaged changes in precipitation intensity (defined as the annual total precipitation divided by the number of wet days) for a low (SRES B1), middle (SRES A1B) and high (SRES A2) scenario. (b) Changes in spatial patterns of simulated precipitation intensity between two 20-year means (2080–2099 minus 1980–1999) for the A1B scenario. (c) Globally averaged changes in dry days (defined as the annual maximum number of consecutive dry days). (d) Changes in spatial patterns of simulated dry days between two 20-year means (2080–2099 minus 1980–1999) for the A1B scenario. Solid lines in (a) and (c) are the 10-year smoothed multi-model ensemble means; the envelope indicates the ensemble mean standard deviation. Stippling in (b) and (d) denotes areas where at least five of the nine models concur in determining that the change is statistically significant. Extreme indices are calculated only over land following Frich et al. (2002). Each model's time series was centred on its 1980 to 1999 average and normalised (rescaled) by its standard deviation computed (after de-trending) over the period 1960 to 2099. The models were then aggregated into an ensemble average, both at the global and at the grid-box level. Thus, changes are given in units of standard deviations.*

HURACANES Y MEDICANES: RESPUESTA AL CALENTAMIENTO GLOBAL

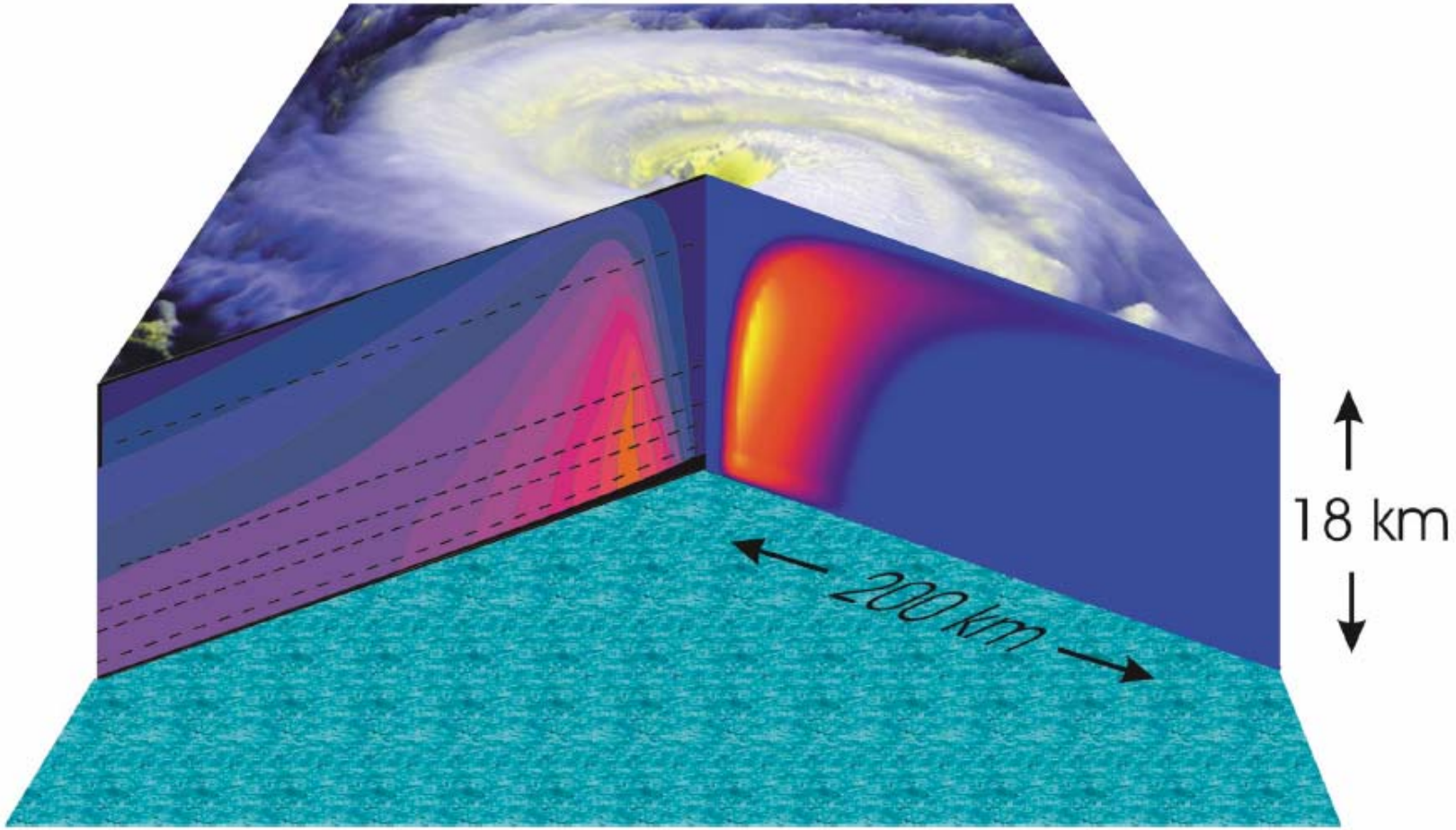

Figure 3 Cutaway view of the structure of a tropical cyclone. The top of the storm is based on a satellite photograph of the cloud structure of Hurricane Fran of 1996. The right-hand cut shows the vertical component of velocity, from a numerical simulation of a hurricane using the model of Emanuel (1995a); maximum values (yellow) are approximately 8 ms^{-1}. The left-hand cut shows the magnitude of the tangential wind component measured in Hurricane Inez of 1966 by aircraft flying at levels indicated by the black dashed lines; from Hawkins & Imbembo (1976). Maximum values are approximately 50 ms^{-1}.

Energía del Huracán (ciclo de Carnot)

a-b: Expansión isotérmica **b-o**: Expansión adiabática **o-o'**: Compresión isotérmica **o'-a**: Compresión adiabática

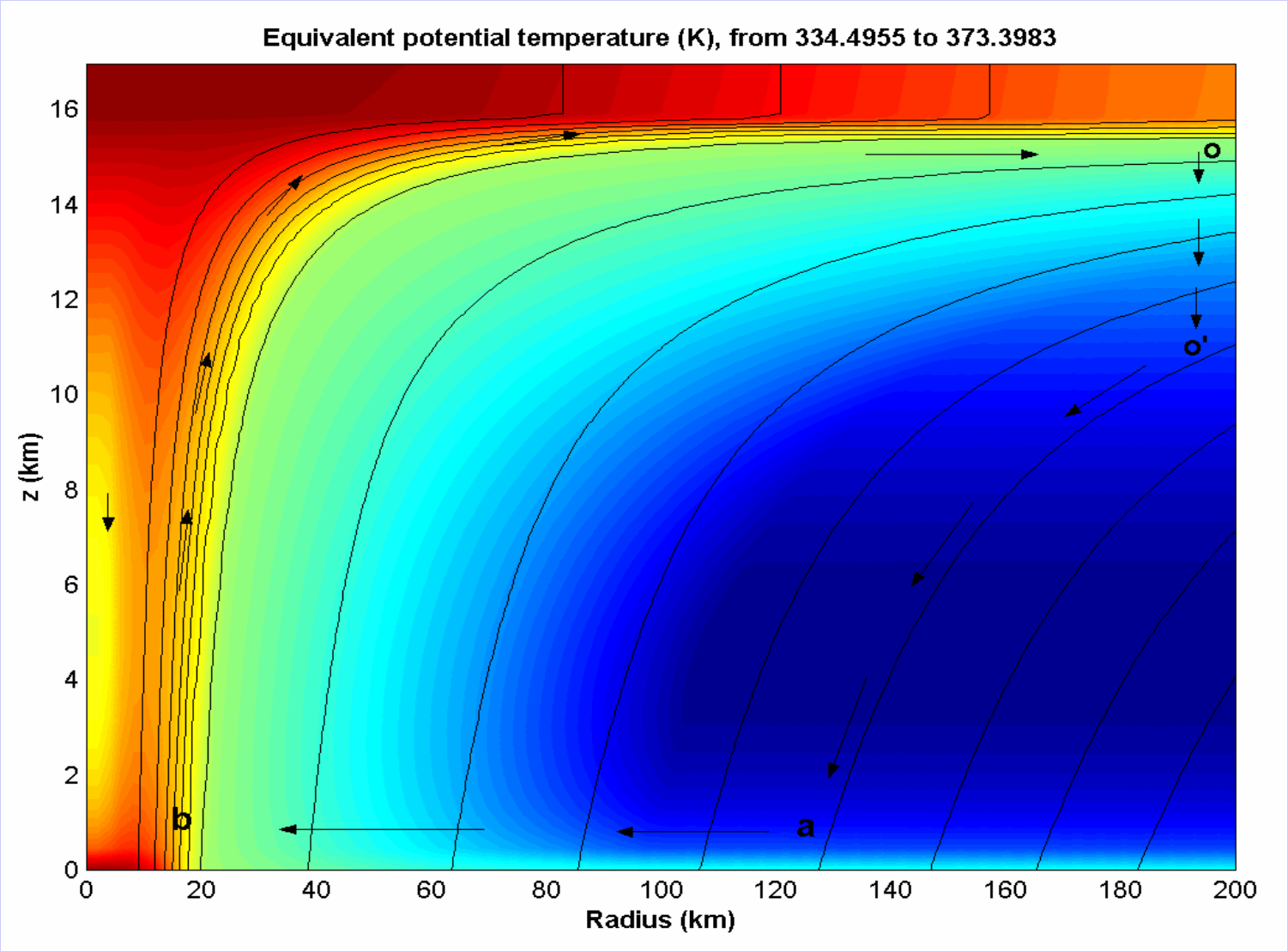

Balance Energético (Estado Estacionario)

$$\mathrm{P} = 2\pi \frac{T_s - T_o}{T_s} \int_a^b \left[C_k \rho |V| \left(k_0^* - k \right) + C_D \rho |V|^3 \right] r dr$$

$$\mathrm{D} = 2\pi \int_a^b C_D \rho |V|^3 r dr$$

$$\rightarrow |V_{\max}|^2 \simeq \frac{C_k}{C_D} \frac{T_s - T_o}{T_o} \left(k_0^* - k \right)$$

→ P_{min} using the gradient-wind relationship

TEORÍA: La Intensidad Potencial Aumenta con la SST (Emanuel, 1987)

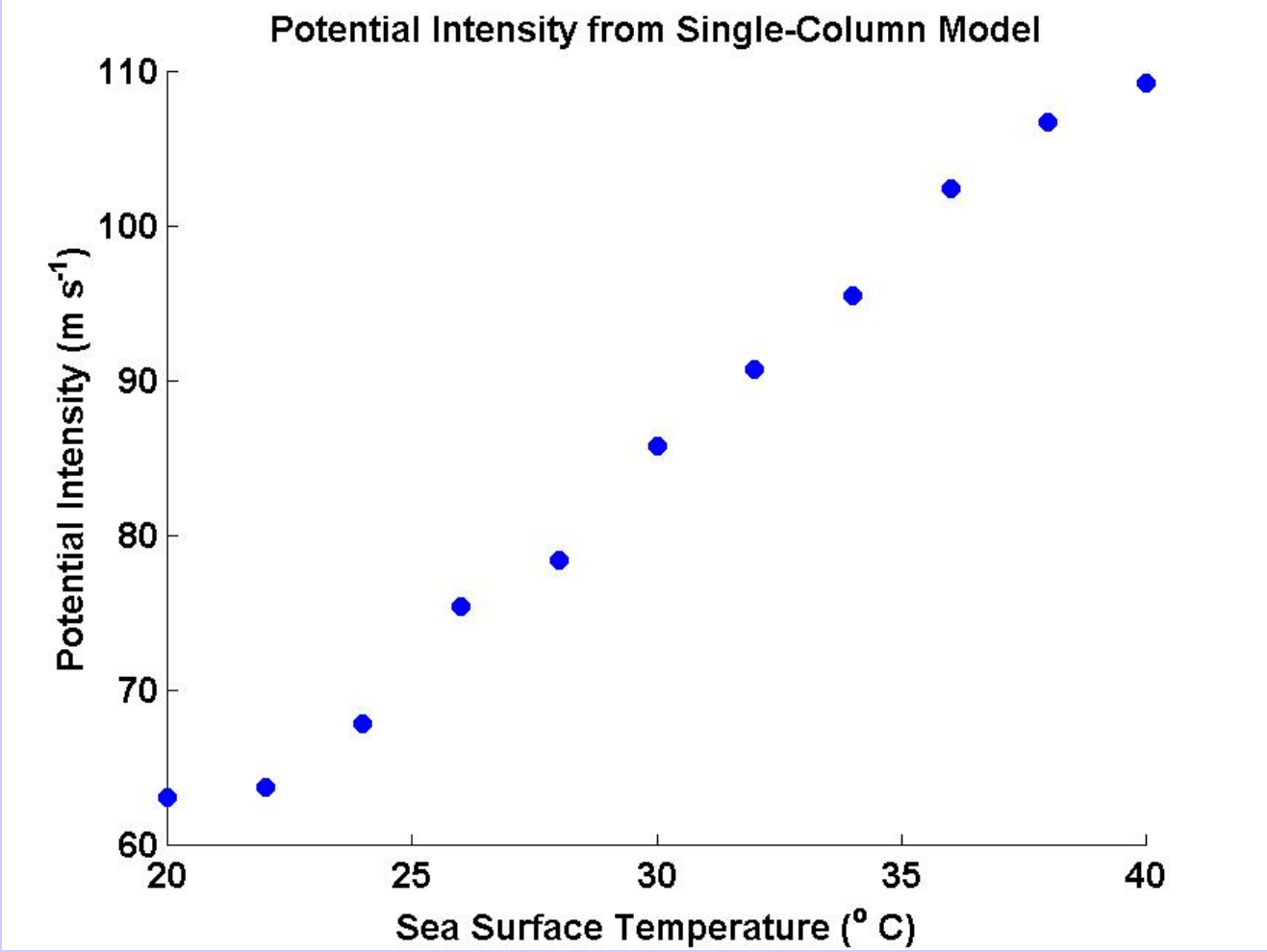

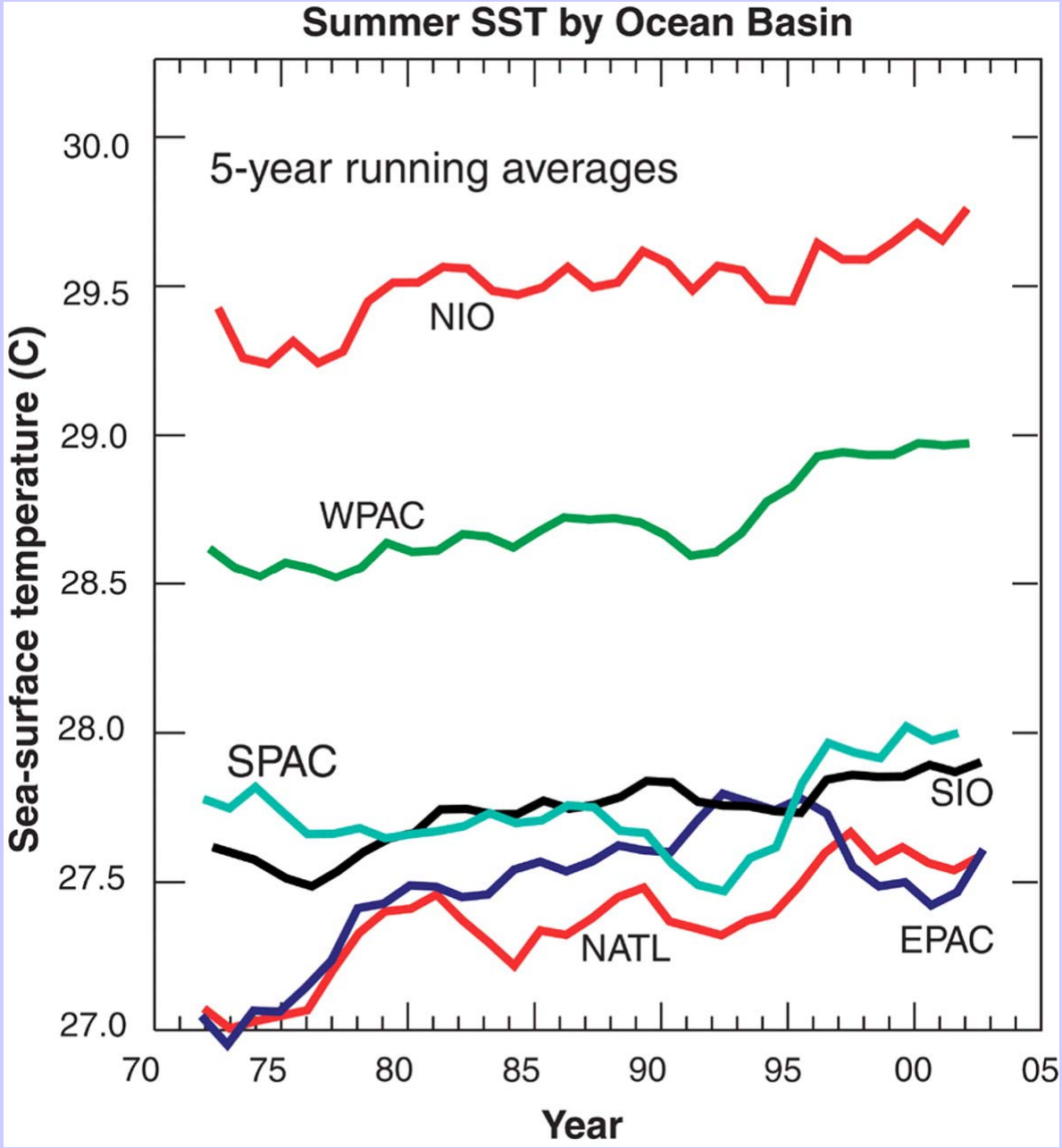
Summer SST by Ocean Basin
5-year running averages
NIO
WPAC
SPAC
SIO
NATL
EPAC
Sea-surface temperature (C)
30.0
29.5
29.0
28.5
28.0
27.5
27.0
70
75
80
85
90
95
00
05
Year

La frecuencia no ha cambiado significativamente

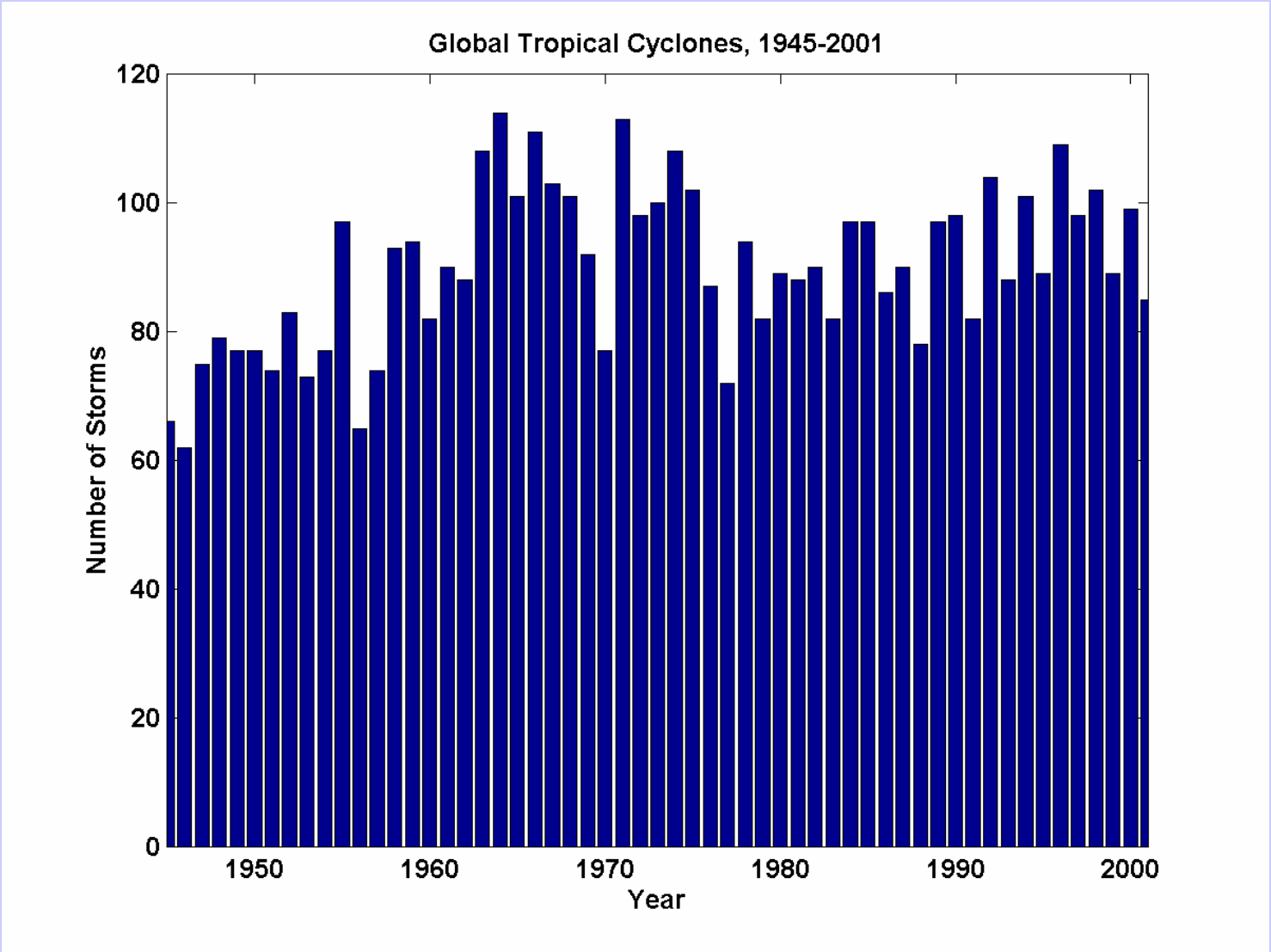

Webster et al. (Science, 2005)

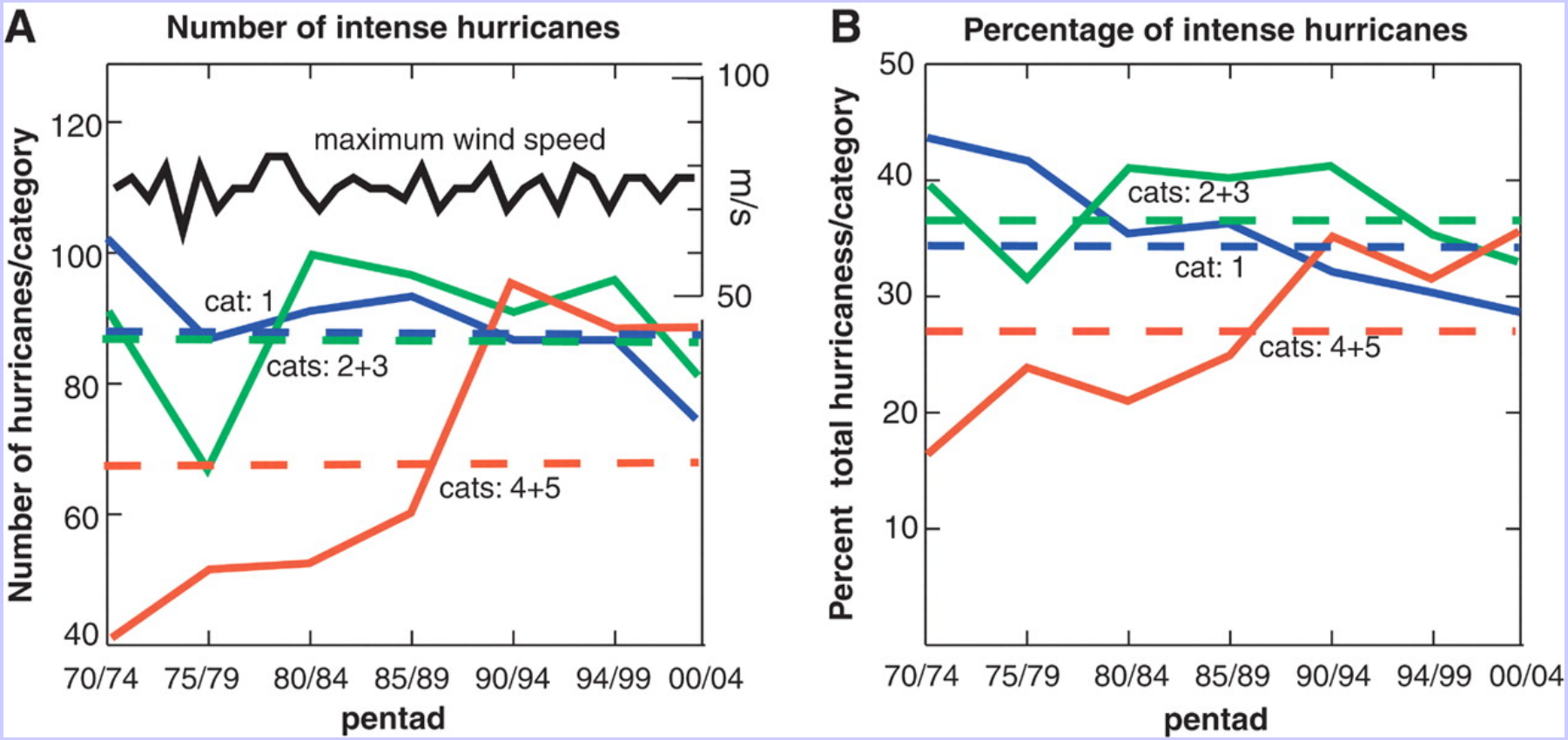

Medida de la actividad del ciclón tropical

$$Power\ dissipation = 2\pi \int_0^{\tau} \int_0^{r_0} C_D \rho \,|\, \mathbf{V} \,|^3 \, r dr dt.$$

Simplified "Power Dissipation Index":

$$PDI \equiv \int_0^{\tau} V_{max}^3 dt$$

Atlántico

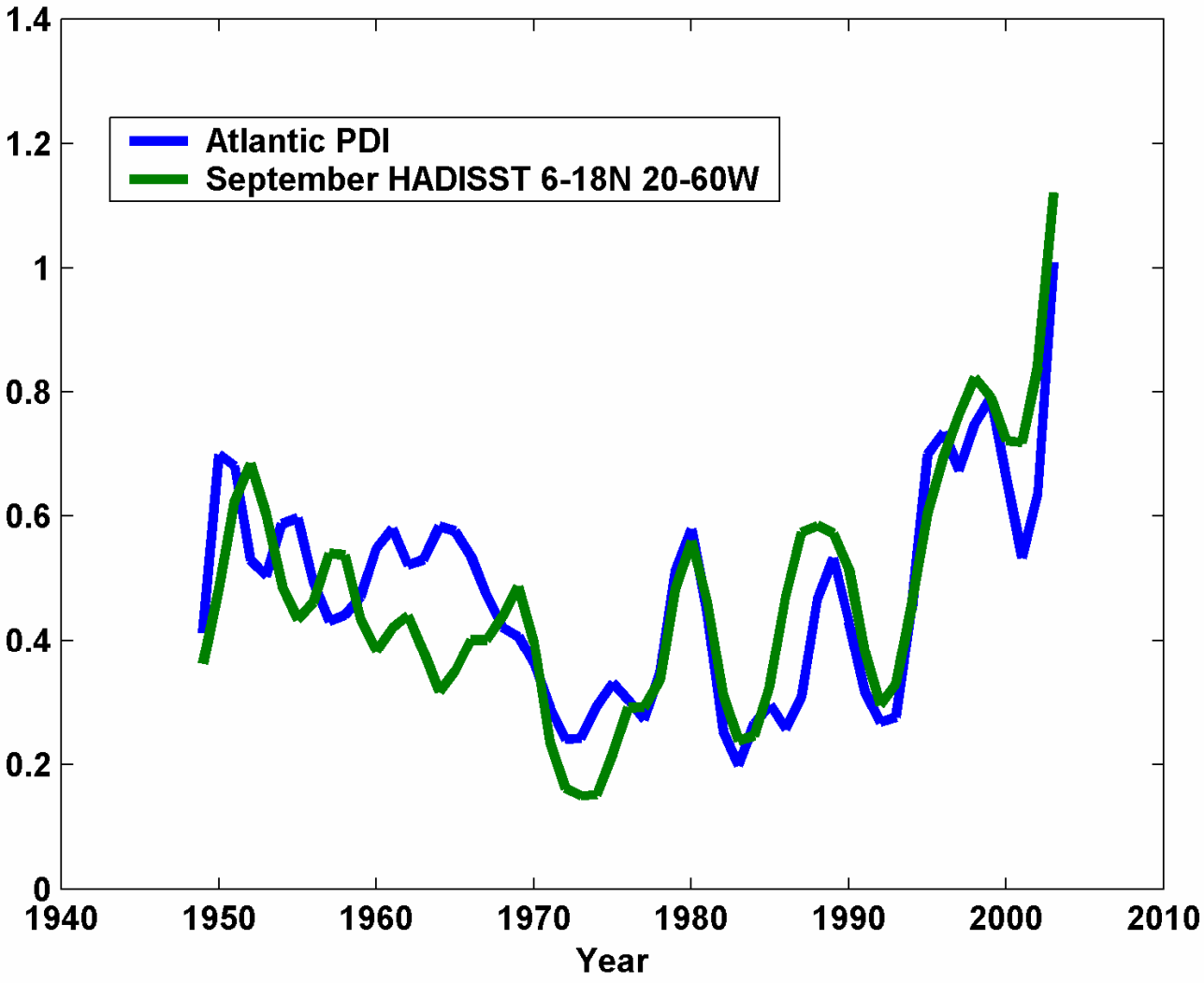
Atlantic PDI
September HADISST 6-18N 20-60W
1.4
1.2
1
0.8
0.6
0.4
0.2
0
1940
1950
1960
1970
1980
1990
2000
2010
Year

Pacífico NW

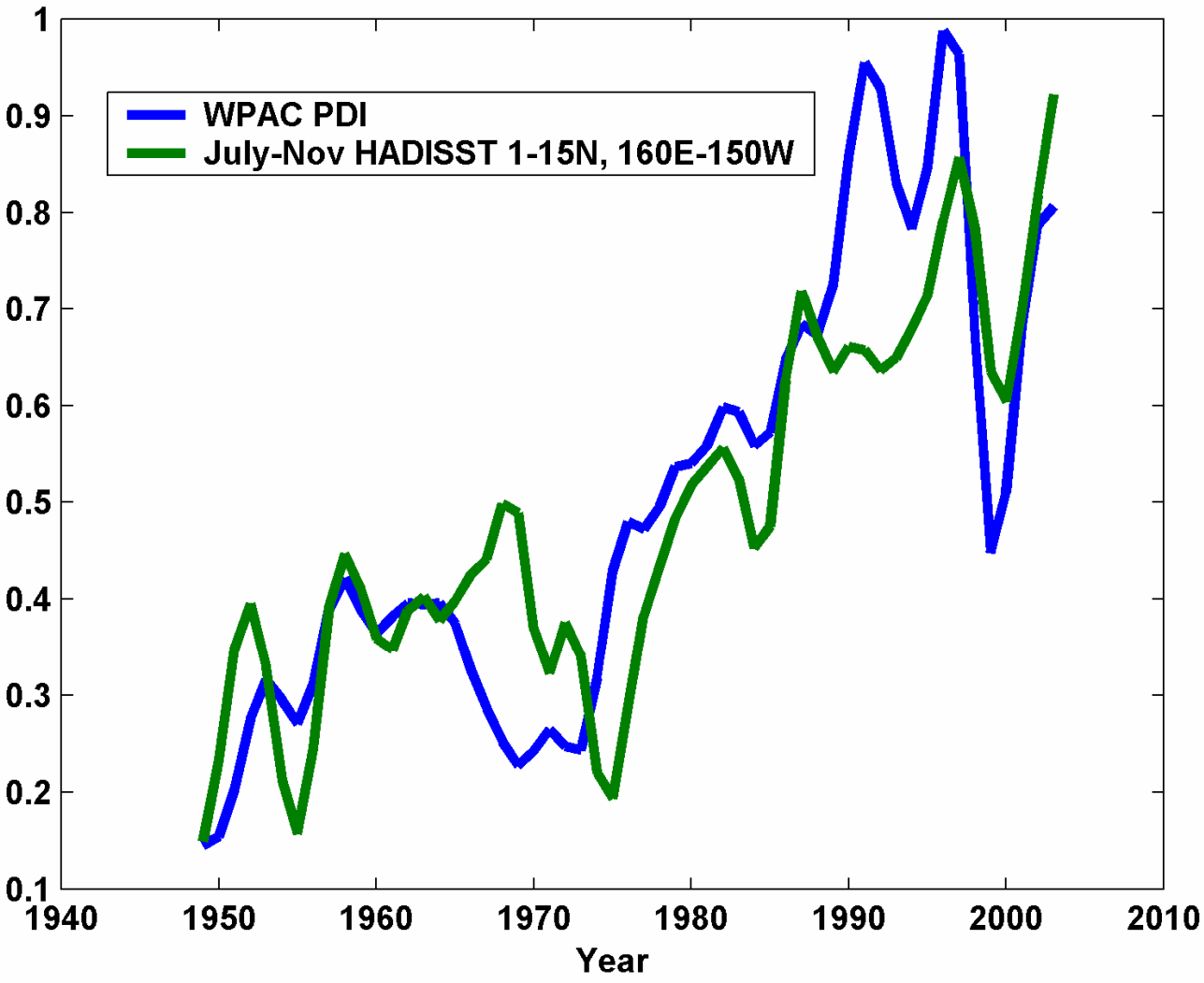
WPAC PDI
July-Nov HADISST 1-15N, 160E-150W
1
0.9
0.8
0.7
0.6
0.5
0.4
0.3
0.2
0.1
1940
1950
1960
1970
1980
1990
2000
2010
Year

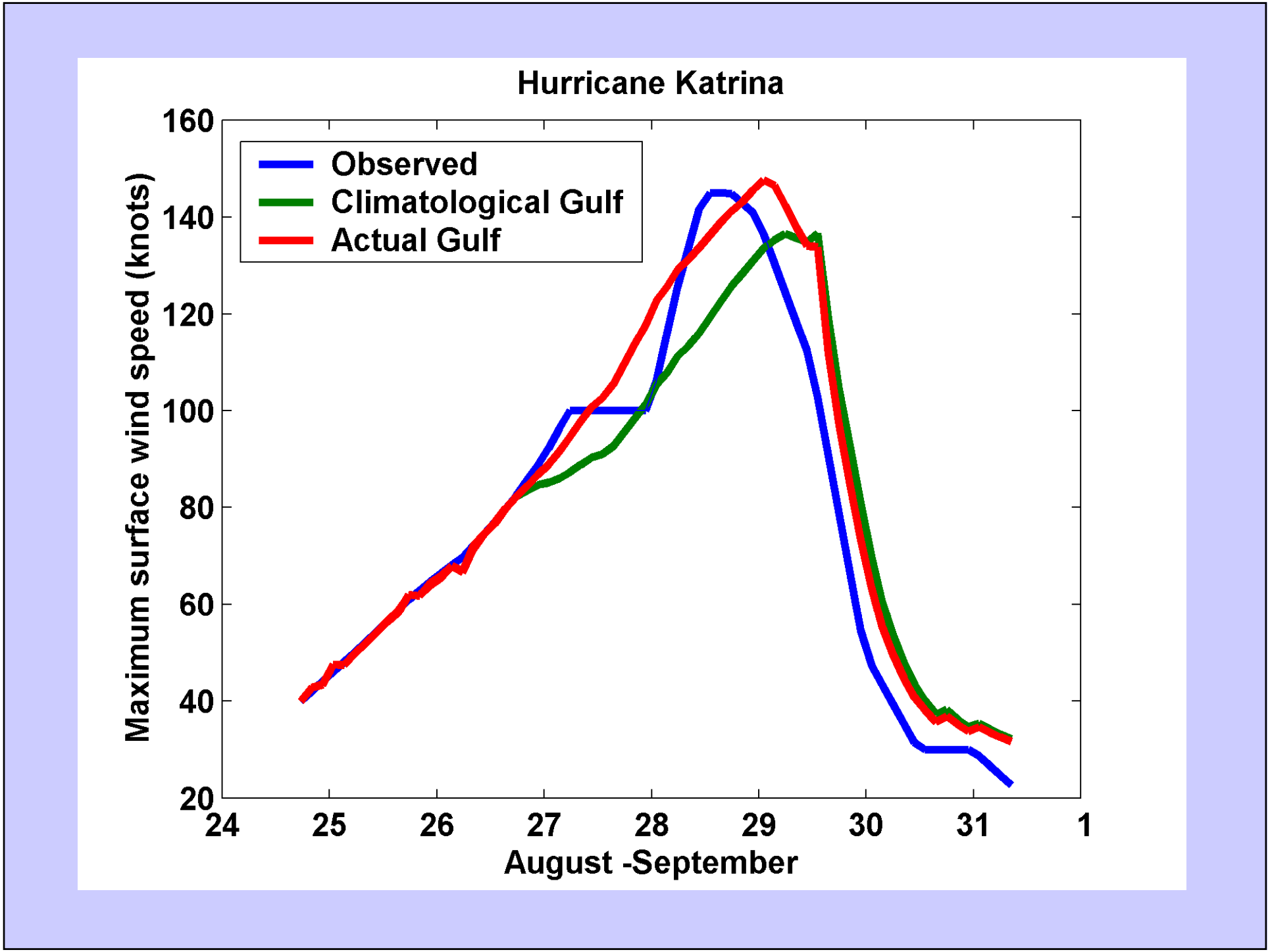
Hurricane Katrina
Observed
Climatological Gulf
Actual Gulf
Maximum surface wind speed (knots)
160
140
120
100
80
60
40
20
24
25
26
27
28
29
30
31
1
August -September

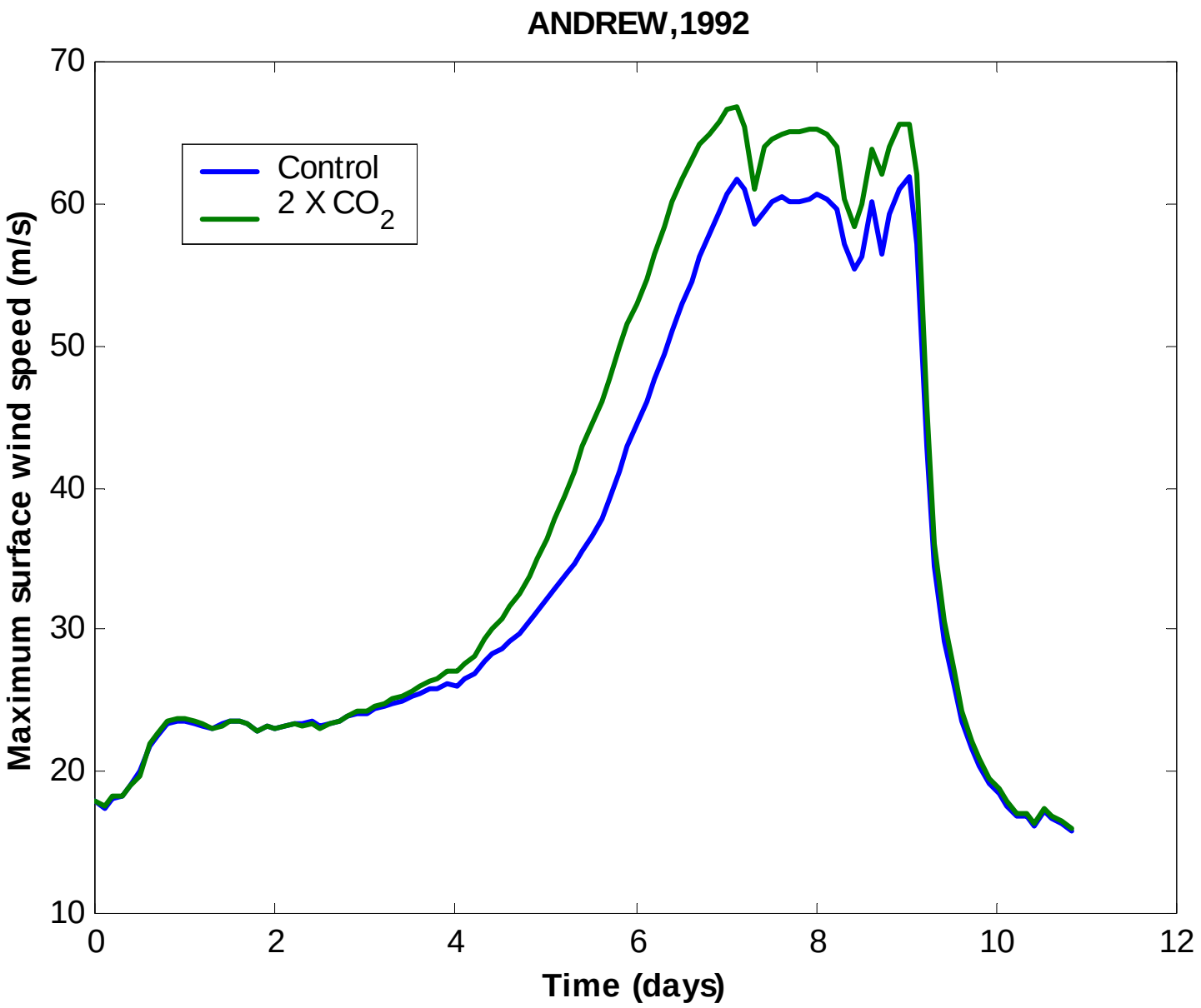
ANDREW,1992
Control
2 X CO2
Maximum surface wind speed (m/s)
Time (days)
70
60
50
40
30
20
10
0
2
4
6
8
10
12

Knutson and Toleya (J. Climate, 2004)

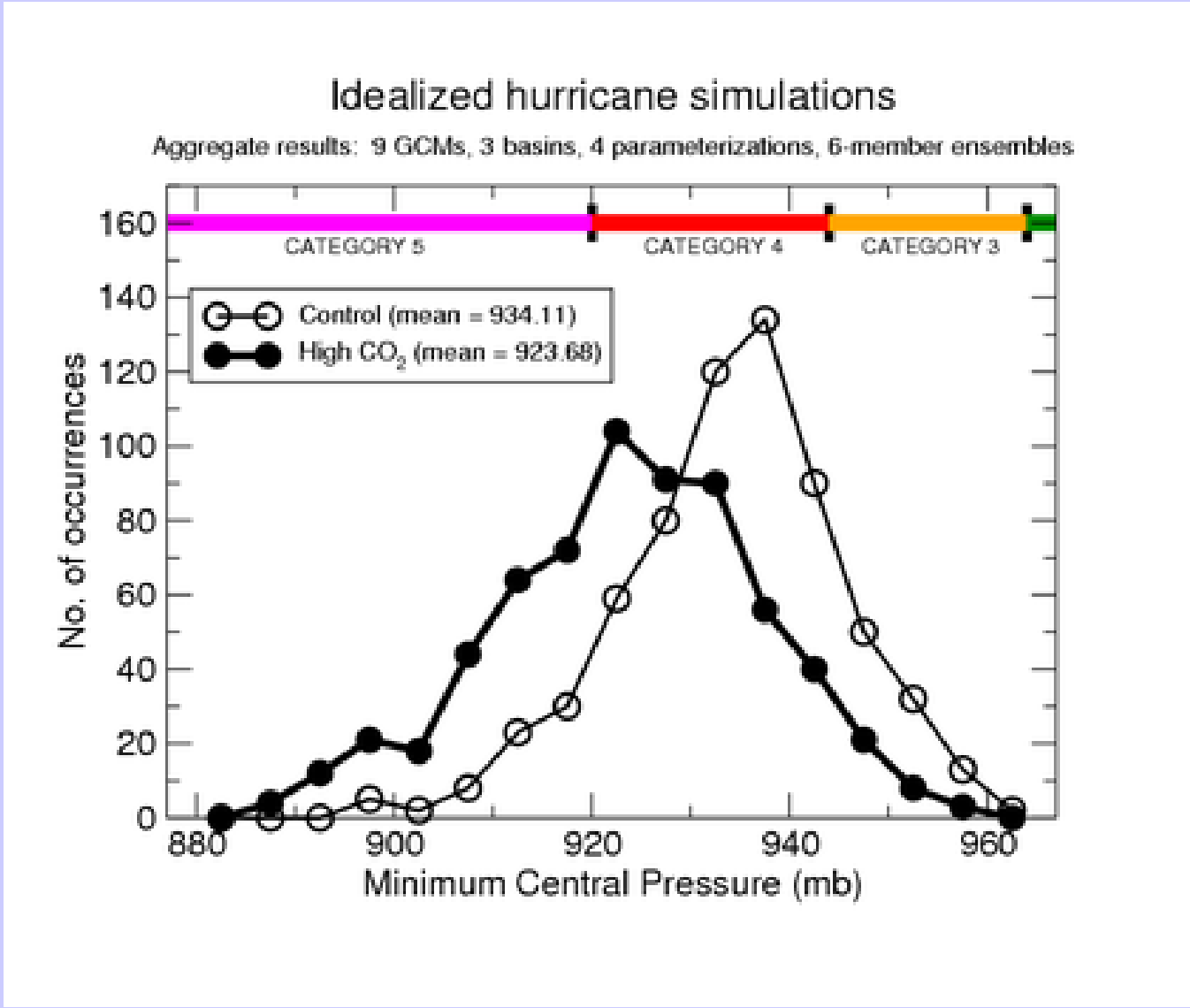

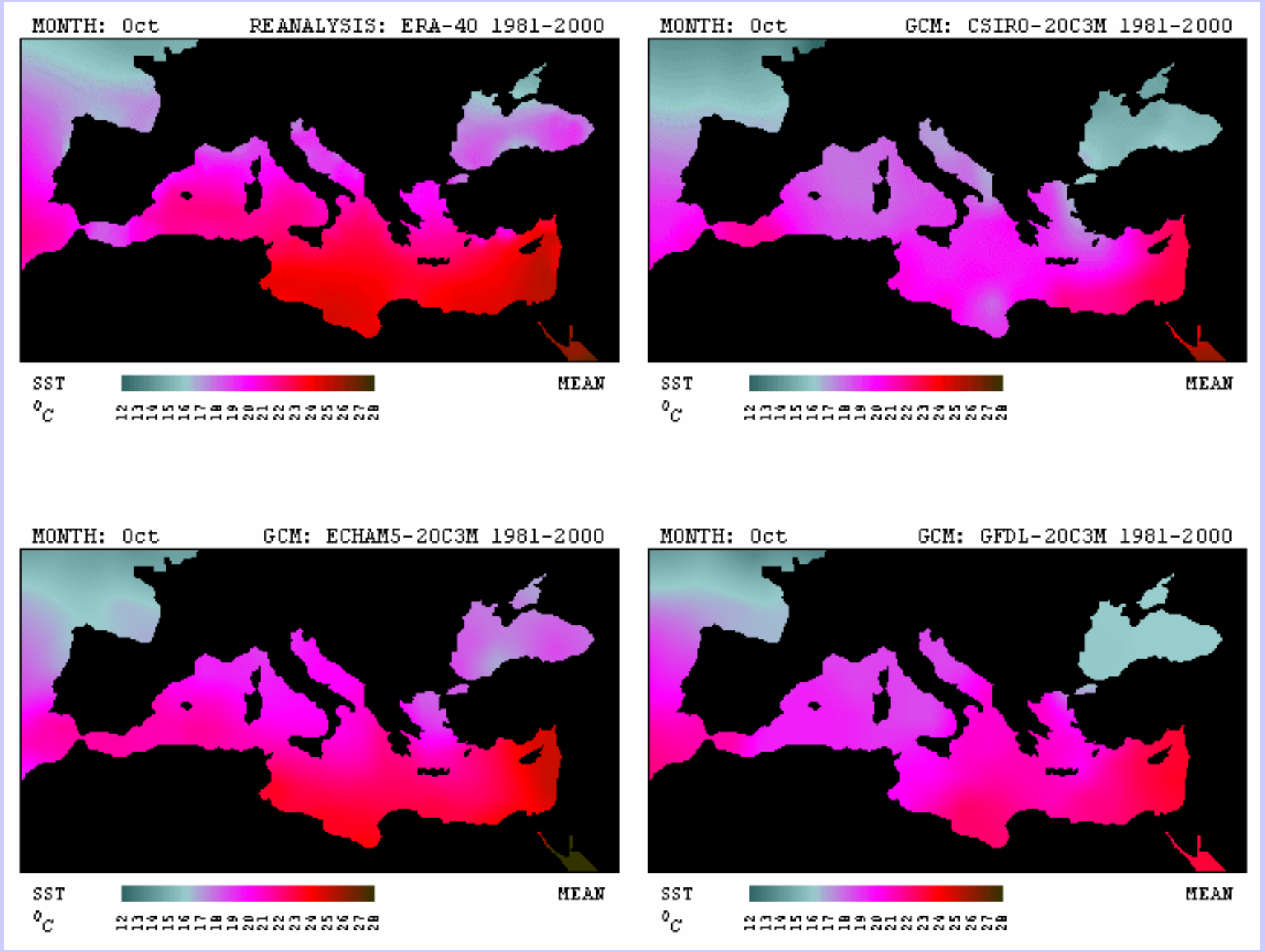
MONTH: Oct
REANALYSIS: ERA-40 1981-2000
SST
MEAN
°C
12 13 14 15 16 17 18 19 20 21 22 23 24 25 26 27 28
MONTH: Oct
GCM: CSIRO-20C3M 1981-2000
SST
MEAN
°C
12 13 14 15 16 17 18 19 20 21 22 23 24 25 26 27 28
MONTH: Oct
GCM: ECHAM5-20C3M 1981-2000
SST
MEAN
°C
12 13 14 15 16 17 18 19 20 21 22 23 24 25 26 27 28
MONTH: Oct
GCM: GFDL-20C3M 1981-2000
SST
MEAN
°C
12 13 14 15 16 17 18 19 20 21 22 23 24 25 26 27 28

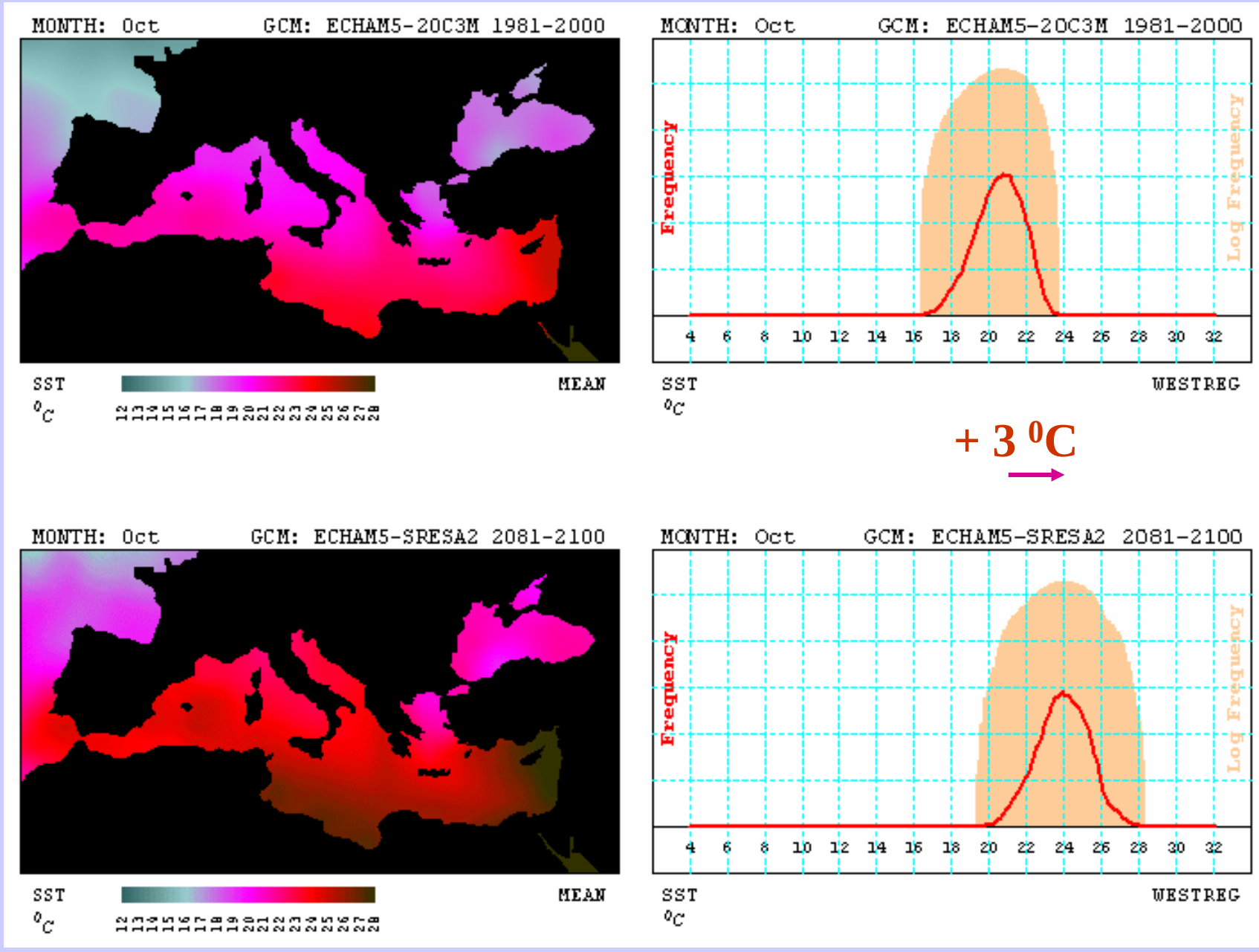
MONTH: Oct
GCM: ECHAM5-20C3M 1981-2000
SST
°C
12 13 14 15 16 17 18 19 20 21 22 23 24 25 26 27 28
MEAN
MONTH: Oct
GCM: ECHAM5-20C3M 1981-2000
Frequency
Log Frequency
4 6 8 10 12 14 16 18 20 22 24 26 28 30 32
SST
°C
WESTREG
+ 3 °C
MONTH: Oct
GCM: ECHAM5-SRESA2 2081-2100
SST
°C
12 13 14 15 16 17 18 19 20 21 22 23 24 25 26 27 28
MEAN
MONTH: Oct
GCM: ECHAM5-SRESA2 2081-2100
Frequency
Log Frequency
4 6 8 10 12 14 16 18 20 22 24 26 28 30 32
SST
°C
WESTREG

Índice Empírico de Génesis

$$I = \left| 10^5 \eta \right|^{3/2} \left(\frac{H}{50} \right)^3 \left(\frac{V_{pot}}{70} \right)^3 \left(1 + 0.1 V_{shear} \right)^{-2},$$

$\eta \equiv 850\, hPa\ absolute\ vorticity\ (s^{-1})$,

$V_{pot} \equiv$ *Potential wind speed* (ms^{-1}),

$H \equiv 600\, mb\ relative\ humidity\ (\%)$,

$V_{shear} \equiv \left| \mathbf{V}_{850} - \mathbf{V}_{250} \right|$ (ms^{-1}).

Variabilidad Estacional

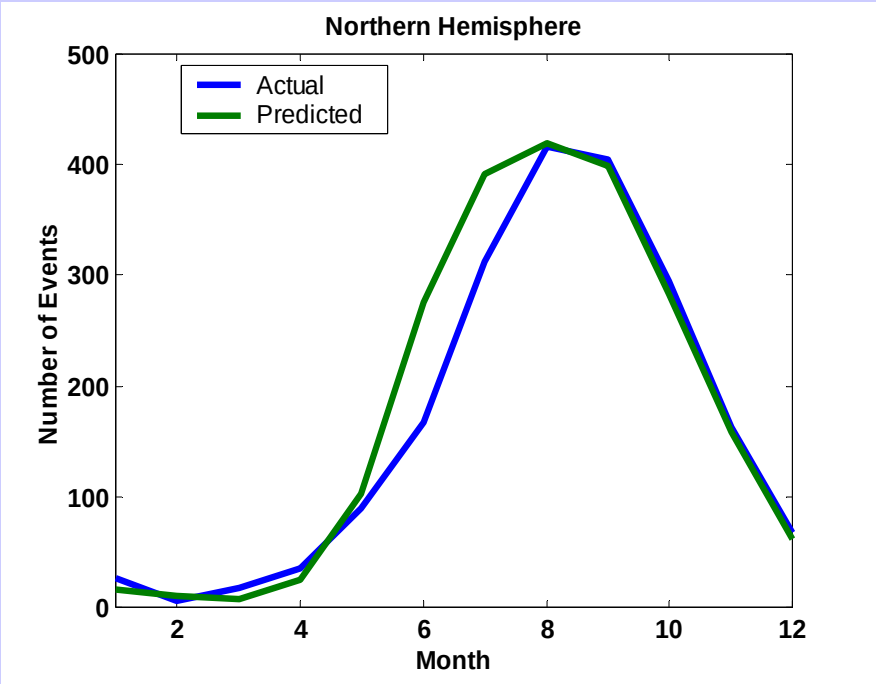

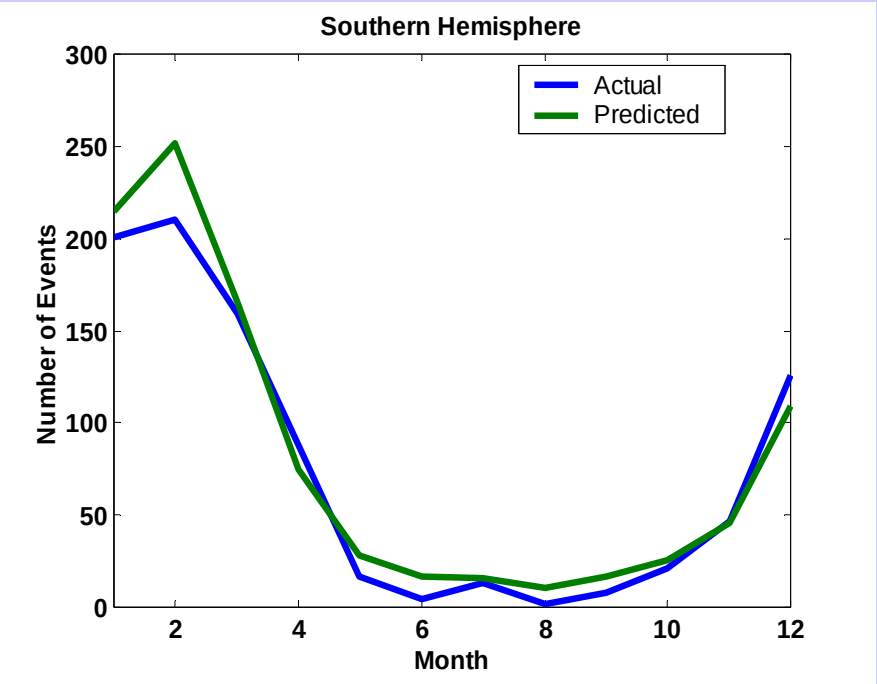

Variabilidad Espacial (H.S)

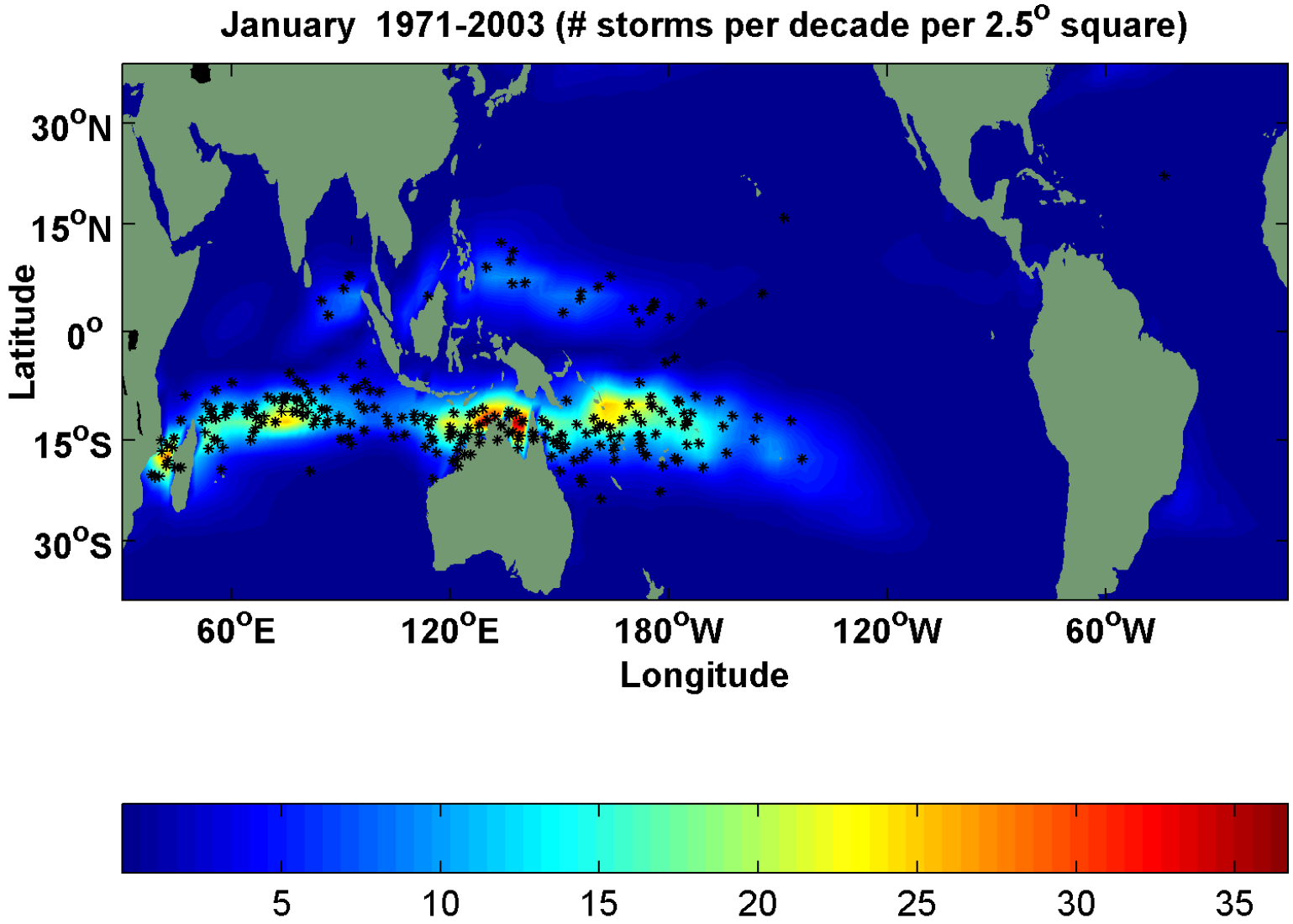

Variabilidad Espacial (H.N)

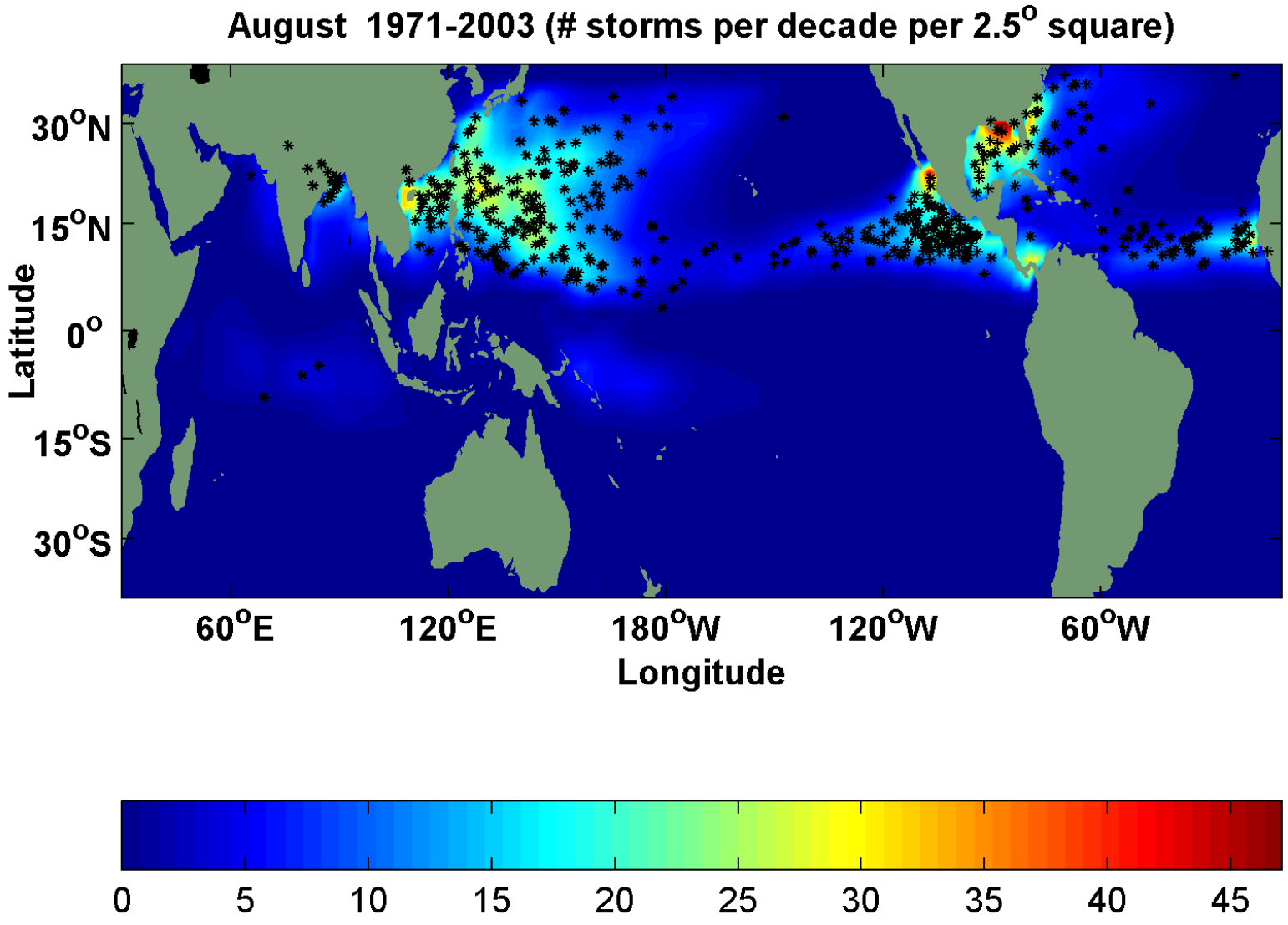

RELATIVE TIME: -24 h EVENT: ECMWF-ANALYSIS

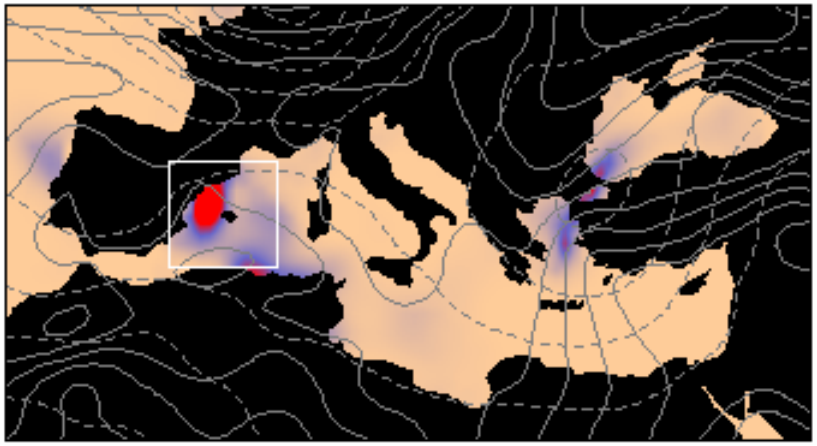

GENPDF 71092500

no dim 0 2 4 6 8 10 12 14 16 18 20 22 24

RELATIVE TIME: -24 h EVENT: ECMWF-ANALYSIS

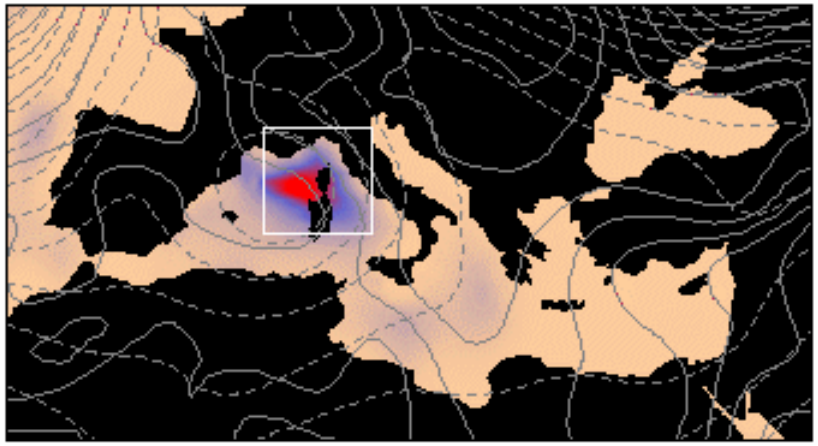

GENPDF 83093012

no dim 0 2 4 6 8 10 12 14 16 18 20 22 24

RELATIVE TIME: -24 h EVENT: ECMWF-ANALYSIS

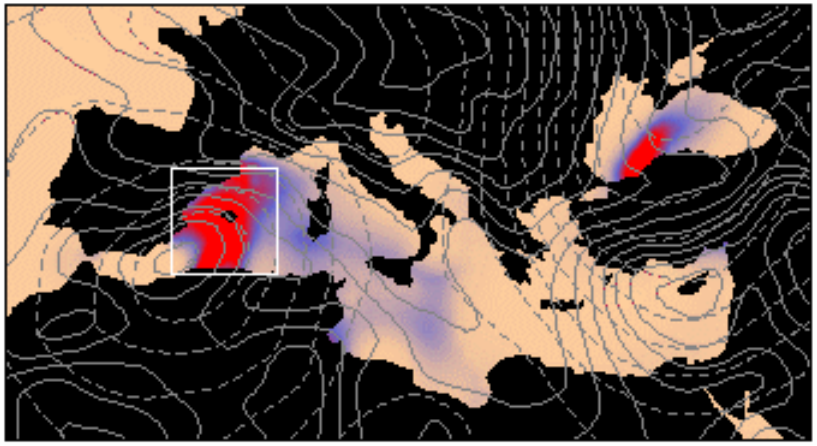

GENPDF 86100200

no dim 0 2 4 6 8 10 12 14 16 18 20 22 24

RELATIVE TIME: -24 h EVENT: ECMWF-ANALYSIS

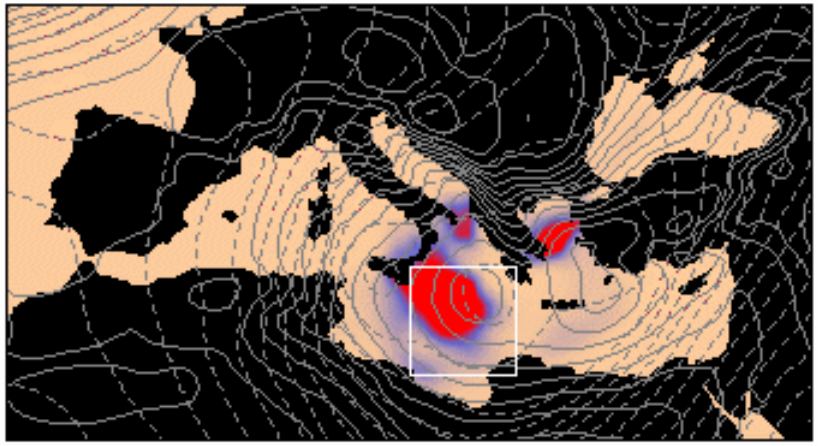

GENPDF 95011612

no dim 0 2 4 6 8 10 12 14 16 18 20 22 24

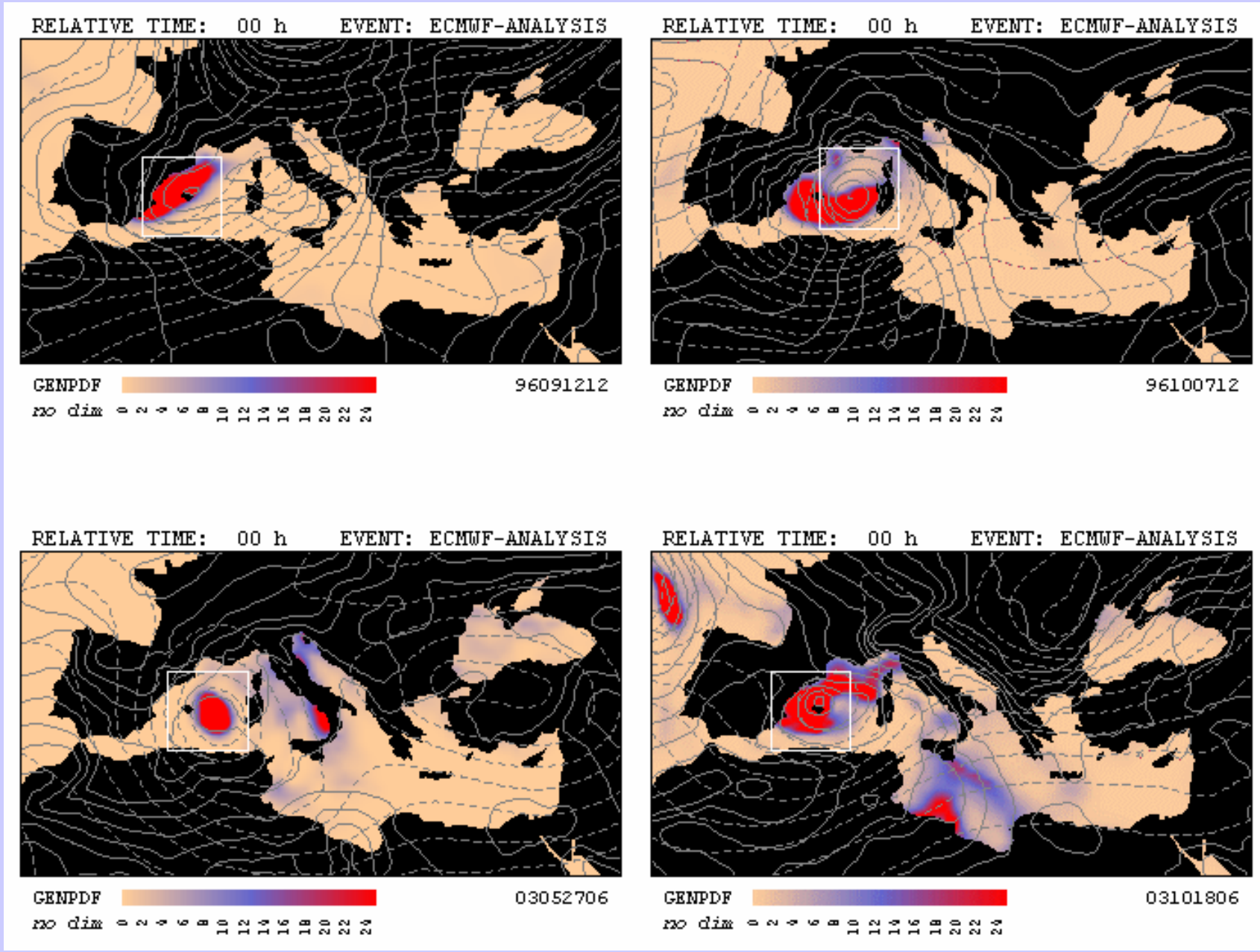
RELATIVE TIME: 00 h EVENT: ECMWF-ANALYSIS
GENPDF
96091212
no dim 0 2 4 6 8 10 12 14 16 18 20 22 24
RELATIVE TIME: 00 h EVENT: ECMWF-ANALYSIS
GENPDF
96100712
no dim 0 2 4 6 8 10 12 14 16 18 20 22 24
RELATIVE TIME: 00 h EVENT: ECMWF-ANALYSIS
GENPDF
03052706
no dim 0 2 4 6 8 10 12 14 16 18 20 22 24
RELATIVE TIME: 00 h EVENT: ECMWF-ANALYSIS
GENPDF
03101806
no dim 0 2 4 6 8 10 12 14 16 18 20 22 24

RELATIVE TIME: -06 h EVENT: ECMWF-ANALYSIS

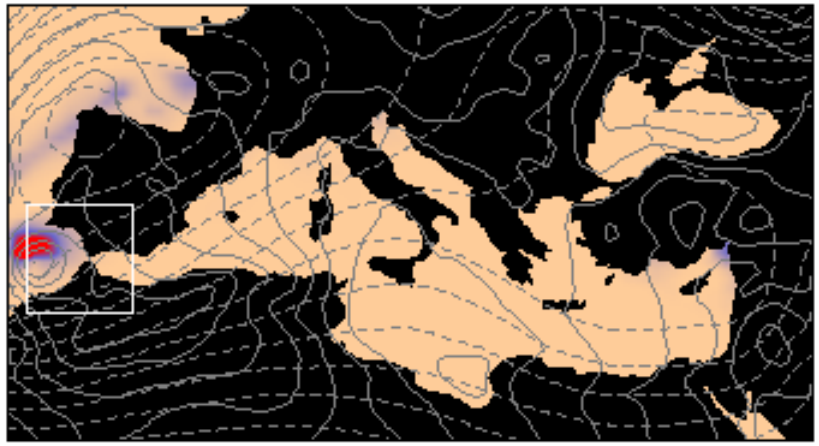

GENPDF 04050218

no dim 0 2 4 6 8 10 12 14 16 18 20 22 24

RELATIVE TIME: -06 h EVENT: ECMWF-ANALYSIS

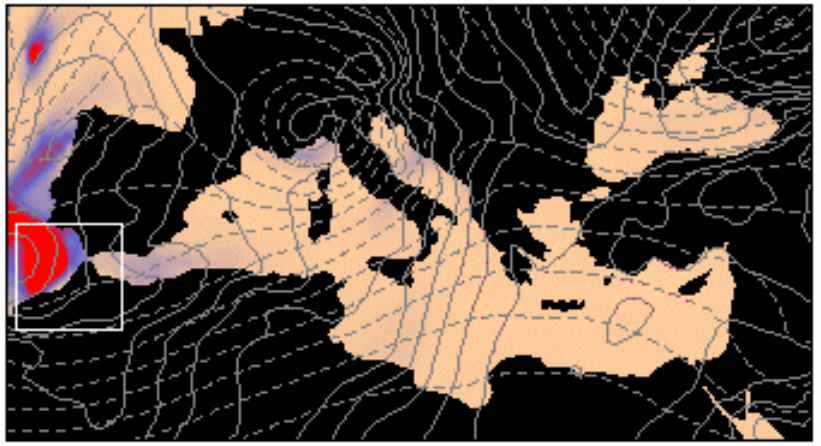

GENPDF 04120100

no dim 0 2 4 6 8 10 12 14 16 18 20 22 24

RELATIVE TIME: -06 h EVENT: ECMWF-ANALYSIS

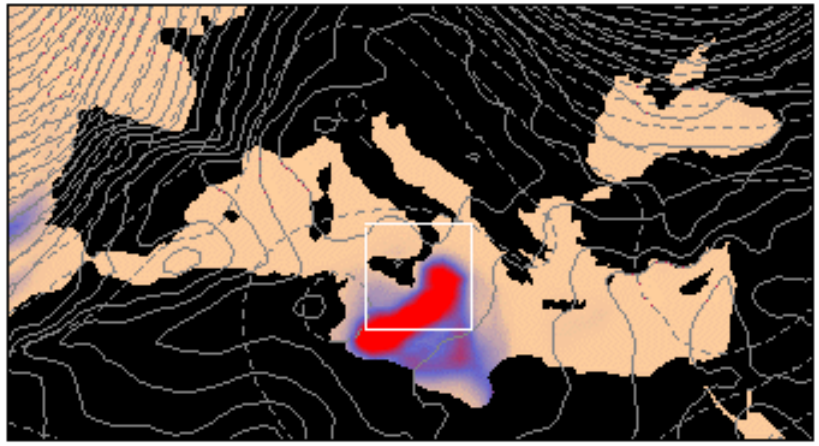

GENPDF 05102712

no dim 0 2 4 6 8 10 12 14 16 18 20 22 24

RELATIVE TIME: -06 h EVENT: ECMWF-ANALYSIS

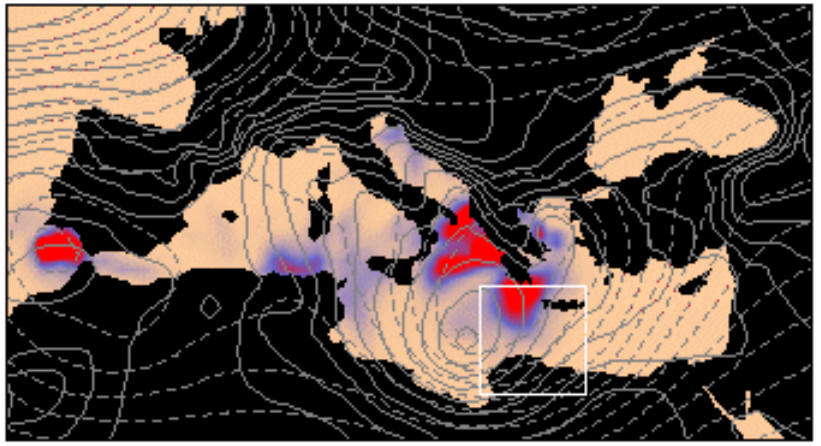

GENPDF 05121506

no dim 0 2 4 6 8 10 12 14 16 18 20 22 24

MONTH: Oct REANALYSIS: ERA-40 1981-2000

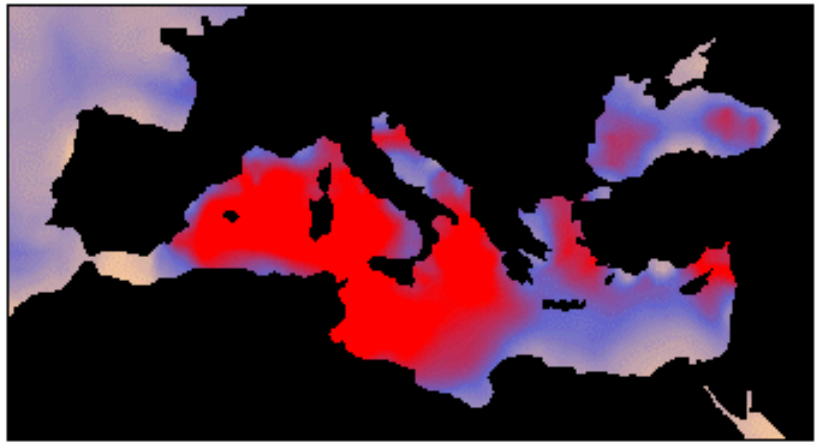

GENPDF MEAN

no dim 0.0 0.2 0.4 0.6 0.8 1.0 1.2 1.4 1.6 1.8 2.0 2.2 2.4

MONTH: Oct GCM: CSIRO-20C3M 1981-2000

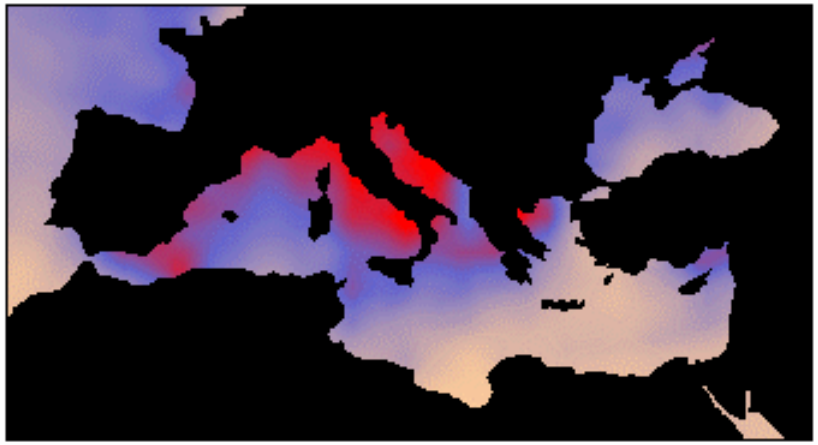

GENPDF MEAN

no dim 0.0 0.2 0.4 0.6 0.8 1.0 1.2 1.4 1.6 1.8 2.0 2.2 2.4

MONTH: Oct GCM: ECHAM5-20C3M 1981-2000

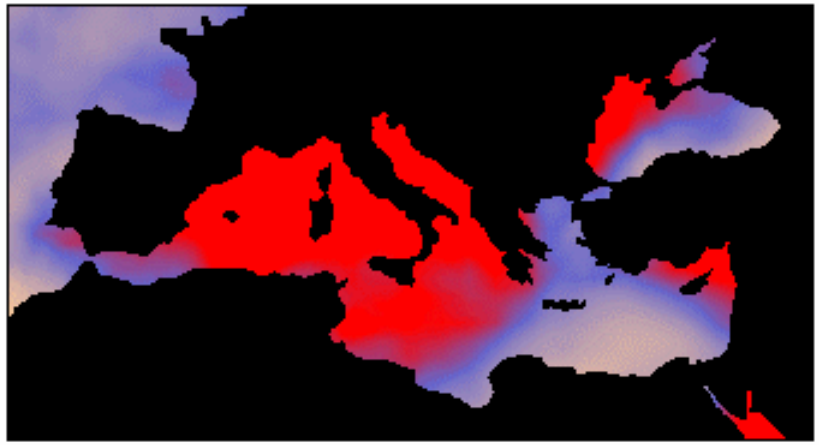

GENPDF MEAN

no dim 0.0 0.2 0.4 0.6 0.8 1.0 1.2 1.4 1.6 1.8 2.0 2.2 2.4

MONTH: Oct GCM: GFDL-20C3M 1981-2000

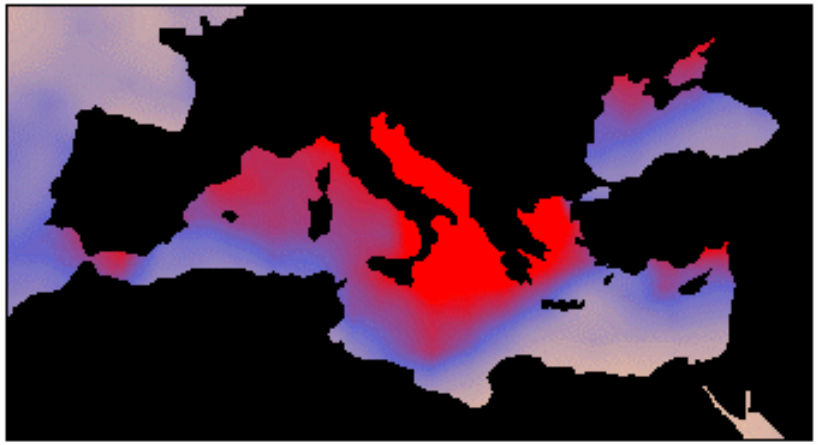

GENPDF MEAN

no dim 0.0 0.2 0.4 0.6 0.8 1.0 1.2 1.4 1.6 1.8 2.0 2.2 2.4

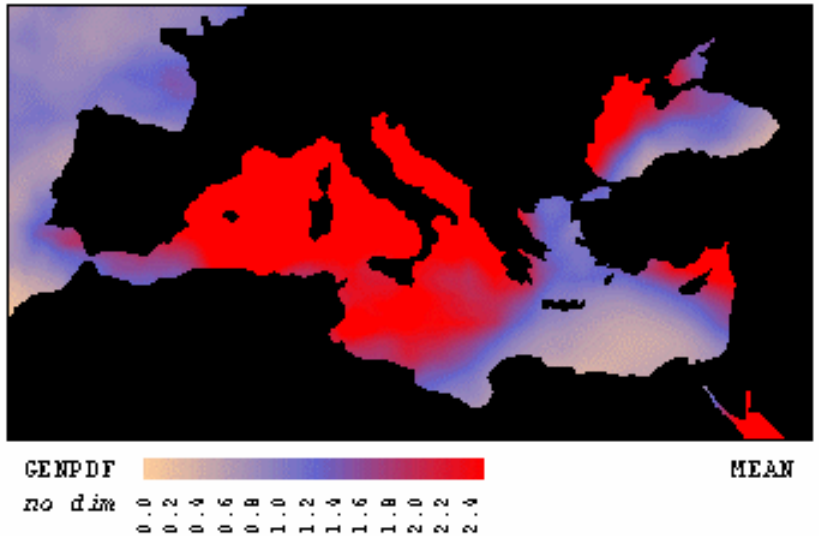
MONTH: Oct
GCM: ECHAM5-20C3M 1981-2000
GENPDF
MEAN
no dim
0.0 0.2 0.4 0.6 0.8 1.0 1.2 1.4 1.6 1.8 2.0 2.2 2.4

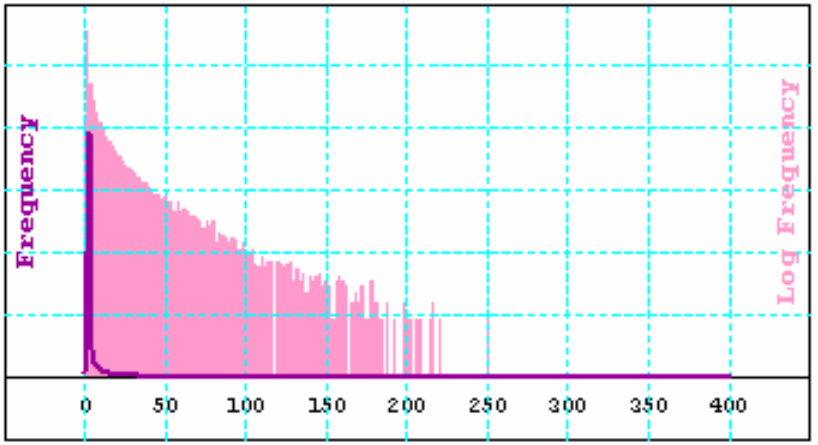
MONTH: Oct
GCM: ECHAM5-20C3M 1981-2000
Frequency
Log Frequency
0 50 100 150 200 250 300 350 400
GENPDF
WESTREG
no dim

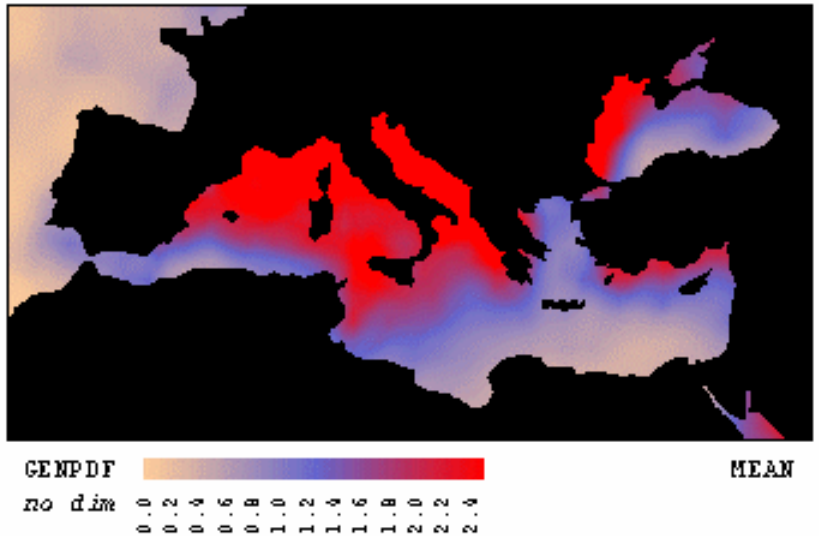
MONTH: Oct
GCM: ECHAM5-SRESA2 2081-2100
GENPDF
MEAN
no dim
0.0 0.2 0.4 0.6 0.8 1.0 1.2 1.4 1.6 1.8 2.0 2.2 2.4

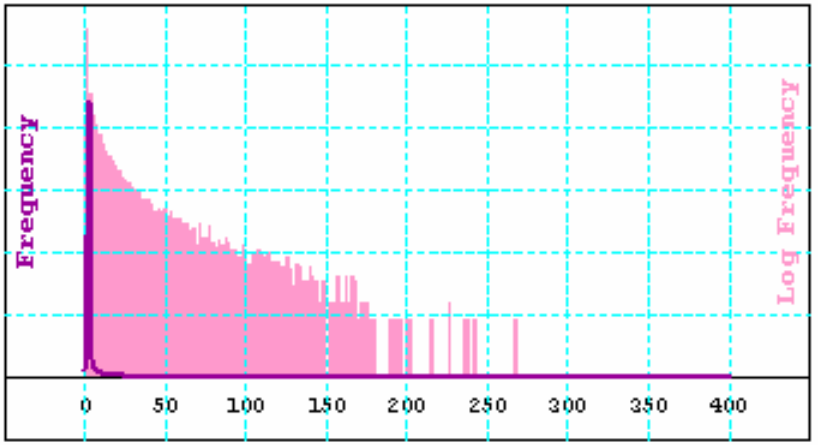
MONTH: Oct
GCM: ECHAM5-SRESA2 2081-2100
Frequency
Log Frequency
0 50 100 150 200 250 300 350 400
GENPDF
WESTREG
no dim

MEDICANE RISK IN A CHANGING CLIMATE :

Results of two methods

MOTIVATION

***Medicanes** are warm-core, surface flux-driven **extreme windstorms** potentially threatening the islands and coastal areas:*

- *Are there favoured locations for medicane development ?*
- *How intense can they become ?*
- *How could they react in frequency and intensity to global warming ?*

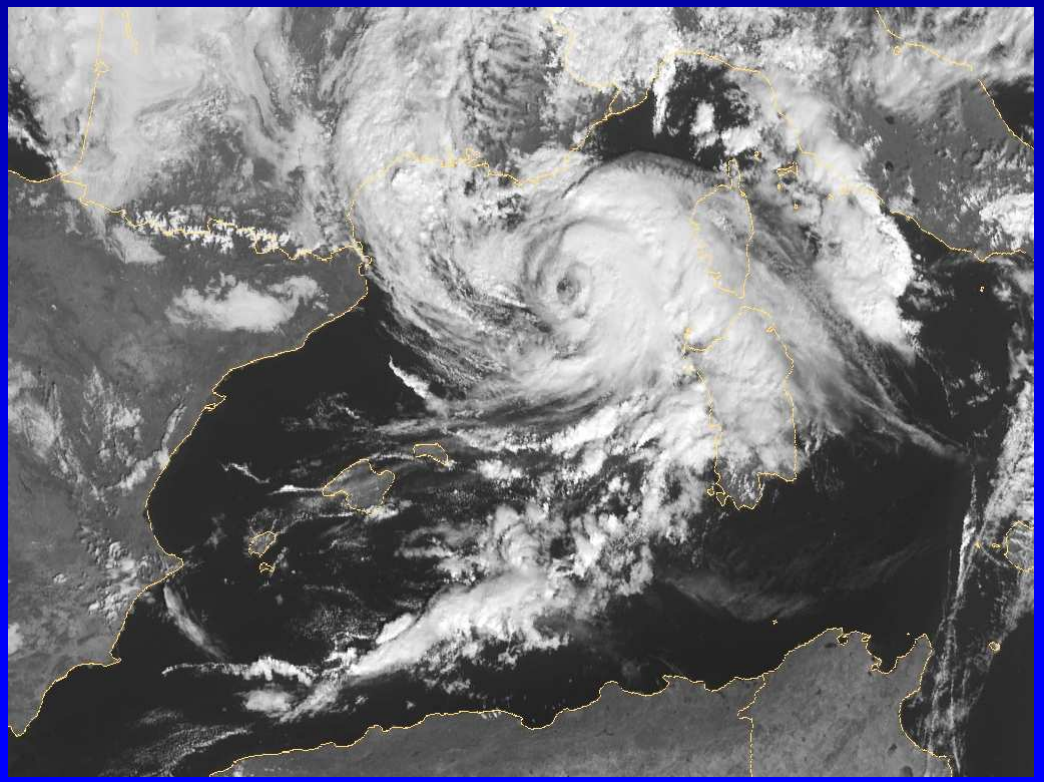

MEDICANE RISK ???

With an average frequency of only 1-2 events per year and given the lack of systematic, multidecadal databases, an objective evaluation of the long-term risk of medicane-induced winds is impractical with standard methods

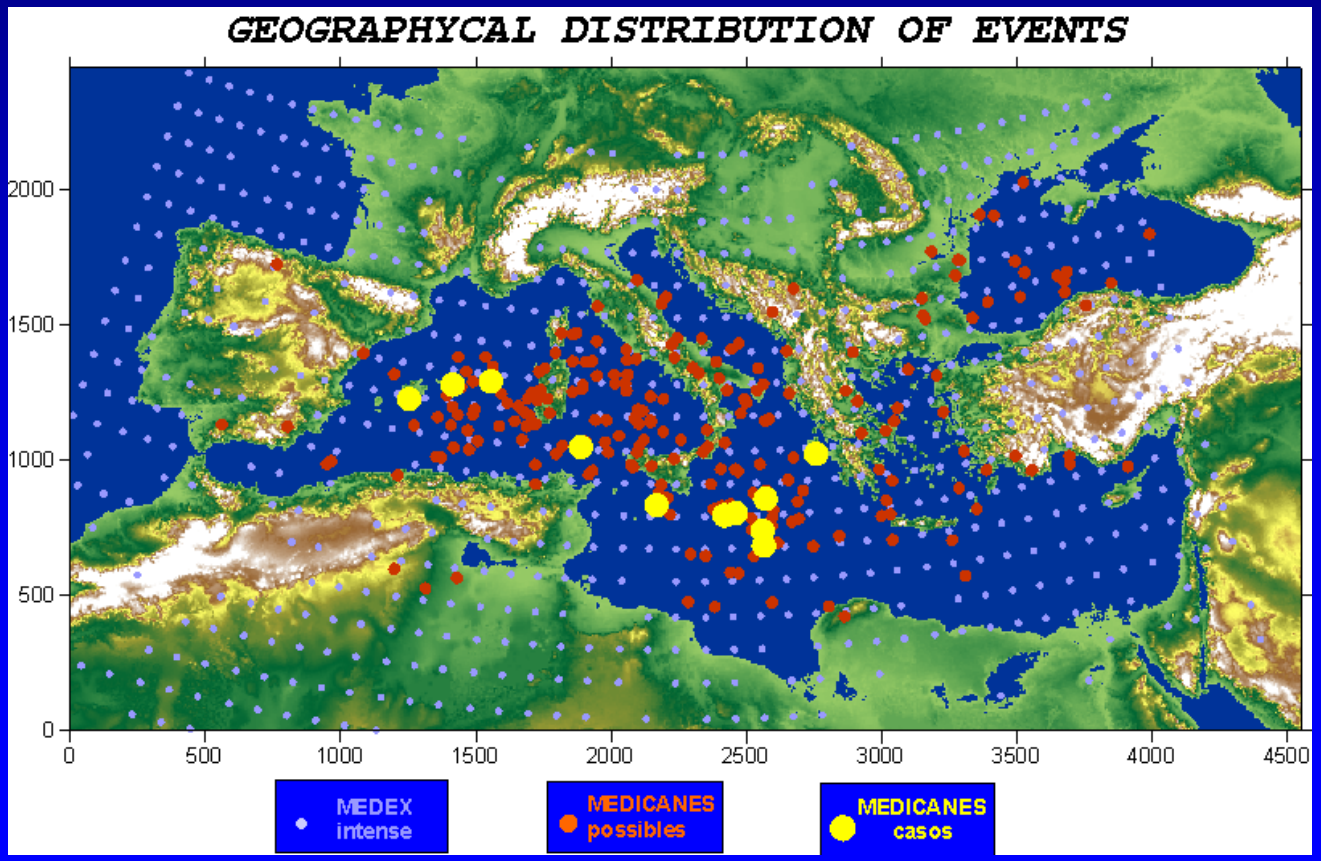

Database from satellite

(Tous and Romero, 2012)

APPROACH: Large-scale environmental proxies

***Synoptic** analyses of a few studied cases show that an inevitable precursor is the presence of a deep, **cut-off, cold-core** low in the upper and middle troposphere:*

- ***But** the infrequent occurrence of medicanes suggests that **additional and very special meteorological conditions** are necessary for these storms to occur …*

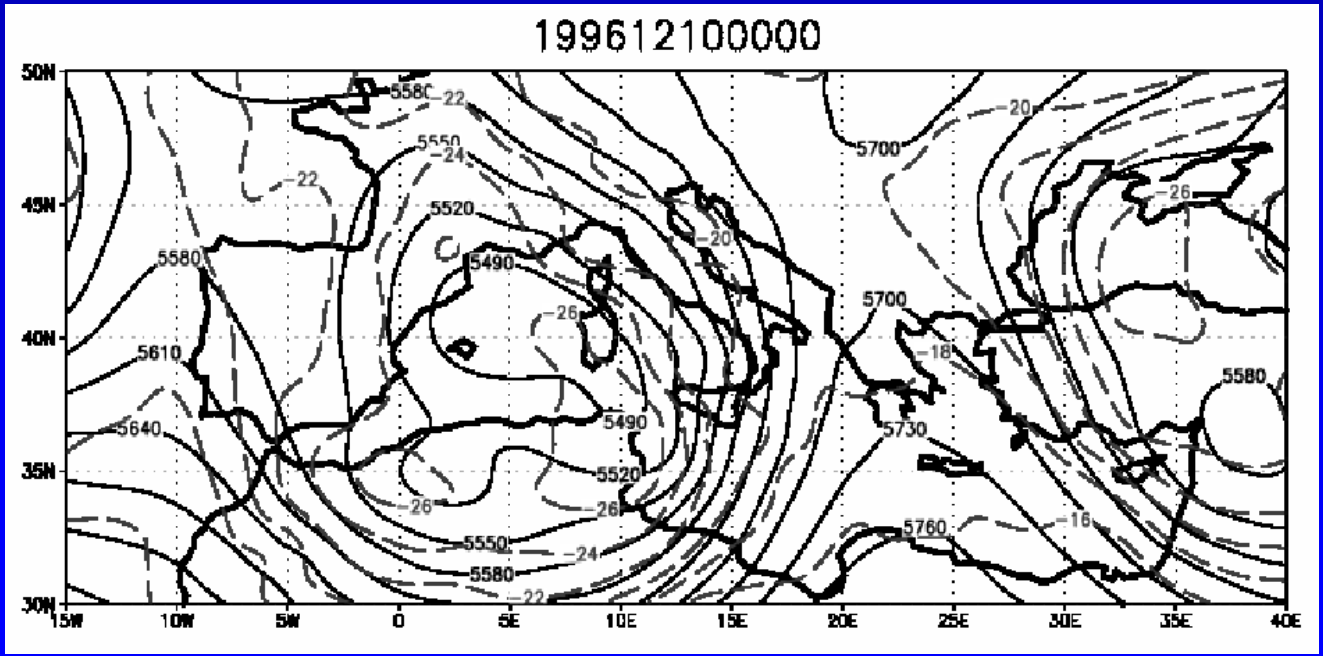

APPROACH: Large-scale environmental proxies

Application of an empirical index of genesis:

$$I = \left| 10^5 \eta \right|^{3/2} \left(\frac{H}{50} \right)^3 \left(\frac{V_{pot}}{70} \right)^3 \left(1 + 0.1 V_{shear} \right)^{-2},$$

GENIX parameter
(Emanuel and Nolan, 2004)

- **But these environmental proxies behave as necessary but no sufficient ingredients for the successful genesis of a medicane …**

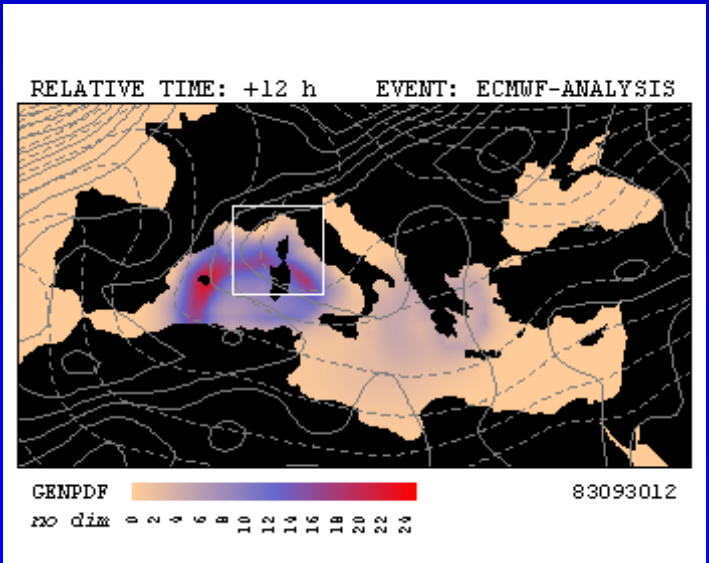

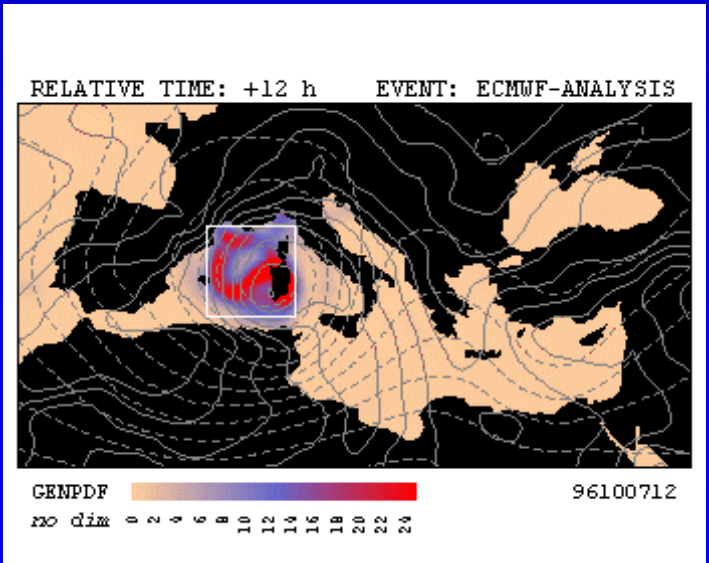

FIRST METHOD: Nested climatic simulations

Detection and tracking *of symmetric warm-core cyclonic disturbances generated* ***in mesoscale simulations*** *forced by Reanalysis and GCM data:*

- ***But high computational cost****: Limited horizontal resolution; Too few climatic realizations to permit a full sampling of the PDF of storms* ***…***

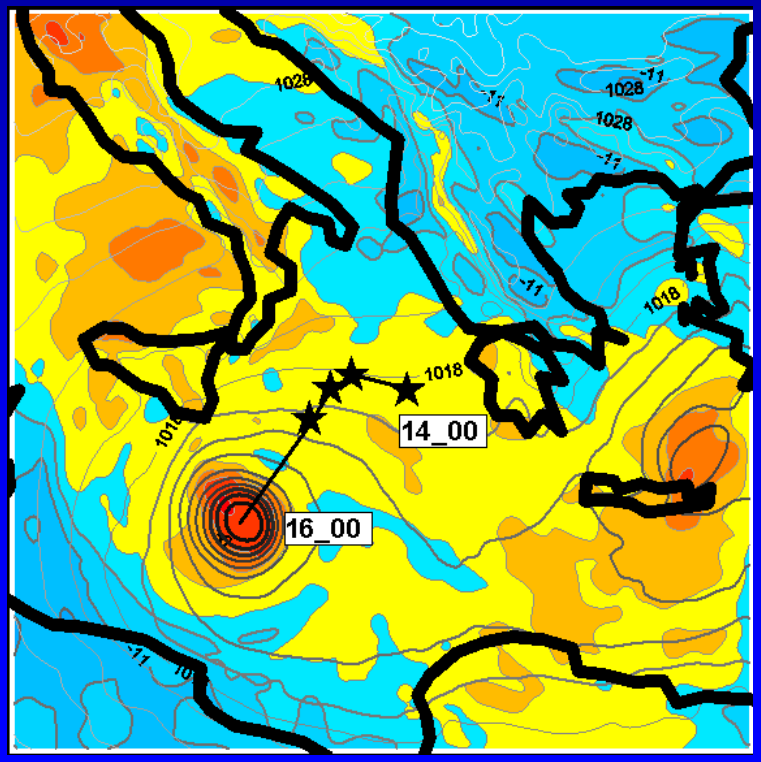

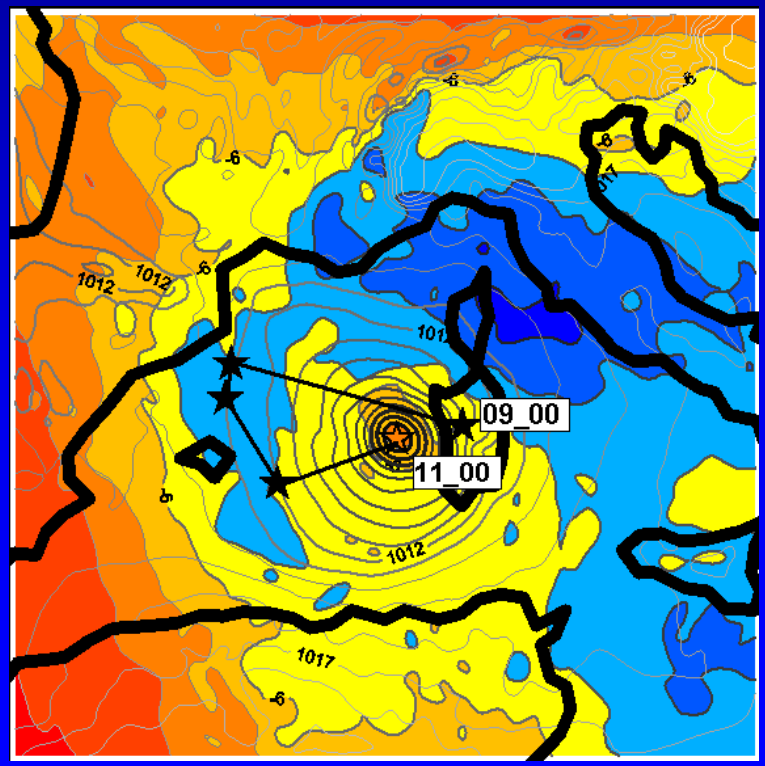

SECOND METHOD: Statistical-deterministic approach

Developed by Kerry Emanuel and his team in the context of the long-term wind risk associated with tropical cyclones:

- ***Low-cost generation of thousands of synthetic storms***
- ***Statistically robust assessment of risk (e.g. return periods for winds)***

- ***Genesis: Random draws from observed PDF or Random seeding***
- ***Track: Randomly varying synthetic winds (respecting climatology)***
- ***Environment: Previous winds + monthly-mean thermodynamic fields***
- ***Intensity and radial distribution of winds: CHIPS model***

ADAPTATION OF THE SECOND METHOD

The separation of timescales made in the tropics between the synthetic wind field (fast scale) and the thermodynamic environment (slow scale) is not appropriate to represent the movement, growth and decay of mid-latitude weather systems. In addition, the history of medicane genesis is far too sparse to form a reasonable PDF of genesis, and random seeding would be very inefficient:

- *For each month, decomposition through PCA of 10-day synoptic evolutions of z250, z850, T600, R600 and PINT into the new space of independent PCs*
- *Random selection + random perturbation of the set of PCs*
- *This perturbed set of PCs is converted back into physical space*
- *This is tantamount to generating 10-day sequences of spatiotemporal coherent z250, z850, T600, R600 and PINT synthetic fields which also respect their mutual covariances*

- *Potential Genesis: Based on the GENIX parameter*

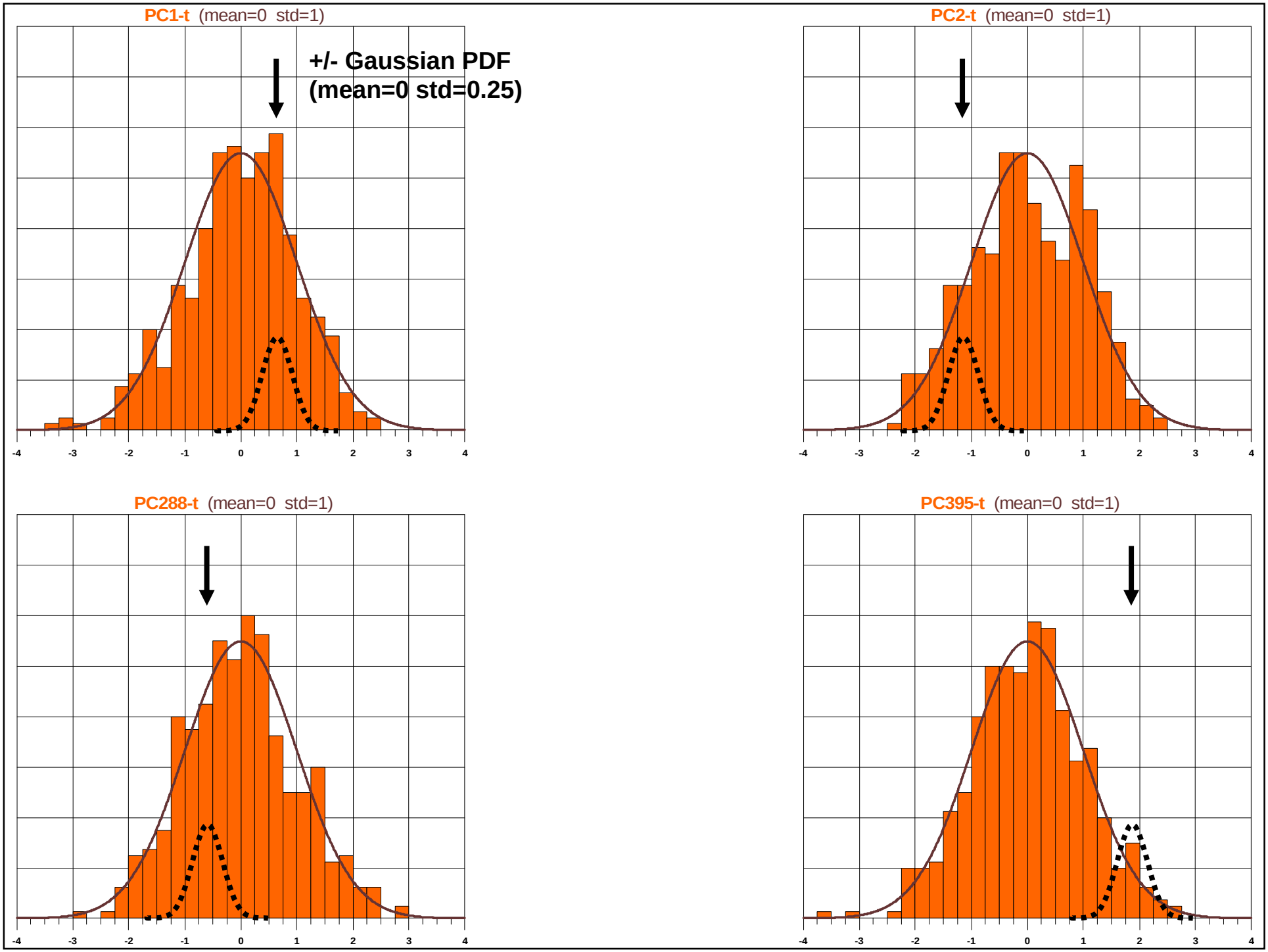
PC1-t (mean=0 std=1)
+/- Gaussian PDF
(mean=0 std=0.25)
PC2-t (mean=0 std=1)
PC288-t (mean=0 std=1)
PC395-t (mean=0 std=1)
-4
-3
-2
-1
0
1
2
3
4

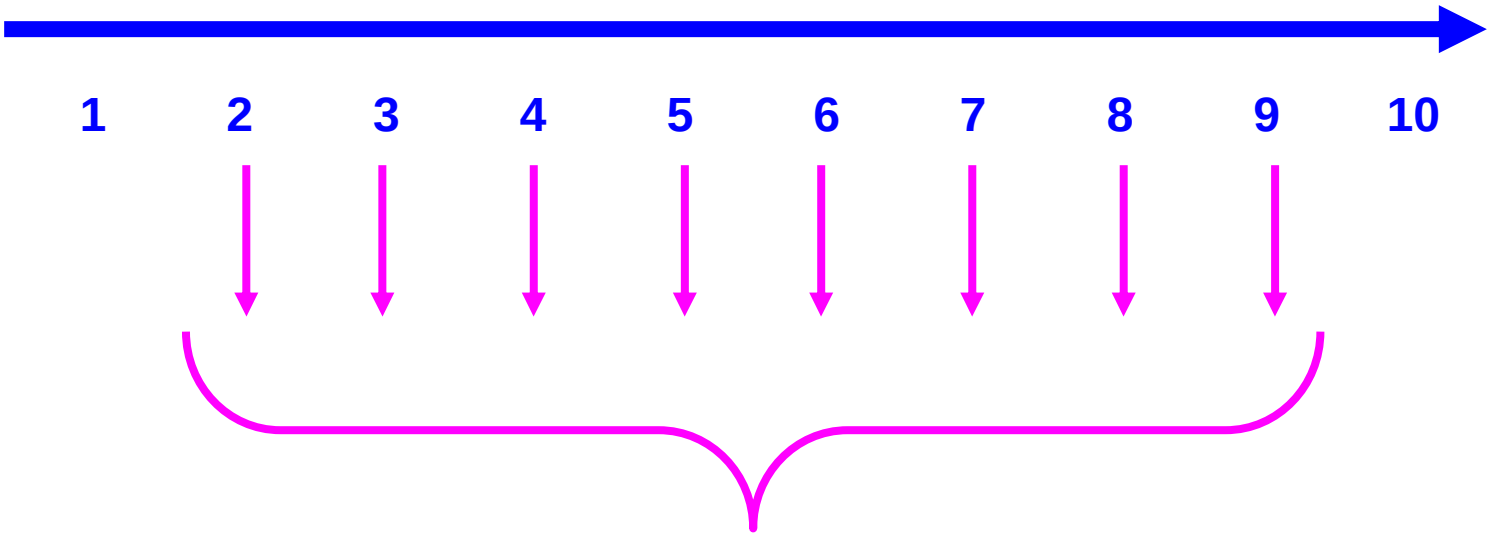

OPEN-SEA POINT + MAX OF GENIX > 20 + ABS VOR > 10 units ???

YES

Backward

(Max: 6 h)

Forward

(Max: 2 days over land)

POTENTIAL TRACK

(Δt = 30 min)

$$\begin{cases} u_{track} = \alpha\, u_{850} + (1 - \alpha)\, u_{250} \\ v_{track} = \alpha\, v_{850} + (1 - \alpha)\, v_{250} + v_{\beta} \end{cases}$$

$\alpha = 0.8$ $v_{\beta} = 2.5$ m/s


EXEMPLE FOR A
REAL EVENT

(d)

19-March-1999, 18 UTC

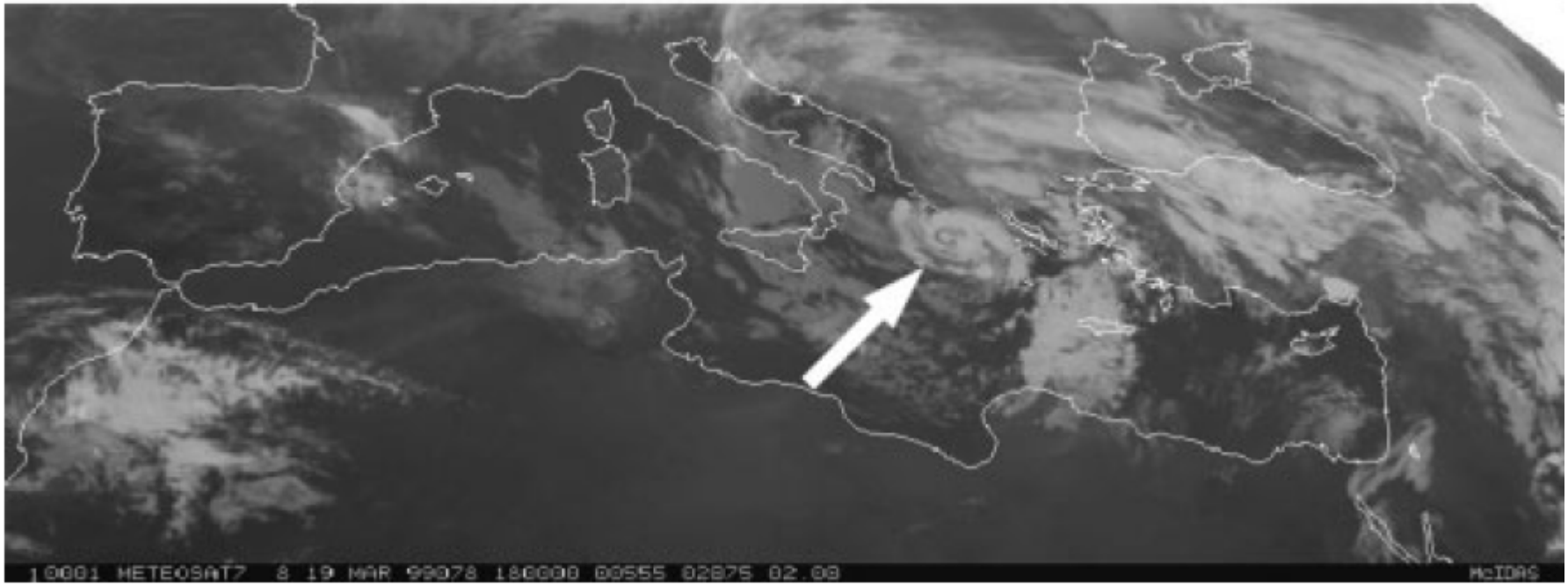

M11

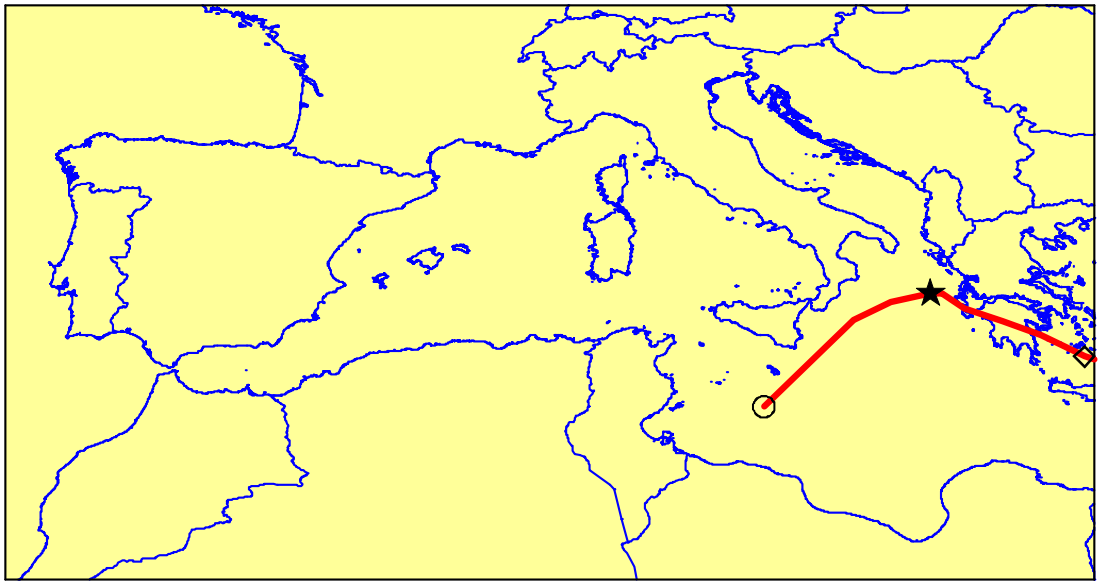

ERA-40
2 tracks

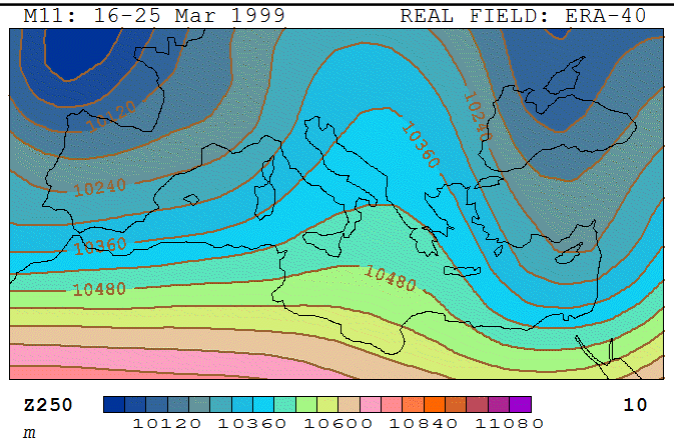

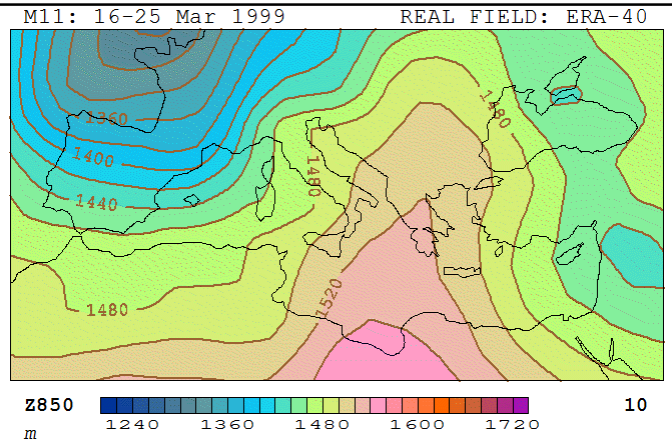

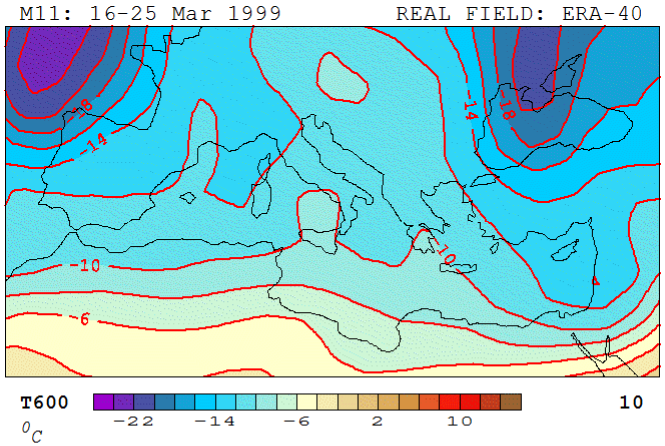

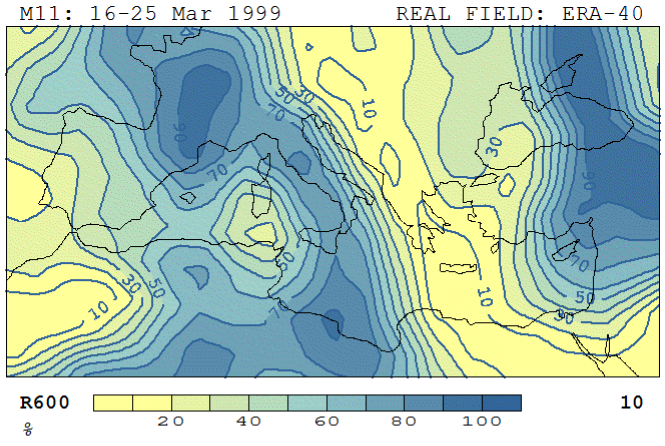

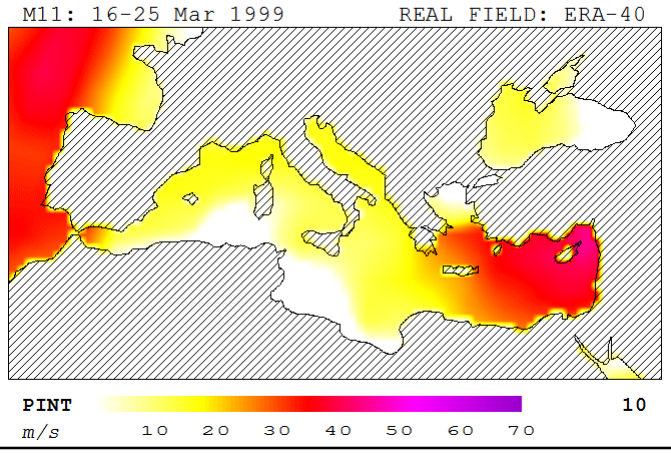

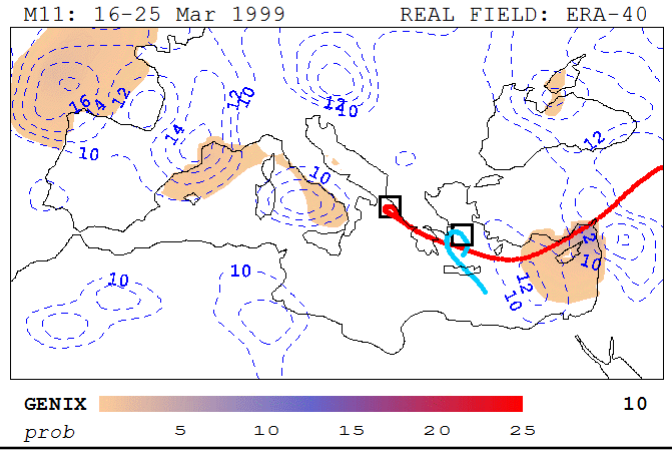

RND 1
1 tracks

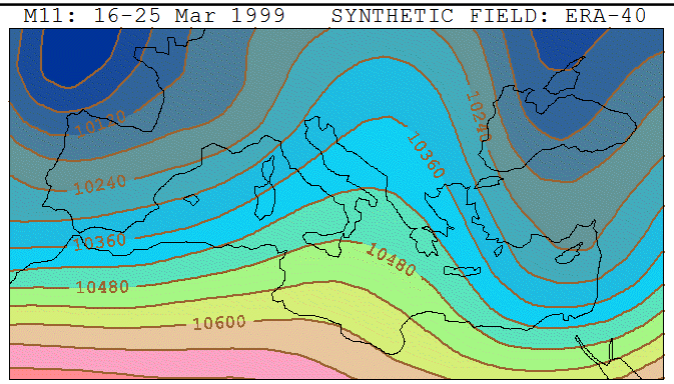

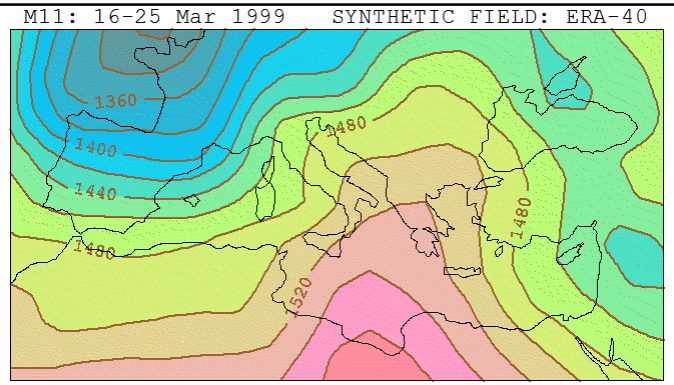

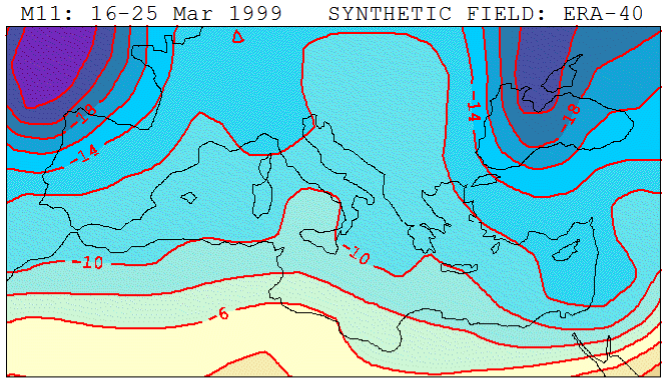

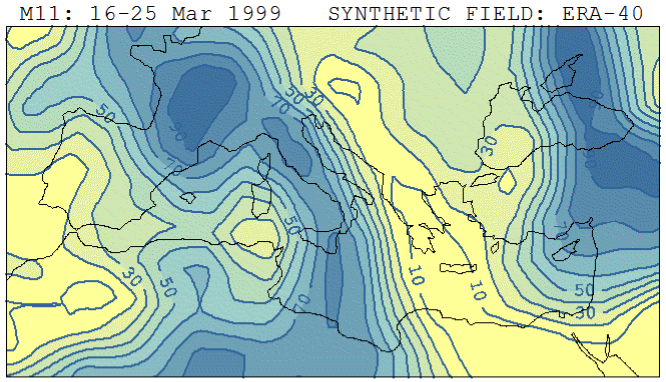

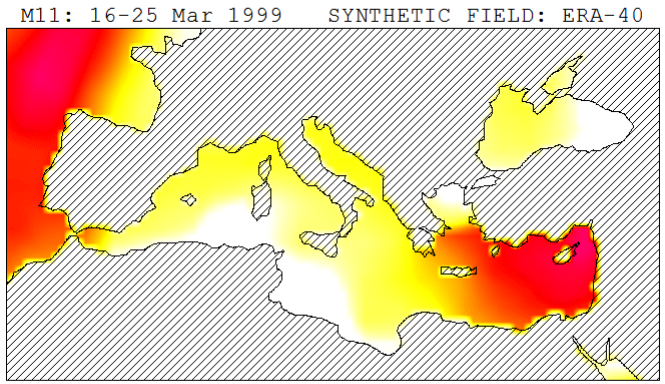

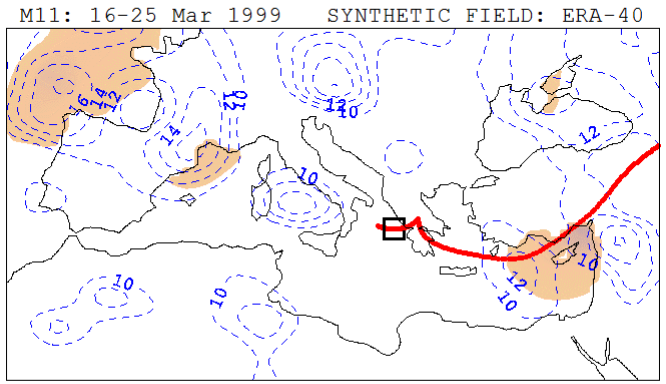

RND 2
4 tracks

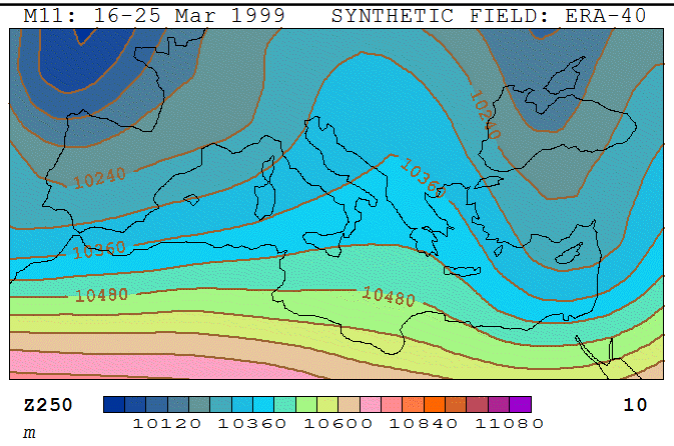

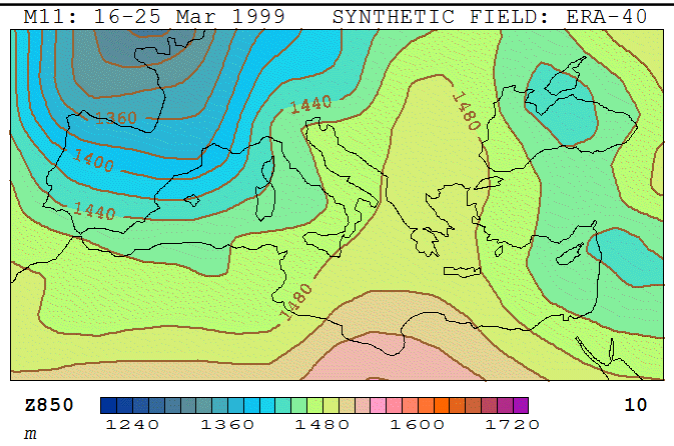

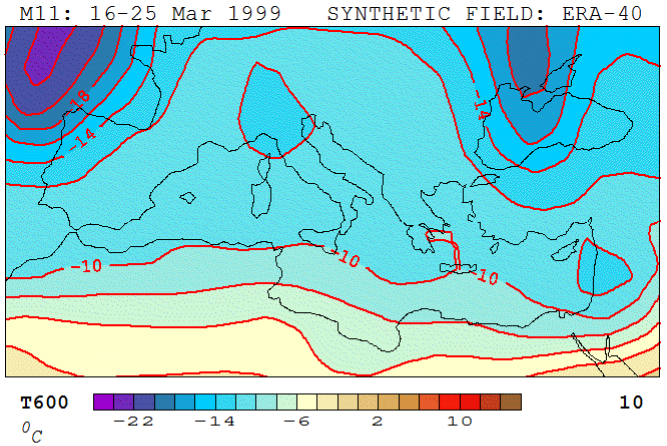

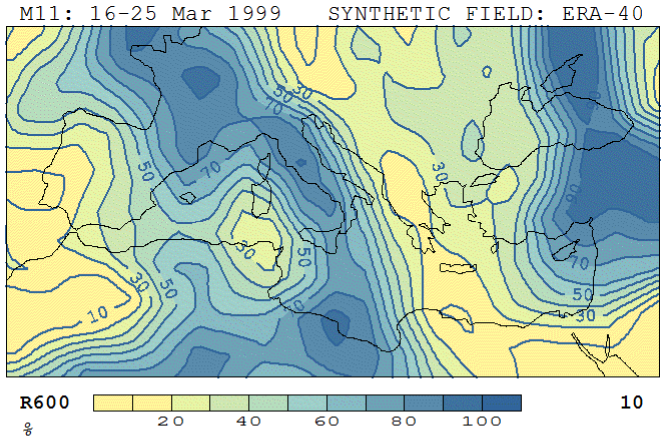

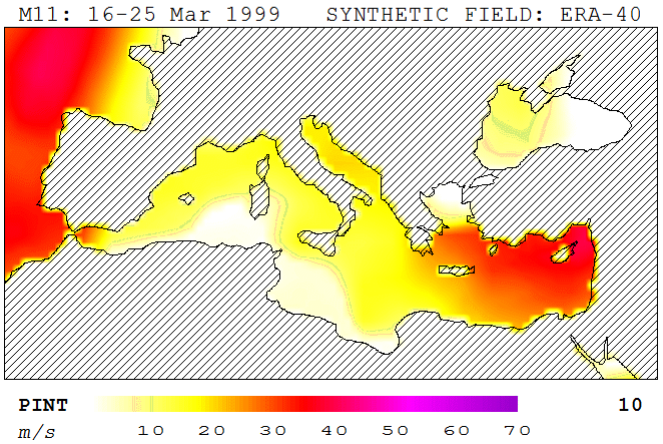

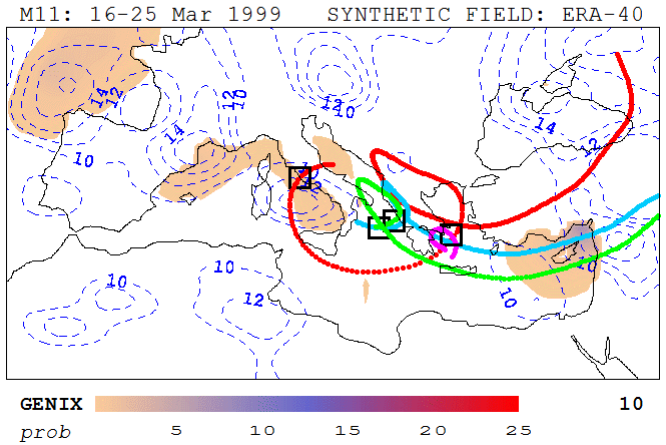

RND 3
5 tracks

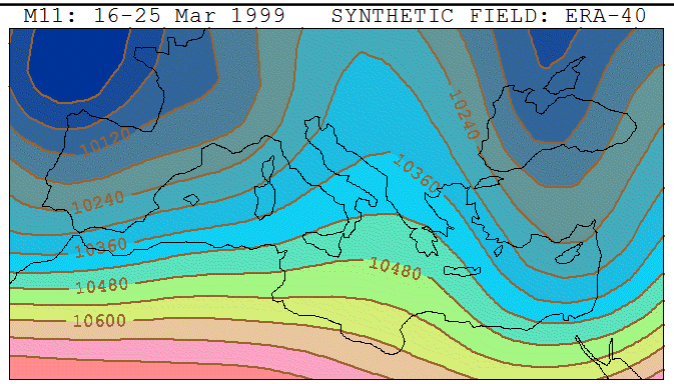

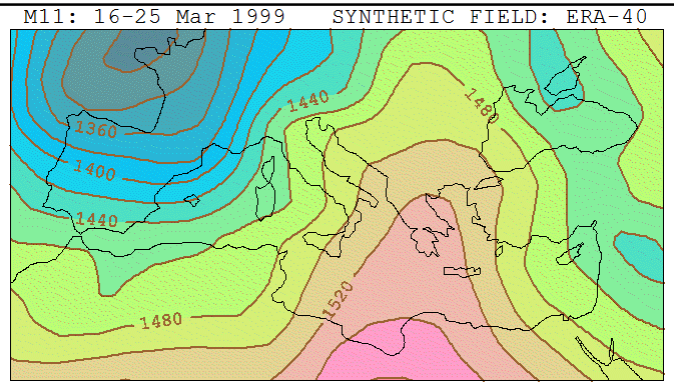

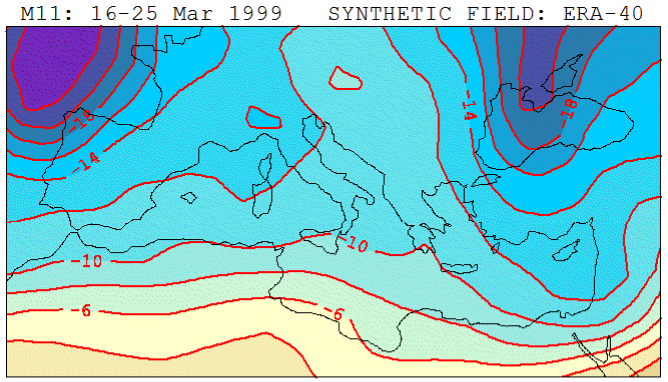

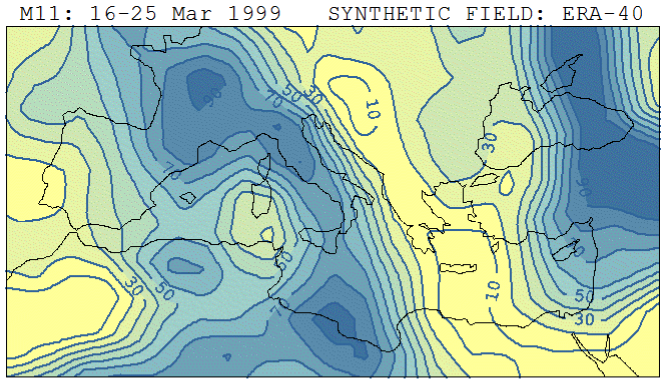

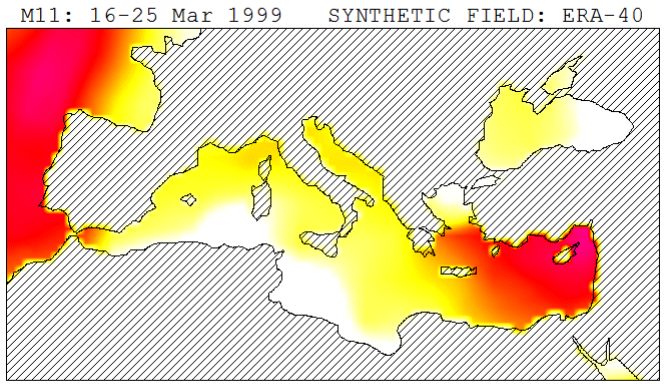

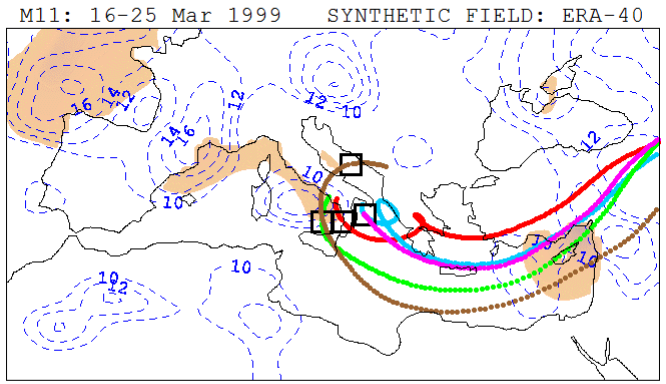

RND 4
5 tracks

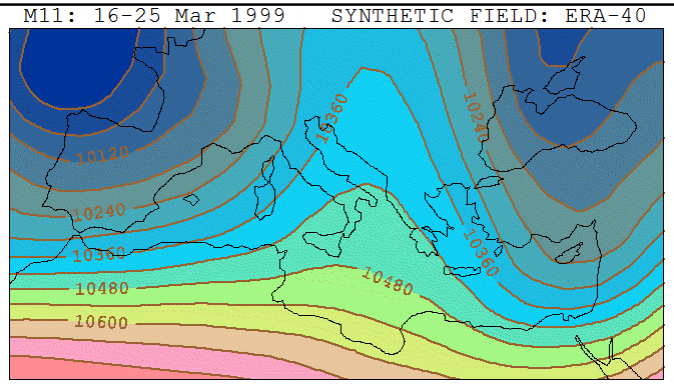

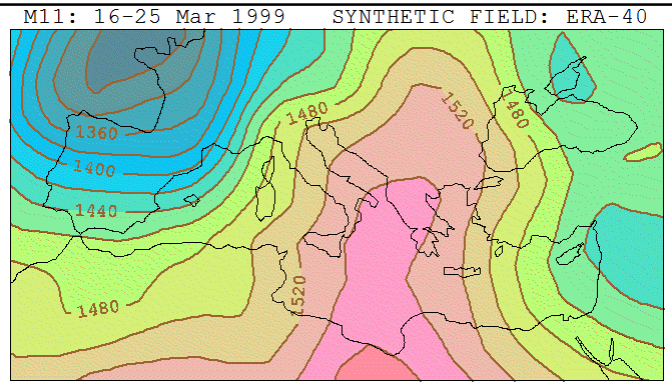

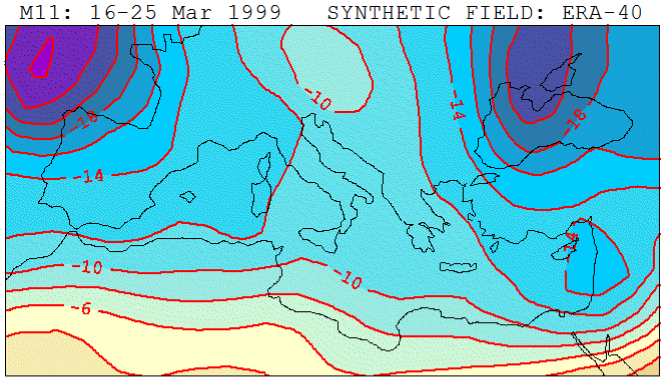

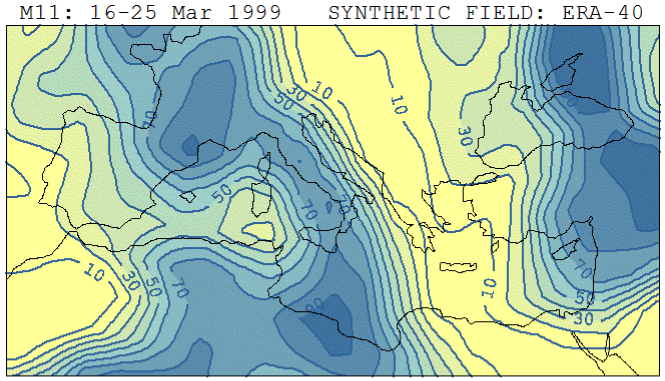

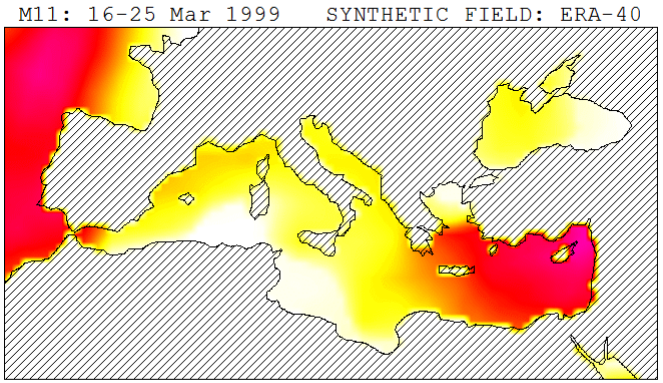

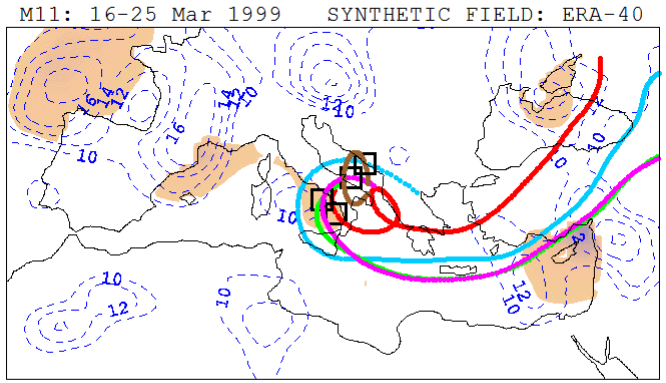

RND 5
1 tracks

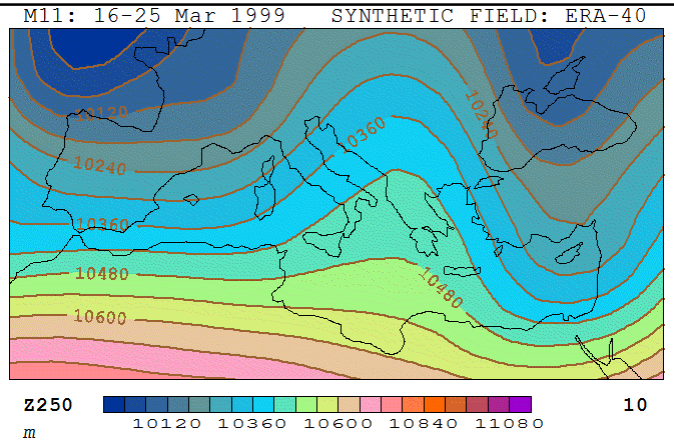

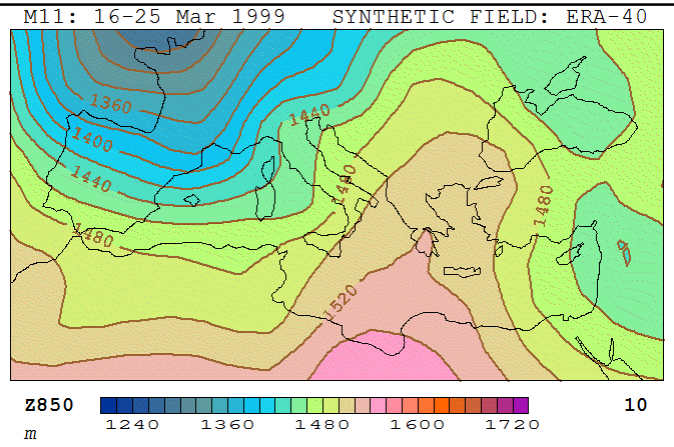

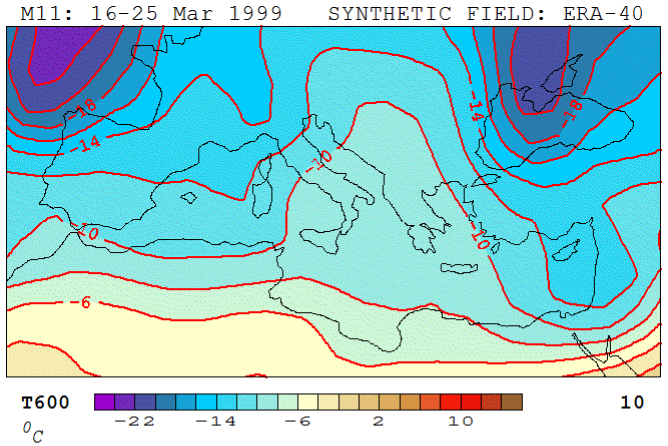

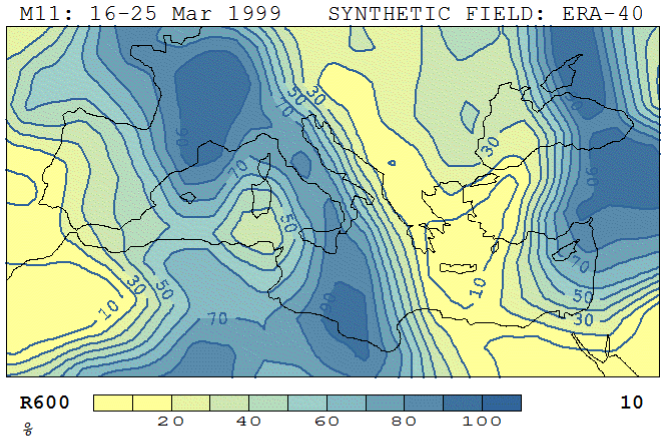

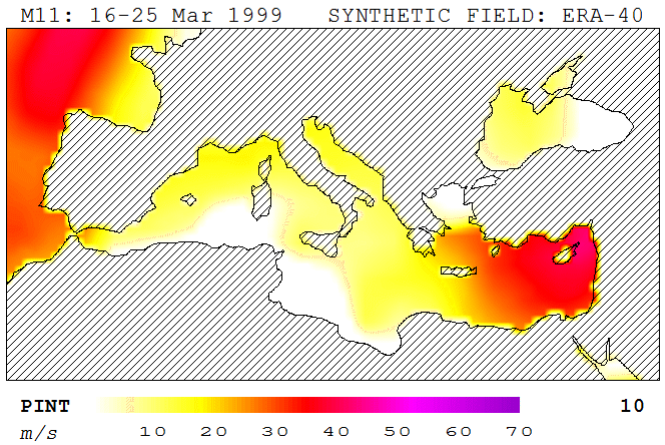

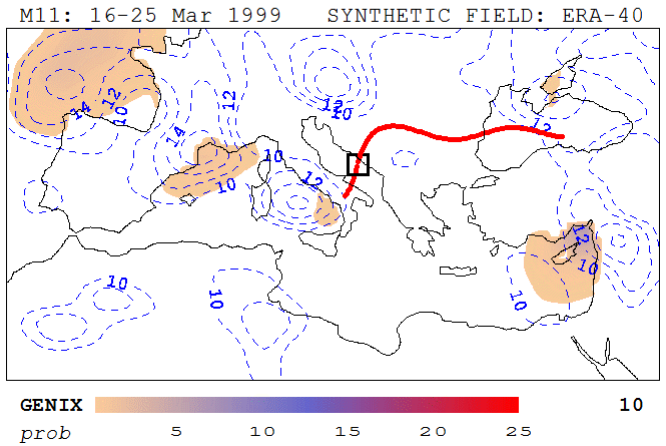

APPLICATION OF THE SECOND METHOD

We synthetically generate a total of ~15000 potential tracks for each climate/model. These are simulated with CHIPS and checked for intensification above TS category (34 kt):

Climate Scenario	Reanalysis or GCM	Successful Storms	Storms per century
PRESENT 1981 – 2000	*ERA40*	3048	**200**
	CSIRO	3286	**200**
	ECHAM	1924	**200**
	GFDL	1343	**200**
	MIROC	1567	**200**
FUTURE 2081 – 2100 SRES A2	*CSIRO*	2857	**174**
	ECHAM	1072	**111**
	GFDL	1226	**183**
	MIROC	2389	**152**

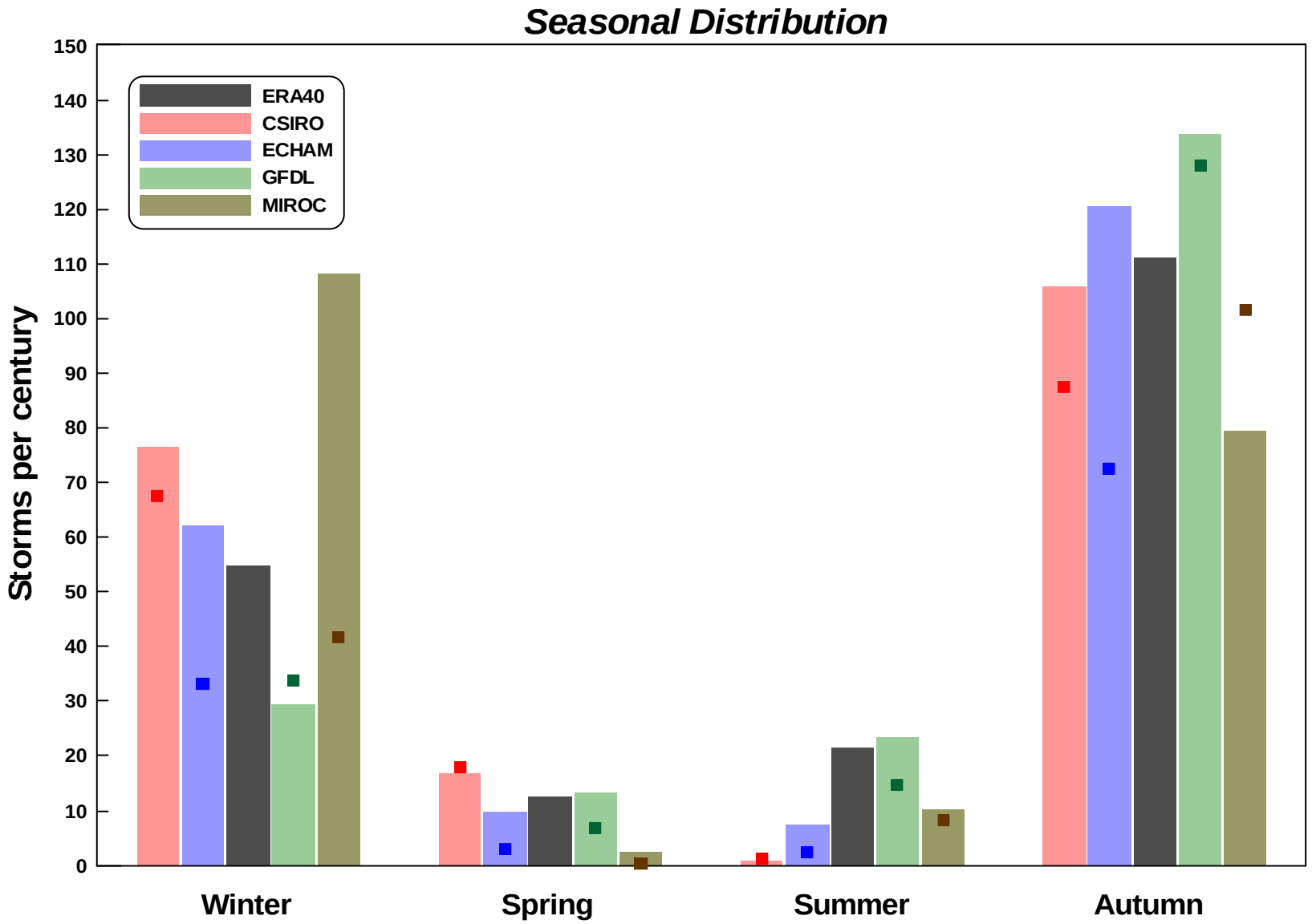
Seasonal Distribution
Storms per century
150
140
130
120
110
100
90
80
70
60
50
40
30
20
10
0
ERA40
CSIRO
ECHAM
GFDL
MIROC
Winter
Spring
Summer
Autumn

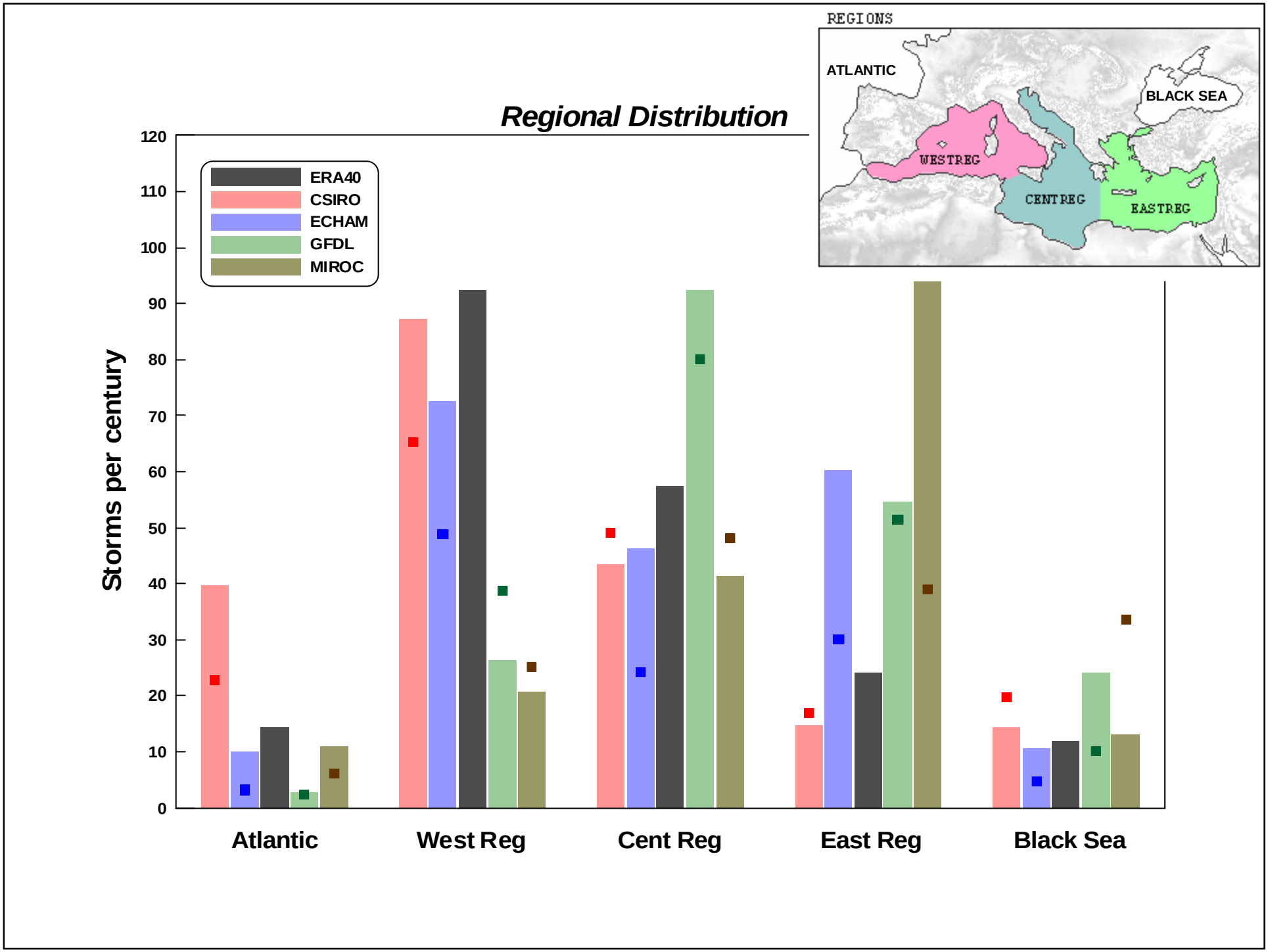
Regional Distribution
REGIONS
ATLANTIC
BLACK SEA
WESTREG
CENTREG
EASTREG
ERA40
CSIRO
ECHAM
GFDL
MIROC
Storms per century
0
10
20
30
40
50
60
70
80
90
100
110
120
Atlantic
West Reg
Cent Reg
East Reg
Black Sea

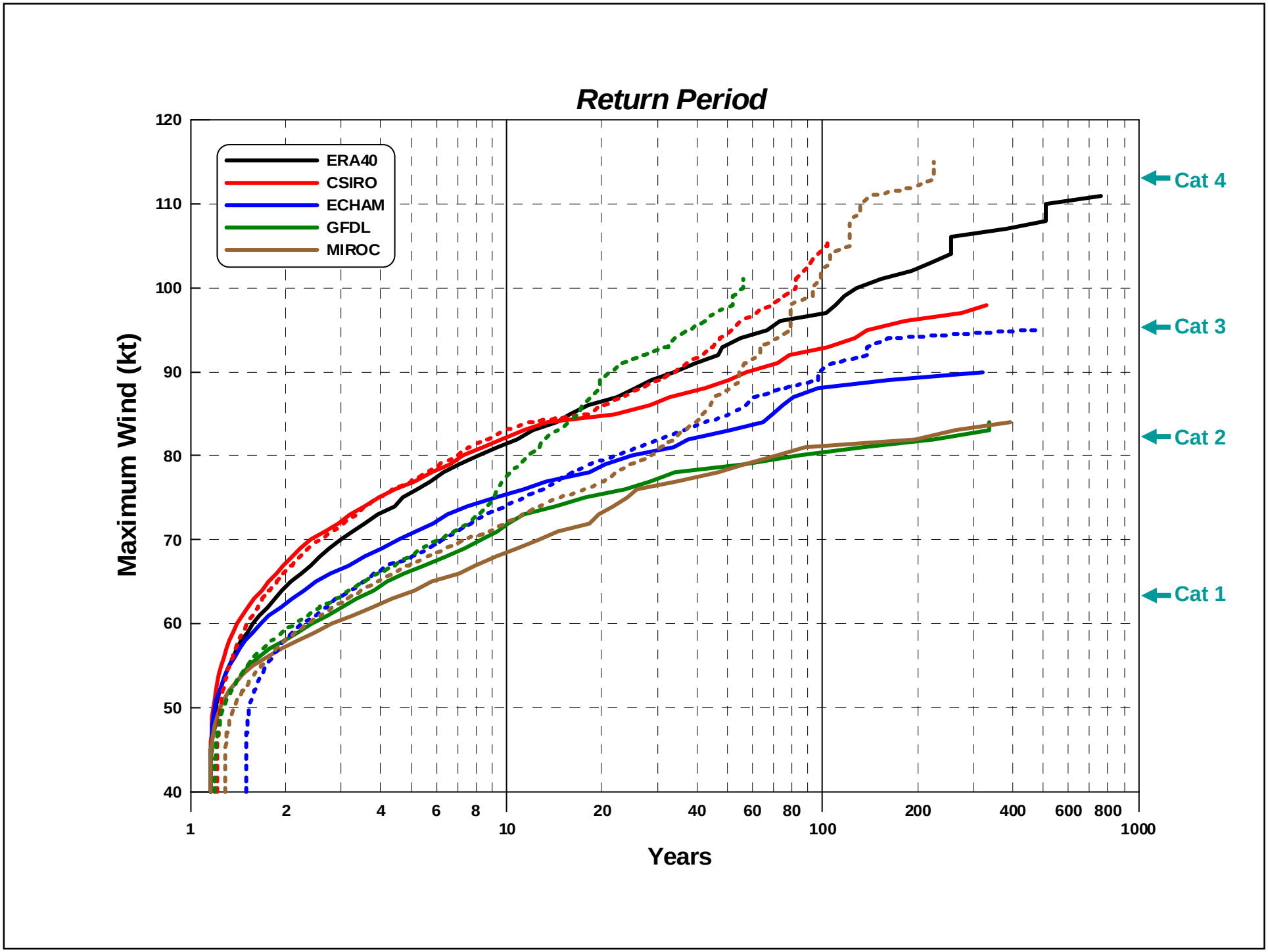
Return Period
ERA40
CSIRO
ECHAM
GFDL
MIROC
Cat 4
Cat 3
Cat 2
Cat 1
Maximum Wind (kt)
120
110
100
90
80
70
60
50
40
1
2
4
6
8
10
20
40
60
80
100
200
400
600
800
1000
Years

20C3M
scenario

CSIRO - Present

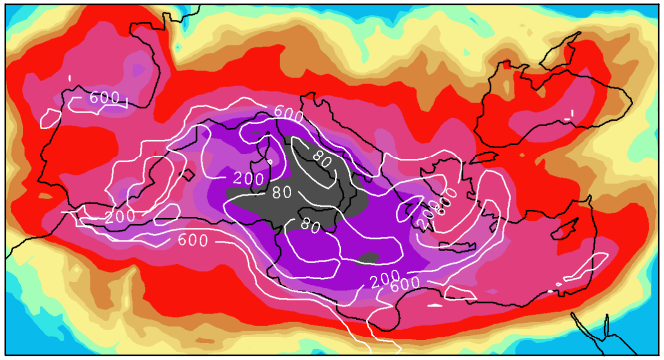

Years
2 4 6 8 10 40 80 200 600

ECHAM - Present

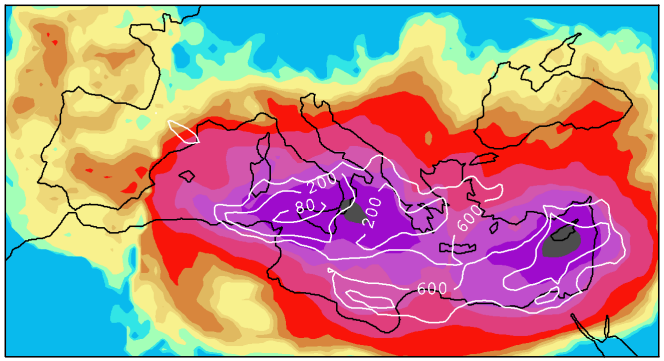

Years
2 4 6 8 10 40 80 200 600

GFDL - Present

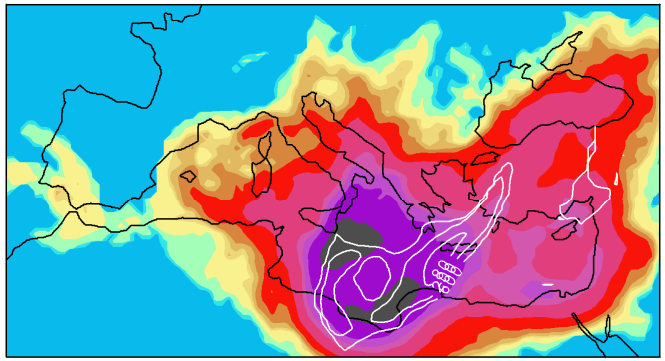

Years
2 4 6 8 10 40 80 200 600

MIROC - Present

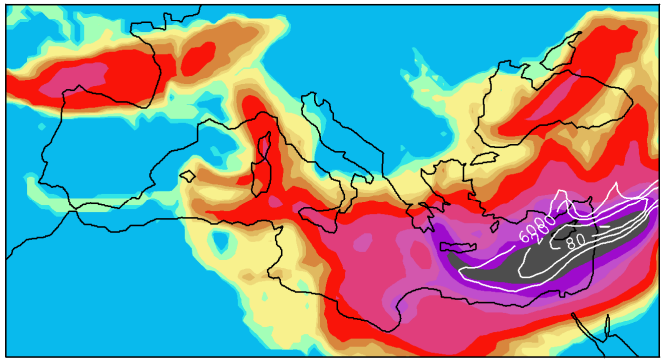

Years
2 4 6 8 10 40 80 200 600

ERA40 - Present

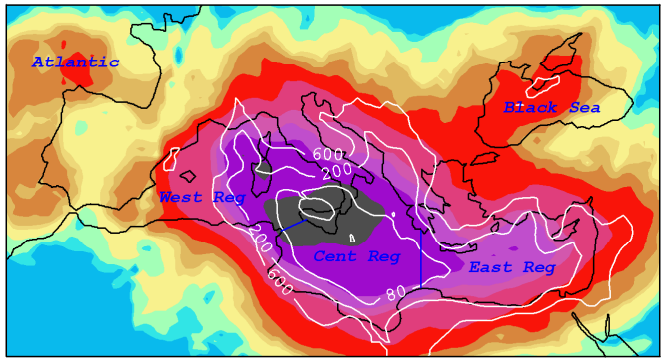

Years
2 4 6 8 10 40 80 200 600

SRESA2
scenario

CSIRO - Future

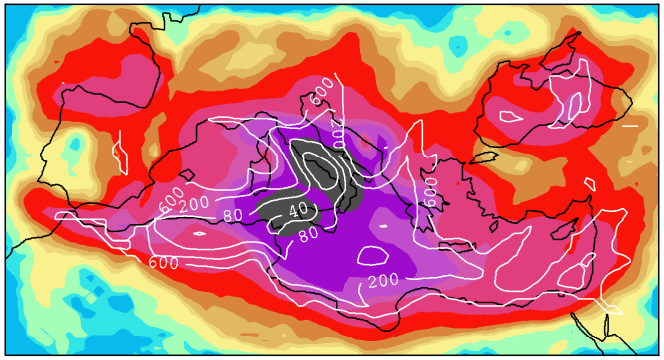

Years
2 4 6 8 10 40 80 200 600

ECHAM - Future

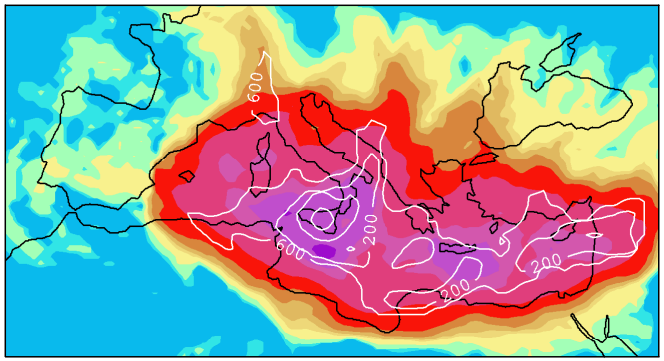

Years
2 4 6 8 10 40 80 200 600

GFDL - Future

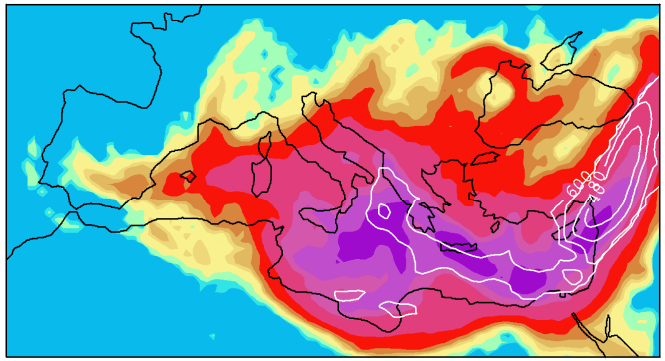

Years
2 4 6 8 10 40 80 200 600

MIROC - Future

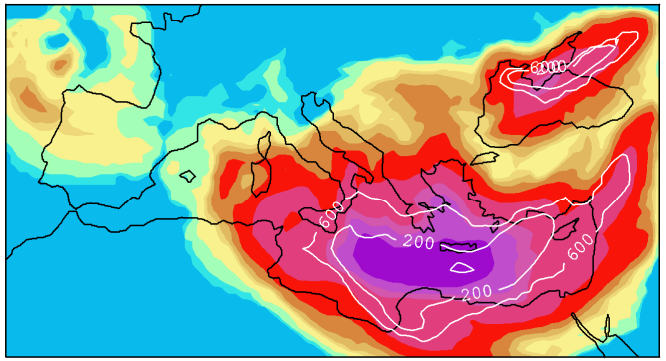

Years
2 4 6 8 10 40 80 200 600

COMPARISON OF BOTH METHODS

SYNTHETIC generation

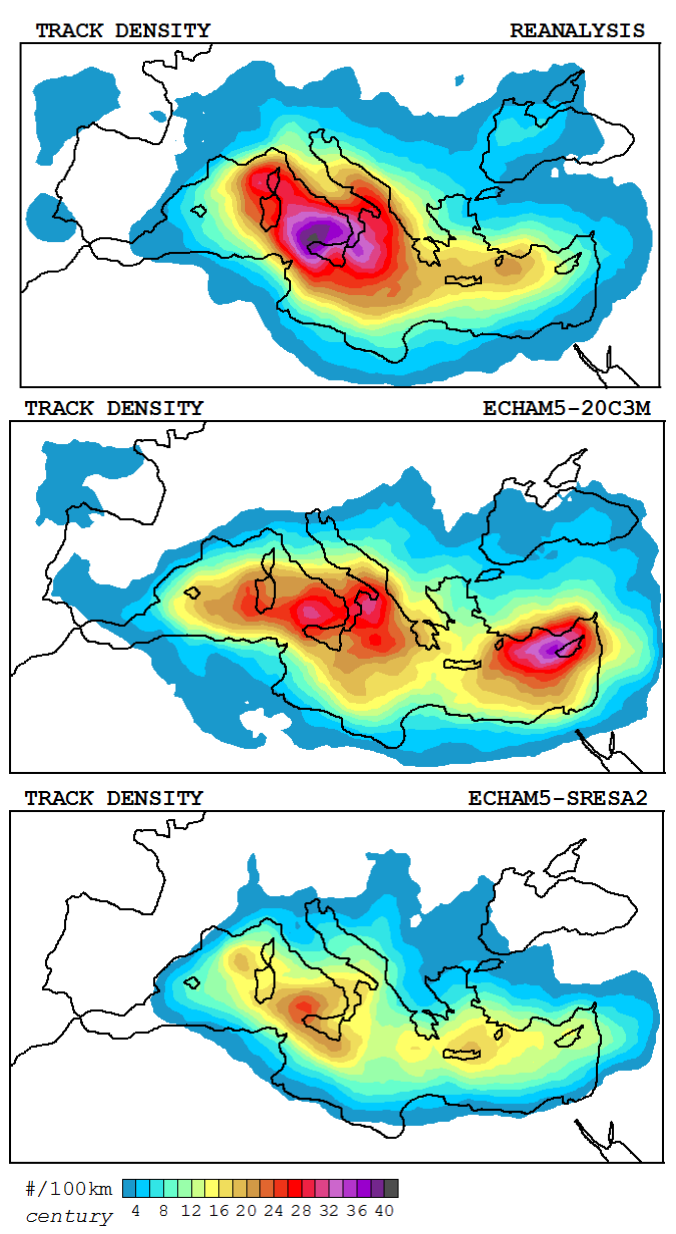

DYNAMICAL downscaling

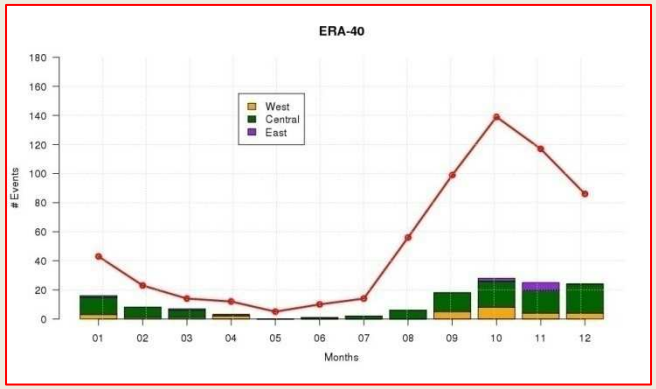

28
101
9

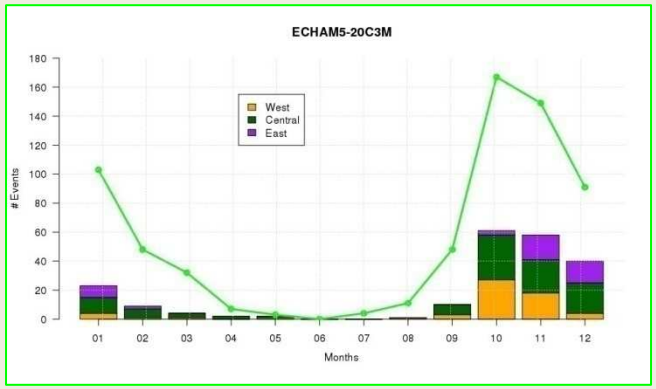

60
105
45

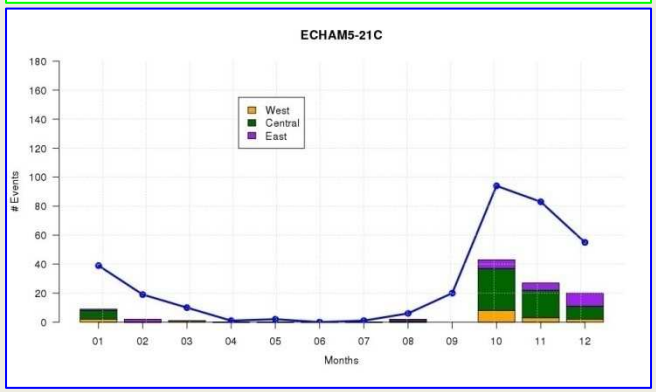

16
64
23

CONCLUSIONS

- The statistical-deterministic approach is a good alternative to computationally expensive classical methods (e.g. dynamical downscaling of medicanes), with the extra benefit of producing statistically large populations of events

- We attained unprecedented medicane-wind risk maps for the Mediterranean region

- General agreement with the “known” phenomenology of medicanes in the current climate (e.g. maximum in the cold season and central Mediterranean) and between both methods

- In spite of some geographical uncertainties, GCMs tend to project fewer medicanes at the end of the century compared to present but a higher number of violent storms, suggesting an increased probability of major economic and social impacts as the century progresses


GRACIAS POR
VUESTRA ATENCIÓN !!!